Microfluidic Applications of Magnetic Particles for Biological Analysis and Catalysis

Martin A. M. Gijs,* Frédéric Lacharme, and Ulrike Lehmann

Laboratory of Microsystems, Ecole Polytechnique Fédérale de Lausanne, 1015 Lausanne EPFL, Switzerland

Received May 14, 2009

Contents

* To whom correspondence should be addressed. Tel.: +41 21 693 67 34. Fax: +41 21 693 59 50. E-mail: martin.gijs@epfl.ch.

1. Introduction

1.1. Microfluidic Systems

Since the introduction of the concept of Micro Total Analysis System or μTAS in 1990,[1] the interest in and impact of such devices, also called lab-on-a-chip or miniaturized analysis systems, has grown explosively. Clinical diagnosis, as practiced in blood screening laboratories, is for economic reasons dominated by high-throughput, highly reliable, and robust modular automated systems. Such systems generate a minimum of consumables per test indeed. However, microfluidics has shown to provide attractive solutions for many problems in chemical and biological analysis, especially for in-field use or point-of-care testing. A detailed overview of the various fluidic operations in microfluidic systems, such as sample preparation, sample injection, sample manipulation, reaction, separation, and detection, published in the 1990−2008 period, was presented in a series of review articles by the group of A. Manz.[2−4] Three of the most important advantages of using fluidic systems of reduced dimension for analytical applications are (i) the possibility of using only minute quantities of sample and reagents (down to picoliters), as problems of fluidic connectors with large dead volumes can be avoided for an integrated lab-on-a-chip, (ii) comparatively fast reaction times, when molecular diffusion lengths are of the order of the microchannel dimension, and (iii) a large surface-to-volume ratio offering an intrinsic compatibility between the use of microfluidic systems and surface-based assays. The long-range nature of viscous flows and the reduced device dimensions imply that the influence of boundaries or "channel walls" is very significant for a microfluidic system. A variety of strategies have been implemented to manipulate fluids by exploiting

10.1021/cr9001929
Published on Web 12/04/2009

Martin A. M. Gijs received his degree in physics in 1981 from the Katholieke Universiteit Leuven, Belgium, and his Ph.D. degree in physics at the same university in 1986. He joined the Philips Research Laboratories in Eindhoven, The Netherlands, in 1987. Subsequently, he has worked there on micro- and nanofabrication processes of high critical temperature superconducting Josephson and tunnel junctions, the microfabrication of microstructures in magnetic multilayers showing the giant magnetoresistance effect, the design and realization of miniaturized motors for hard disk applications, and the design and realization of planar transformers for miniaturized power applications. He joined the Ecole Polytechnique Fédérale de Lausanne (EPFL) in 1997. He presently is a professor in the Institute of Microengineering, where he is responsible for the Microsystems Technology Group. His main interests are in developing technologies for novel magnetic devices, new microfabrication technologies for Microsystems fabrication in general, and the development and use of microfluidics for biomedical applications in particular. He is on the editorial board of Microfluidics and Nanofluidics and the Journal of Micromechanics and Microengineering. He has published over 160 papers in peer-reviewed journals and holds over 20 patents.

Frédéric Lacharme was born in Bordeaux, Gironde, France in 1978. He received his Master's degree in Physical-Chemistry from the University of Bordeaux 1 "Sciences and Technologies" in 2002. In 2003, he joined the laboratory of Professor Martin Gijs at the Ecole Polytechnique Fédérale de Lausanne, where he received his Ph.D. degree in 2008. His research was focused on the development of analytical microfluidic systems using magnetic nanoparticles. He is currently working on the development of microchips for analytical and diagnostic applications.

boundary effects, among them electrokinetic effects, droplet generation, acoustic streaming, and fluid−structure interactions, topics that were also reviewed extensively.[5−8]

Multiple technologies for the realization of fluidic microsystems have been developed, as shown for example in the book of Madou[9] and the review of Reyes et al.[10] The basic microfabrication sequence of a fluidic chip usually involves the patterning of a microchannel structure, a bonding operation to seal the open channel, followed by surface coating or functionalization steps. Glass and silicon have been the dominating material for the realization of microfluidic chips in the early years,[11] but have been more and more replaced by polymers. Still, borosilicate glass forms an interesting option for more demanding microreactor applications in harsh environments, for example, during catalytic reactions at high temperatures. Fused silica is a material with low autofluorescence in the ultraviolet region, making it a preferred choice for high-resolution fluorescent detection methods. However, microfabrication of glass[9] can be expensive due to the requirement of clean room-based technologies such as deep plasma etching or hydrofluoric acid-based wet etching. This explains the increasing interest in the replication of microchannel master structures in an elastomeric material like poly dimethylsiloxane (PDMS),[12,13] which has become a preferred microfluidic technology for the lab-on-a-chip research community. Also, high-throughput polymer microfabrication techniques such as microinjection molding and hot embossing[14] have emerged for affordable and disposable microfluidic analytical applications.

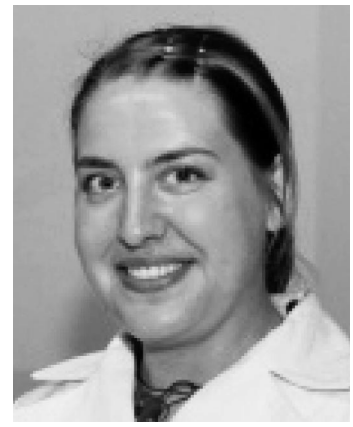

Ulrike Lehmann was born in Rostock, Germany in 1978. She obtained her Dipl-Ing. degree in electrical engineering, with a specialization on MEMS, in 2003, at the Chemnitz Technical University, Chemnitz, Germany. She subsequently joined the group of Prof. Gijs in the Laboratory for Microsystems at the Ecole Polytechnique Fédérale de Lausanne to work on her Ph.D. In 2008, she obtained her Ph.D. for her work on the manipulation of magnetic microparticles in liquid phases for application in biomedical systems, which included the magnetic manipulation of droplets as well as the direct manipulation of single magnetic microparticles. Ulrike Lehmann is currently working at Microsens S.A., where she is involved in the development of environmental sensor probes based on electrochemical and resistive microsensors.

Parallel to the boom of microfluidic systems, nanomaterials and nanoparticles have become a hot topic in research. When brought into a microfluidic channel, nano- and microparticles offer a relatively large specific surface for chemical binding. Such particles are also called in general "beads" in literature, independent of what their size is. A polymer colloid or microsphere solution has a low viscosity as compared to solutions having the same amount of solid, giving it special properties. Also, such small particles can be advantageously used as a "mobile substrate" in catalysis, for bioassays or even for in vivo applications; they can be easily recovered from a dispersion, reversibly redispersed, etc. Several reviews on the preparation and use of polymer particles and polymer colloids for medical, biological, and optical applications exist.[15,16] Moreover, the technologies for the realization of nano- and microparticle handling systems, with a focus on the integration of the latter with microfluidic systems, were reviewed.[17] With respect to open or "empty" microchannels, microfluidic structures with packed beds of functionalized beads or containing bead suspensions profit from an even

larger surface-to-volume ratio, an enhanced interaction of reactive surfaces with fluids passing by, and an improved recuperation of reaction products.

1.2. Basic Characteristics of Magnetic Beads

If a magnetic material is placed in a magnetic field of strength **H**, the individual atomic moments in the material contribute to its overall response, resulting in the magnetic induction $\mathbf{B} = \mu_0(\mathbf{H} + \mathbf{M})$,where μ_0 is the permeability of free space, and the magnetization $\mathbf{M} = \mathbf{m}/V$ is the magnetic moment per unit volume, where **m** is the magnetic moment of a volume V of the material. The magnetic character of a material depends on its atomic structure and temperature. Materials may be conveniently classified in terms of their volumetric magnetic susceptibility, χ, where $\mathbf{M} = \chi\mathbf{H}$ describes the magnetization induced in a material by **H**. In SI units, χ is dimensionless, **B** is expressed in tesla (T), and both **M** and **H** are expressed in A/m.

Magnetic beads have additional advantages beyond those mentioned for nonmagnetic particles: having embedded magnetic entities, they can be magnetically manipulated using permanent magnets or electromagnets, independent of normal microfluidic or biological processes. This additional degree of freedom is the basis of a still improved exposure of the functionalized bead surface to the surrounding liquid, due to the increased relative motion of the bead with respect to the fluid. It is important to note that a magnetic field gradient is required to exert a translation force, because a uniform field solely gives rise to a torque, but no translational action. The magnetic force acting on a point-like magnetic dipole or "magnetic moment" **m** in a magnetic induction **B** can be written as a function of the derivative of the magnetic induction:[18−23]

$$\mathbf{F}_m = \frac{1}{\mu_0}(\mathbf{m}\cdot\nabla)\mathbf{B} \tag{1}$$

As an example, for a constant moment **m** in the x-direction, leading to $\mathbf{m}\cdot\nabla = m_x((\partial)/(\partial x))$, a force will be exerted on the moment, provided there is a magnetic field gradient in the x-direction. Figure 1a is a schematic diagram of a ferromagnetic microparticle, which can either have a homogeneous magnetic core or be composed of an ensemble of primary magnetic nanoparticles that each have a dimension s that is in the nanometer range. The magnetization measurement of an ensemble of such microparticles results in a magnetization loop as shown in Figure 1b, which is characterized by a remnant magnetization M_{rem} close to the saturation magnetization M_{sat}. Such particles will be subjected to substantial forces when brought into a magnetic field gradient, but suffer from magnetic clustering and agglomeration effects due to the magnetic dipole interaction. Superparamagnetic nanoparticles, as schematically shown in Figure 1c, have zero magnetization in the absence of a magnetic field, as their magnetic anisotropy energy (proportional to their magnetic volume V) is typically smaller than the thermal energy. They therefore essentially behave as nonmagnetic particles in the absence of a magnetic field and are characterized by a magnetization curve as shown in Figure 1d. The slope at low fields is characterized by the magnetic susceptibility χ. The susceptibility of a particle is also called effective susceptibility and is related to the intrinsic susceptibility of the material χ_{mat} by $\chi = \chi_{mat}/(1 + N_d\chi_{mat})$, with N_d the demagnetization factor (1/3 for a spherical particle).[24]

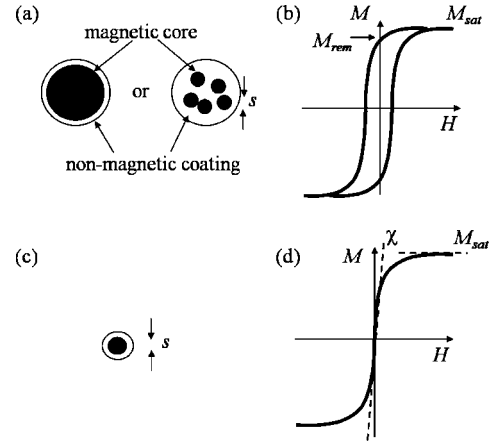

Figure 1. (a) Schematic of a ferromagnetic microparticle containing either a single magnetic core or a core composed of an ensemble of magnetic nanoparticles of size s. (b) Schematic magnetization curve of ferromagnetic particles with indication of the saturation magnetization M_{sat} and the remnant magnetization M_{rem}. (c) Schematic of a superparamagnetic nanoparticle having a single magnetic nanoparticle of size s as a core. (d) Schematic magnetization curve of superparamagnetic particles with indication of the magnetic susceptibility χ and the saturation magnetization M_{sat}.

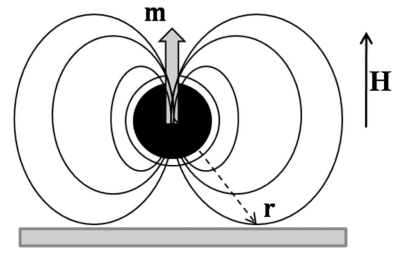

Figure 2. Schematic diagram of the dipole field of a magnetic particle. When a superparamagnetic particle is placed in a magnetic field **H**, the resulting moment **m** leads to a stray magnetic induction at each position vector **r** on the sensor surface, given by eq 3.

In case of superparamagnetic particles in a biological medium, one can describe the moment at small fields by the linear relation $\mathbf{m} = V\mu_0\mathbf{M} = V\mu_0\Delta\chi\mathbf{H}$, with **M** the magnetization of the particle and $\Delta\chi$ the difference in magnetic susceptibility between the magnetic particle and the surrounding liquid medium. Using the relation $\mathbf{B} = \mu_0\mathbf{H}$, eq 1 for a superparamagnetic particle in the linear susceptibility regime becomes

$$\mathbf{F}_m = \frac{V\Delta\chi}{\mu_0}(\mathbf{B}\cdot\nabla)\mathbf{B} \tag{2}$$

The magnetic moment of a superparamagnetic nanoparticle generally is smaller than that of a larger ferromagnetic microparticle. Hence, the magnetic force on a superparamagnetic particle will be smaller, which will result in slower magnetic separation processes. However, the advantage of superparamagnetic particles is the possibility to simply "switch off" the magnetic effects by removing the magnetic induction field.

Besides actuation of magnetic beads, the latter can also be used as labels for detection by a magnetic field sensor. The magnetic dipole stray field of a point-like magnetic bead is schematically shown in Figure 2 and is given by

$$\mathbf{B}(\mathbf{r}) = \frac{1}{4\pi}\left[-\frac{\mathbf{m}}{r^3} + \frac{3(\mathbf{m}\cdot\mathbf{r})\mathbf{r}}{r^5}\right] \tag{3}$$

Typically, the sensor output will be proportional to the total magnetic induction integrated over the sensor area. Another consequence of eq 3 is that, when a magnetic bead is in the magnetic induction field of other beads, the particles will interact via the magnetic dipole interaction, and chain-like or more complicated magnetic supraparticle structures (SPS) can be formed.

1.3. Scope of This Review

Pankhurst et al.,[25] Gijs,[26] and Pamme[27] reviewed the applications of magnetic beads, with focus on the underlying physics[25] and microfluidic aspects.[26,27] Here, we intend to present a comprehensive overview of recent research on the manipulation of magnetic beads in microfluidic systems and their utilization for biological analysis and chemical catalysis. We start with a discussion on the production of various types of magnetic beads and their chemical/biological functionalization. We then discuss the main forces that act on magnetic particles, that is, magnetic forces that provide the primary means of actuation, viscous drag forces in the liquid that oppose the magnetically induced bead motion, and electrostatic forces that can be responsible for agglomeration or sticking of the particles to microchannel walls. Thereafter we discuss the basic manipulation steps of magnetic particles: retention, separation, mixing, and transport. We also discuss the use of beads as magnetic detection labels, or contained as actuators/substrates in discrete droplets for digital microfluidics. We then focus on the applications of magnetic beads: the handling, detection, and separation of biological cells, on-chip nucleic acid assays, and immunoassays. Finally, the promising application area of magnetic micro- and nanoparticles for chemical catalysis is discussed. Throughout this Review, we try to compare the use of magnetic beads in microfluidic systems with alternative solutions and point out the advantages. We end this Review with an outlook section on possible future developments.

2. Magnetic Beads

Magnetic bead suspensions or magnetic fluids are stable dispersions of magnetic beads or encapsulated magnetic nanoparticles in an organic or aqueous carrier medium. Requirements of the bead matrix such as biocompatibility, biodegradability, and stability in different media must be combined with a preferable uniform size distribution and a correct shape. The magnetic material content determines the magnetic behavior of the beads and must be associated with suitable measures of protection against corrosion. For example, the primary magnetic nanoparticles (schematically shown as the black dots on the left of Figure 1a and in Figure 1c) can be coated with polymers or surfactants, with silica or carbon, or can be embedded in a chemically inert protective matrix. Moreover, for use in specific target applications, the bead surface needs to be functionalized (hydrophilicity versus hydrophobicity, chemical functionality at the surface, etc.) to allow covalent bonding or simple aspecific adsorption of biomolecules (proteins, antibodies, nucleic acids) or cells. Many types of magnetic beads are commercially available nowadays and are usually tailor-made for a specific final application. The synthesis, protection, and functionalization of magnetic nanoparticles were reviewed by Lu et al.[28] and Horák et al.[29] Also, the articles of Landfester and Ramírez,[30] Bergemann et al.,[31] Grüttner et al.,[32,33] and Latham et al.[34] present specific short review sections on the synthesis and chemical modifications of magnetic beads. Therefore, we only provide representative examples of bead synthesis, protection, and functionalization in this Review, rather than covering this vast field of literature in a comprehensive way.

2.1. Synthesis

Reviews of the synthesis of inorganic nanoparticles in the liquid phase (not limited to magnetic materials) were presented by Grieve et al.,[35] Trindade et al.,[36] Murray et al.,[37] and Lu et al.,[28] while a review of the synthesis of such particles from the vapor phase was presented by Swihart.[38] The synthesis and applications of (nonmagnetic) polymer micoparticles were reviewed by Kawaguchi.[15] The synthesis of magnetic beads is also a well-covered subject in patent literature. Magnetic nanoparticles have been synthesized with a number of different compositions that include iron oxides, such as magnetite (Fe_3O_4) and maghemite (γ-Fe_2O_3),[39,40] pure metals,[41,42] such as Fe and Co, or alloys,[43,44] such as $CoPt_3$ and FePt. Among the practiced magnetic nanoparticle synthesis methods, coprecipitation, thermal decomposition, microemulsion, and hydrothermal technologies are mentioned here. To date, magnetic nanoparticles prepared from coprecipitation and thermal decomposition are the most widely studied. Synthesis in microfluidic chips is an alternative technique for very controlled realization of magnetic particles.[45−47]

Coprecipitation

In early publications, magnetic bead solutions ("ferrofluids") were produced by grinding magnetite with long-chain hydrocarbons and a grinding agent.[48] Later, magnetic fluids were produced by precipitating an aqueous Fe^{3+}/Fe^{2+} solution with a base, coating these particles with an adsorbed layer of oleic acid, and then dispersing them in a nonaqueous fluid.[49] Both types of processes result in very small magnetic particles with a surfactant coating in a nonaqueous liquid carrier, in which the hydrophobic magnetite particles are dispersed. However, a lot of applications of magnetic beads rely on water as the continuous phase. A water-based magnetic fluid was realized by conversion of iron products to magnetic iron oxide in an aqueous medium under controlled pH conditions.[50] The experimental challenge in the synthesis of Fe_3O_4 by coprecipitation is in the control of the particle size and the achievement of a narrow particle size distribution. To produce monodisperse iron oxide magnetic nanoparticles in a coprecipitation reaction, a process with a short burst of nucleation followed by a slow controlled growth is necessary.

Thermal Decomposition

Monodisperse magnetic nanoparticles can be synthesized through the thermal decomposition of organometallic compounds in boiling organic solvents that contain stabilizing surfactants.[51] The ratios of the starting reagents, including the organometallic compounds, surfactant, and solvent, are, together with the reaction temperature and reaction time, the main parameters for controlling the nanoparticle synthesis. For example, nearly monodisperse iron oxide crystals with sizes adjustable over a wide size range (3−50 nm) have been prepared.[52,53] The reaction system was composed of iron fatty acid salts, fatty acids, hydrocarbon solvents, and activation

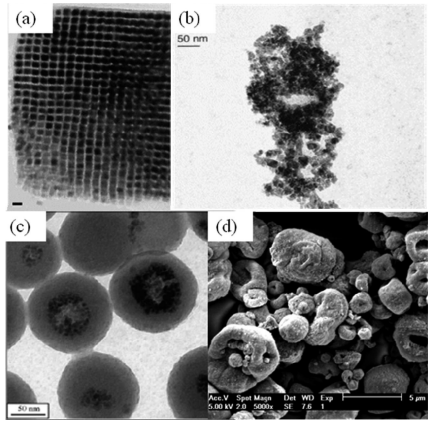

Figure 3. (a) Three-dimensional superlattice of iron nanocubes as deposited on a carbon-coated copper grid from a toluene dispersion. Bar: 10 nm. (b) TEM photograph of dextran nanoparticles; the dextran coating is not visible in the TEM picture, and the particles have an irregular shape. (c) More regular polystyrene particles with encapsulated magnetite nanoparticles. (d) SEM photograph of irregular magnetic glass particles [obtained from the MagNA Pure LC DNA isolation Kit from Roche Diagnostics (Rotkreuz, Switzerland)]. (a) Reprinted with permission from ref 54. Copyright 2004 American Association for the Advancement of Science. (b) Reprinted with permission from ref 33. Copyright 1999 Elsevier. (c) Reprinted with permission from ref 30. Copyright 2003 The Institute of Physics Publishing Ltd.

reagents. The thermal-decomposition method can also be used to prepare metallic nanoparticles. A metallic ferromagnet has a larger magnetization as compared to a magnetic oxide; therefore, the magnetic force (eq 1) on such particles will be larger. As an example, the reaction at 150 °C of the metal−organic precursor $Fe[N(SiMe_3)_2]_2$ with H_2 in the presence of a long-chain acid and a long-chain amine produces monodisperse cubic nanoparticles that have edges of 7 nm and are incorporated into extended superlattices[54] (see Figure 3a).

Microemulsion Techniques

A microemulsion is a stable dispersion of two immiscible liquids in which small-size droplets are stabilized by an interfacial film of surfactant molecules. In water-in-oil microemulsions, the aqueous phase forms droplets (1−50 nm diameter) in a continuous hydrocarbon phase. By mixing two identical water-in-oil emulsions containing the desired reactants, the droplets will collide, coalesce, and split and induce the formation of precipitates. Adding a solvent like ethanol to the microemulsion allows extraction of the precipitate by filtering or centrifuging the mixture. Also, the preparation of magnetizable polymer particles from aqueous dispersions is known. The particles can be prepared by dispersing magnetic elements in an organic phase containing an organosoluble initiator and/or monomer(s), mixing the dispersion with an aqueous solution made of water and emulsifier, homogenizing the mixture to give droplets of organic phase with (sub)micrometer size, and finally polymerizing the homogenized mixture after the addition of monomer(s), if necessary.[55] The distribution of the droplets (and hence of the polymer particles) is a function of the proportion of emulsifier present in the aqueous solution, and the ratio of the organic to the aqueous phase. The size distribution of the polymer particles obtained by this process is generally wide. By applying a purification process to the initial polydisperse crude emulsion, it is possible to obtain a set of highly monodisperse samples with high magnetic content (up to 70%).[56] The purification method is analogous in principle to a fractionated crystallization process.[33,56,57]

Hydrothermal Synthesis

Hydrothermal reactions with mixed oxides or hydroxides of iron and other metals can be carried out in water under supercritical conditions, that is, at temperatures around or higher than 200 °C under a pressure higher than 14 MPa. Under these conditions, water plays the role of a hydrolytic reactant. The size and morphology of the reaction products are controlled by the reaction time and temperature. However, hydrothermal reaction procedures are experimentally demanding.

Synthesis in Microfluidic Chips

Microfluidic devices provide an alternative for the controlled generation of monodisperse emulsion droplets by coflowing two immiscible fluids to induce droplet formation. The size of the monodiperse emulsion droplets can be controlled by tuning the relative flow rates of the two fluids. In these devices, spherical emulsion droplets are usually generated because the disperse phase seeks to minimize its interfacial free energy.[45,46] However, also nonspherical hydrogel microparticles with embedded magnetic nanoparticles have been synthesized using ultraviolet-initiated photopolymerization.[47]

2.2. Protection and Stabilization

Maintaining the stability of magnetic beads for a long time without agglomeration or precipitation problems is a prerequisite for applications. Especially pure metallic particles are subjected to oxidation or degradation, but also magnetite nanoparticles are not very stable under ambient conditions, and can be easily oxidized to maghemite or dissolved in an acid medium. Particle protection results in magnetic beads having a core−shell structure, where the role of the shell is to protect the magnetic core against environmental influence. Also, some particle compounds, in particular cobalt, are considered extremely toxic, and thus the leakage of this into the liquid medium must be avoided. Several coating strategies exist, ranging from coating the magnetic nanoparticles with organic shells containing surfactants and polymers, with inorganic compounds like silica, with carbon, to coating with precious metals. Besides simply coating individual magnetic nanoparticles, it is also possible to embed a number of magnetic nanoparticles or magnetic material in a polymer or silica matrix to form composites. This way, one can synthesize microbeads that, due to a higher magnetic content, are more easy and rapid to manipulate magnetically than the primary magnetic nanoparticles. Such types of beads (size around 1 μm) are therefore often used in microfluidic systems.

Surfactant and Polymer Coating

To stabilize magnetic nanoparticles after synthesis, electrostatic or steric repulsion can be used to keep the nanoparticles dispersed in a nonagglomerated colloidal state. For the so-called ferrofluids,[48] the stability results from a control of surface charges and the use of specific surfactants; both water- and oil-based ferrofluids are available. Surfactants or polymers can be chemically linked to or physically adsorbed

to the magnetic nanoparticles, creating repulsive forces (due to steric hindrance) that balance the attractive magnetic, electrostatic, and van der Waals force. Polymers containing functional groups, such as carboxylic acids, phosphates, and sulfates, can bind to the surface of iron oxide,[58] while surface-modified magnetic nanoparticles with certain biocompatible polymers are intensively studied for magnetic-field-directed drug targeting[59] and as contrast agents for magnetic resonance imaging.[60,61] For metallic magnetic nanoparticles, a thin polymer coating may not be sufficient to prevent oxidation of the highly reactive metal particles, while, more generally, such coating will also be less stable at higher temperatures.

Precious-Metal and Carbon Coating

Several precious-metal coating procedures have been proposed. Gold seems to be an ideal coating due to its low reactivity. Coating magnetic particles directly with gold is difficult due to the dissimilar nature of the two surfaces. However, gold-coated iron nanoparticles with 11 nm core size and 2.5 nm gold shell thickness have been prepared by a partial replacement reaction in a polar aprotic solvent.[62] Gold-coated iron nanoparticles were also prepared by a reverse microemulsion method.[63] Coating with gold is interesting, because the gold surface can be easily chemically functionalized with ligands via thiol groups.

Carbon-based coatings can be advantageous over polymers or silica, due to their higher chemical and thermal stability, as well as their biocompatibility. For example, a sonochemical coating procedure was developed that leads to air-stable cobalt nanoparticles.[64]

Silica Coating

Silica coatings are attractive due to their relatively good stability under aqueous conditions, their easy surface modification, and control of interparticle interactions via the variation of shell thickness. The Stöber process[65] and other sol−gel techniques[66,67] are the preferred methods for coating the magnetic nanoparticles with silica. The coating thickness can be varied by tuning the concentration of ammonium and the ratio of tetraethoxysilane (TEOS) to water. Silica-coated magnetic nanoparticles are hydrophilic and can be easily functionalized with several groups.[68] On pure metal nanoparticles, direct silica deposition is complicated because of the lack of hydroxyl groups on the metal surface. Another problem can be the oxidation of a metal like iron or cobalt in the presence of dissolved oxygen in the reaction medium. Although silica coatings are in general robust, silica is unstable under basic conditions and in addition may contain pores through which oxygen can diffuse.

Embedding Nanoparticles in a Protective Matrix

Matrix-dispersed magnetic nanoparticles can be created in different ways. The nanoparticles can be homogeneously dispersed in a continuous matrix, they can be dispersed as a coating on other larger particles, or they can form agglomerates that are connected through their protective shells. The preparation of magnetic polymer microbeads was reviewed in detail by Horák et al.[29] For example, polymer-coated magnetic beads can be produced by in situ precipitation of magnetic materials in the presence of a polymer. In this way, single or multiple magnetic core beads surrounded by a hydrophilic polymer shell have been made, choosing for the polymer the water-soluble dextran,[69] poly-(ethylene imine),[70] poly-(vinyl alcohol),[71] poly-(ethylene glycol),[72] etc. The well-known Dynabeads[73] are magnetic monodisperse microbeads developed in a multistep procedure. They contain iron oxides that are formed in situ by precipitation in preformed porous and monodisperse polymer microspheres, followed by a coating step.[74,75] Such types of polystyrene-coated magnetic particles are known for their excellent size distribution and spherical shape.[73,75] However, their hydrophobic surface results in a high amount of aspecific protein and antibody adsorption on the particle surface, so that it often needs to be modified chemically. Magnetic silica particles are very efficient in adsorbing proteins and DNA on their surface, but are hardly available with a small size distribution and an ideal spherical shape.[76,77] Magnetic polysaccharide particles are important for many in vivo applications. They combine biocompatibility with availability in a size range below 300 nm,[33,78] but the particles are irregular in shape, and the soft particle matrix causes them to be sensitive to mechanical stress. Magnetic poly-(lactic acid) particles also play an important role in the in vivo applications:[79,80] they are biodegradable, and their degradation time in the blood can be adjusted by their molecular weight and exact chemical composition. However, because of their hydrophobic surfaces, these particles stick to plastic surfaces found in microfluidic systems, resulting in problems with particle handling and analytical errors. In other work, nonspherical hydrogel microparticles with embedded magnetic nanoparticles have been synthesized in microfluidic chips using ultraviolet-initiated photopolymerisation.[47] As an example of matrix-dispersed magnetic nanoparticles, Figure 3b is a transmission electron microscopy (TEM) micrograph of dextran nanoparticles; note that the dextran is not visible in the TEM picture and that the particles have an irregular (nonspherical) shape. Figure 3c is a TEM photograph of more regular polystyrene particles with encapsulated magnetite nanoparticles. Figure 3d is a scanning electron microscopy (SEM) micrograph of irregular magnetic glass microparticles.

2.3. Functionalization

As was already indicated in the previous section, a protective shell around a magnetic nanoparticle or a protective matrix not only protects the particle against degradation, but can also be used to functionalize the bead surface with specific molecules, like those used in catalytic applications, or for use in experiments with proteins, cells, etc. Proteins may bind/adsorb to hydrophobic surfaces, such as those found in polymer-coated beads, forming a monolayer that is resistant to washing. It may also be desirable to have a strong covalent binding between the particle surface and the protein. This is achievable through specific groups at the particle surface ($-COOH-NH_2$, $-CONH_2$, $-OH$ groups), which via an activating reagent bind to $-NH_2$ or $-SH$ groups on the proteins.[81] Also, streptavidin, biotin, histidine, protein A, protein G, etc., can be grafted onto the bead surface for specific biorecognition reactions.[29] Small antibody-binding peptides have also been proposed for surface functionalization.[82] Silica-coated beads can be used as-prepared to recover and purify the total DNA content of a lysed cell solution. Sample DNA is for example bound to the silica surface after chemical cell lysis in a guanidine thiocyanate binding buffer. It binds preferentially to the silica surface of the magnetic beads due to the presence of chaotropic salts like guanidine or sodium iodine in the buffer solution.[83]

In many catalytic applications, transition metals are used as catalyst to transform or bond reagents. The good catalytic activity of these elements is due to their ability to have various oxidation states helping electron transfers or, in the case of metals, to adsorb other substances onto their surface and activate them in the process. When used with magnetic beads, different strategies are developed to link the metal atoms to the bead surface. The metal can be either complexed using ligands, chemically bonded to the surface, or directly immobilized on or incorporated into the magnetic bead surface using a supporting matrix (see section 8.2).

3. Forces on Magnetic Beads

3.1. Magnetic Force

The magnetic force (eq 1 or 2) is responsible for the unique possibilities offered by magnetic beads. Particularly interesting are small magnetic monodomain nanoparticles, because they do not express hysteretic magnetization curves and have zero remnance. Leslie-Pelecky and Rieke[84] have reviewed the relation between the morphology of nanostructured materials and their magnetic properties. Magnetic particles are single-domain, when they have a dimension that is typically of the order or smaller than the thickness of a magnetic domain wall $\delta = (JS^2\pi^2/Ka)^{1/2}$, with J the magnetic exchange constant, S the total spin quantum number of each atom, a the interatomic spacing, and K the magnetic anisotropy constant of the magnetic material.[19] For iron, assuming that $S = 1$, and taking $J = 2.16 \times 10^{-21}$ J, $a = 2.86 \times 10^{-10}$ m, and $K = 4.2 \times 10^4$ J/m^3, one calculates a domain wall width of 42 nm. The time over which the magnetization of a single-domain particle is stable and will remain in a certain state is of importance for probing the moment and magnetization. The relaxation time of the magnetic moment of a particle can be written as[25]

$$\tau = \tau_0 \exp\left(\frac{K_{\text{eff}}V}{k_{\text{B}}T}\right) \tag{4}$$

with $\tau_0 \approx 10^{-9}$s, K_{eff} the effective anisotropy constant of the particle, k_{B} the Boltzmann constant, and $k_{\text{B}}T$ the thermal energy. Equation 4 shows that monodomain magnetic particles become superparamagnetic, that is, their time-averaged magnetization without a magnetic field is zero, over a typically supposed experimental time scale $\tau = 100$ s, when their magnetic energy $K_{\text{eff}} \times (4/3)\pi r^3$ is lower than about 20 times the thermal energy $k_{\text{B}}T$, with r the particle radius of a supposed spherical particle.[84] When the particle magnetic moment does not reverse its magnetic moment over the experimental time scale, such a particle is in the "blocked" state. The temperature that separates the two regimes is the blocking temperature and very sensitively depends on the particle size. For example, at room temperature, one finds a maximum radius $r = 6$ nm for a superparamagnetic spherical particle of iron. In the superparamagnetic state, such a nanoparticle behaves similar to a paramagnetic spin but with a much larger moment. The induced magnetization of an ensemble of such particles is described by the Langevin function, which at low fields ($mH \ll k_{\text{B}}T$) behaves as $mH/k_{\text{B}}T$, and at high fields ($mH \gg k_{\text{B}}T$), as $(1 - (k_{\text{B}}T)/(mH))$, with m the size of the individual particle moment.[19]

An additional advantage of using small nanoparticles, besides the possibility to easily switch off the magnetic state and particle interactions by removing the external magnetic induction, is the minimum disturbance such a particle has on reactions, implying the biomolecules attached to the particle[85] and the large surface-to-volume ratio, which is of high interest for chemical binding. A disadvantage, however, of such a particle may be that the magnetic force is small due to the small volume, so that viscous forces dominate and magnetic separations can take a long time (tens of minutes).

This explains the interest of using larger magnetic particles (typically 0.2−5 μm in diameter) in microfluidic applications. These can either have a single magnetic core or have a core composed of multiple (non)interacting nanoparticles in a nonmagnetic matrix (see Figure 1a). Such microparticles often have a multidomain structure and are characterized by a hysteretic magnetization characteristic (see Figure 1b). For example, spherical particles with radius $r = 1.5$ μm, a saturation magnetization $\mu_0 M_{\text{sat}} = 0.2$ T, and a remnant magnetization $\mu_0 M_{\text{rem}} = 1$ mT will have the remnant magnetic moment size $m_{\text{rem}} = V\mu_0 M_{\text{rem}} = (4/3)\pi r^3 \mu_0 M_{\text{rem}} = 1.4 \times 10^{-20}$ T m^3. One notes here that the magnetic moment of a magnetic bead not only depends on its volume or size, but also on its magnetic load, that is, the kind and amount (up to 70%) of magnetic material that is present in the particle. Two of such particles will have the maximum magnetic attraction energy $|U_{\text{max}}| = (m_{\text{rem}}^2/2\pi\mu_0)(1/(2r)^3) = 9.2 \times 10^{-19}$ J, much larger than the thermal energy of $\sim 4 \times 10^{-21}$ J at room temperature, resulting in strong magnetic dipolar forces between the particles.[19] As a consequence, when exposed to an external magnetic induction, such magnetic microparticles coalesce under influence of the magnetic dipole interaction into a SPS consisting of chain-like "columnar" structures along the field direction. The exact shape of this SPS depends on parameters such as the particle concentration and applied magnetic field. Even after removal of the external magnetic induction, such particle structures can stay agglomerated, hindering separation and recovery of the magnetic beads.

While the magnetic character of a magnetic bead is essential for delivering the magnetic force, it is interesting to note that also diamagnetic objects brought in solutions of paramagnetic ions can be displaced on the basis of their repulsive force from a high magnetic field.[86,87] The magnetic force on a magnetic bead can be induced using a magnetic field generated either by permanent magnets or by coils. A permanent magnet typically is characterized by a magnetic induction $B_{\text{m}} = 0.5-1$ T and a field gradient $\nabla B \approx B_{\text{m}}/w$, with w the typical geometrical dimension of the permanent magnet.[88] For a cylindrical permanent magnet with a diameter $Ø = 5$ mm, one induces on a spherical particle with radius $r = 500$ nm and $\Delta\chi = 1$ a magnetic moment $m = 2.6 \times 10^{-19}$ T m^3, resulting in a magnetic force of about 40 pN. For a current-fed coil, the generated field is much smaller: a flat millimeter-size coil with 10 windings and a current of 0.5−1 A generates typically a magnetic induction of 1−10 mT, at least 100 times smaller than the permanent magnet. Consequently, the gradient is also a factor 100 lower, so that the force of eq 2 is a factor 10^4 larger, when using a permanent magnet rather than a coil. On the other hand, a coil offers more flexibility in switching the field on and off by simply controlling the current (and heat dissipation!), whereas a permanent magnet requires a mechanical action to move it away from the microfluidic system containing the magnetic beads.

3.2. Viscous Drag Force

In many applications, a magnetically labeled material is separated from a liquid solution by passing the fluid mixture through a region with a magnetic field gradient that can immobilize the tagged material via magnetic forces. For in vivo applications, magnetic particles can be transported by the blood flow and locally retained with the help of an external magnet. In other applications, there is a magnetic translational driving force, and the liquid solution is static. In the equilibrium state, the magnetic force $\mathbf{F}_m$ is opposed to the hydrodynamic drag force $\mathbf{F}_d$ acting on the magnetic particle. The hydrodynamic drag force is shown in Figure 4 and is a consequence of the velocity difference between the magnetic particle and the liquid $\Delta\mathbf{v}$ and, for a spherical particle with radius r, is given by[89]

$$\mathbf{F}_d = 6\pi\eta r\Delta\mathbf{v}f_D \tag{5}$$

where η is the viscosity of the medium surrounding the particle (for water, $\eta = 8.9 \times 10^{-4}$ N s/m^2). f_D is the drag coefficient of the particle and incorporates the influence of a solid wall in the vicinity of the moving particle and is calculated as[90,91]

$$f_D = \left[1 - \frac{9}{16}\left(\frac{r}{r+z}\right) + \frac{1}{8}\left(\frac{r}{r+z}\right)^3 - \frac{45}{256}\left(\frac{r}{r+z}\right)^4 - \frac{1}{16}\left(\frac{r}{r+z}\right)^5\right]^{-1} \tag{6}$$

Here, z is the distance of the particle to the solid wall; in the limit of small z, $f_D \approx 3$, so that the drag will be a factor 3 higher than when no solid wall is in the vicinity. In a microfluidic system, a particle may be moving at different z from the microchannel wall, under influence of the applied magnetic forces, so that the viscous force of eq 5 will vary along the particle trajectory.

Equalizing eqs 2 and 5 permits one to determine the maximum flow rate a particle can withstand when exposed to a magnetic immobilization force, or the maximum particle flow rate that can be generated by a magnetic force in a surrounding static liquid:

$$\Delta\mathbf{v} = \frac{2r^2\Delta\chi(\mathbf{B}\cdot\nabla)\mathbf{B}}{9\mu_0\eta f_D} \equiv \frac{1}{\mu_0 f_D}\xi(\mathbf{B}\cdot\nabla)\mathbf{B} \tag{7}$$

with

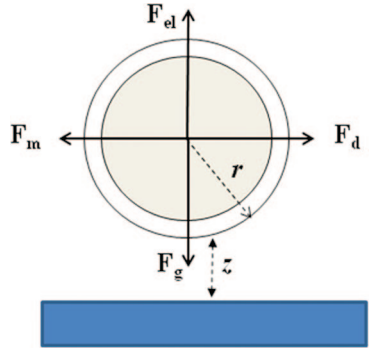

Figure 4. Simplified schematic diagram of the main directions of the most important forces acting on a magnetic particle with radius r and positioned at a distance z from a surface. The particle is in a fluid and is subjected to a magnetic force $\mathbf{F}_m$, a viscous drag force $\mathbf{F}_d$, a gravitational force $\mathbf{F}_g$, and an electrical force $\mathbf{F}_{el}$ originating from the surface.

$$\xi \equiv \frac{2r^2\Delta\chi}{9\eta} = \frac{V\Delta\chi}{6\pi r\eta} \tag{8}$$

the "magnetophoretic mobility" of the particle, a parameter describing how magnetically manipulable the particle is. The quantity $(\mathbf{B}\cdot\nabla)\mathbf{B}$ can be a strongly varying function in space, which implies a similar spatial variation for $\Delta\mathbf{v}$.

3.3. Electrical Interaction with the Microchannel Wall

Both electrostatic and electrodynamic (van der Waals) forces act on a particle in solution. The van der Waals force originates from attractive electromagnetic interactions between permanent electrical dipoles and/or induced dipoles. The van der Waals force between a particle and a substrate or the wall of a fluidic microchannel is expressed in the Hamaker approach as[91,92]

$$\mathbf{F}_{VdW} = -\frac{A_{123}r}{6z^2}\left[\frac{1}{1 + 14(z/\lambda_{ret})}\right]\mathbf{e}_z \tag{9}$$

with A_{123} the Hamaker constant of particle of material 1 on a substrate of material 2 in a medium of material 3, and $\mathbf{e}_z$ the unit vector in the vertical direction; λ_{ret} is a characteristic length scale of the interaction, often assumed to be 100 nm. For example, one finds for an acrylate-coated particle close to a SiO_2 substrate in water a value of $A_{123} = 3.4 \times 10^{-21}$ J.[91,93]

When immersed in an ion-containing aqueous solution, the substrate and particle acquire a surface charge through the adsorption of ions present in the solution and/or the presence of charged surface groups. This surface charge is neutralized by mobile ions of opposite charge also present in the solution, thus forming the well-known double layer. When the double layers of two surfaces overlap, an electrostatic interaction occurs, resulting in either a repulsive or an attractive force. This electrical force $\mathbf{F}_{el}$ is given, for a constant surface charge density on substrate and particle, by[94]

$$\mathbf{F}_{el} = \frac{2\pi\varepsilon\kappa r}{1 - \exp(-2\kappa z)}[2\zeta_s\zeta_p \exp(-\kappa z) + (\zeta_s^2 + \zeta_p^2)\exp(-2\kappa z)]\mathbf{e}_z \tag{10}$$

with ε the permittivity of the medium (7×10^{-10} F/m for water), and ζ_s and ζ_p the zeta-potential of the substrate and particle, respectively.[95] The electrical force is acting over a spatial range given by the Debye−Hückel double layer thickness κ^{-1}:

$$\kappa^{-1} = \sqrt{\frac{k_B T}{2000 N_A e^2 I_c}} \tag{11}$$

with N_A Avogardo's number, and I_c the ionic strength in mol/L of the solution. κ^{-1} is typically in the 10 nm range. Wirix-Speetjens et al.[91] showed how, by changing the pH and ionic strength of the solution, it is possible to obtain repulsive electrical force conditions between the particle and the substrate surface, considering combined van der Waals and electrostatic forces. This is important, if one wants to avoid the issue of unwanted particle sticking to the microfluidic channel. Higher pH values (6−10) and low ionic strength (1−10 mM) are shown to favor repulsive electrical

forces for the acrylate-coated particle/SiO_2 substrate system.[91] Alternatively, at the cost of more complex technology, it is possible to coat the microchannel wall with proteins or polymers to avoid sticking of beads or molecules.[96]

3.4. Other Forces

In addition to the magnetic, viscous, and electrical forces on magnetic beads, several other forces exist. As indicated in Figure 4, a gravitational force acts on a magnetic bead and is given by

$$\mathbf{F}_g = -m_b g \mathbf{e}_z \tag{12}$$

with g the gravitation constant, and $m_b = V(\rho - \rho_{fl})$ the "buoyant mass" that represents the effective mass of the magnetic bead by taking into account the average density of the bead ρ and the surrounding fluid ρ_{fl}. For example, 1.0 μm diameter MyOne Dynabeads[73] have a volume of 0.52 μm^3, 26% iron content, and a density of 1.8 g/cm^3, resulting in a gravitational force of 0.004 pN, which is much smaller than the typical magnetic force generated by a permanent magnet, but of the order of the force generated by a simple coil. When only gravitation is taken into account, these magnetic beads will sink to the bottom of the microchannel, hindered by a viscous force (eq 5) in the z-direction, resulting in a "sinking speed" of 0.5 μm/s. As the ratio of gravitational to viscous forces is proportional to r^2, smaller particles will sink much slower.

When the size of the magnetic bead is in the submicrometer range, stochastic Brownian forces become relatively more important, as the magnetic (and gravitational) forces, being proportional to r^3, are fastly decreasing. In a long-time dynamics, the friction coefficient $6\pi\eta r$ of eq 5 is related to the diffusion coefficient D of the particle by the well-known Stokes−Einstein relation:[97]

$$D = \frac{k_B T}{6\pi\eta r} \tag{13}$$

For example, a MyOne Dynabead has a diffusion coefficient in water of 4.8×10^{-13} m^2/s at room temperature, resulting in the time-dependent diffusion length $\sqrt{(Dt)}$; for example, after 1 s of diffusion, the particle will have moved an average distance of 0.7 μm. Taking a magnetic nanoparticle with radius of 100 nm instead, the diffusion coefficient becomes 2.4×10^{-12} m^2/s, resulting in a more than 2 times increased diffusion. Analysis by optical microscopy of the Brownian motion of magnetic nanoparticles in a magnetic field gradient was used to characterize the basic magnetic parameters of the particles.[98,99] A rotating magnetic field was used to apply a controlled torque on superparamagnetic beads, leading to a tunable bead rotation frequency in fluid, as observed via optical microscopy.[100] It is suggested that control of torque and measurement of the rotation will enable future torsion-based protein assays as well as nucleic acid assays on a single bead.

A combination of magnetic and dielectrophoretic forces to discriminate specific and nonspecific molecular bindings for on-chip magnetic bioassays was reported.[101] Conjugated to the analytes, magnetic particles are used as the agents for dielectrophoretic force generation. Because of a weaker binding strength, the nonspecifically bound particles are removed, while specific bindings remained intact. This technique can not only be used to improve the specificity of on-chip bioassays, but also be developed as a tool of force spectroscopy for the study of biomolecular binding physics.

Additional forces act on magnetic beads, such as hydrodynamic, magnetic, and electrostatic interaction forces originating from other beads,[102] especially when bead concentrations are high and the particles come close to each other. Magnetic interactions between beads lead to the formation of bead clusters or SPS, which have their own dynamics, as well as magnetic and viscous forces.[98,103,104] Finally, to describe the motion of a magnetic bead, one should solve Newton's law involving all forces present, which becomes extremely complex and leads to cumbersome numerical procedures. Therefore, a practical approach is to consider only the most important forces (for example, the magnetic and viscous forces for magnetic microparticles), when designing magnetic bead manipulation systems.

4. Magnetic Bead Manipulation

The spatial and temporal combination of the forces introduced in the previous section allows designing procedures or manipulation protocols, which are at the basis of the applications of magnetic beads in bioanalysis or catalysis. Figure 5 shows diagrams representing basic manipulations of magnetic beads in microfluidic systems. In separation (Figure 5a), magnetic beads are retained from a flow by focusing a magnetic field over the channel using, electromagnets, coils, or permanent magnets. Also, systems with miniaturized soft magnetic microstructures exist, which can be coupled to a macroscopic electromagnet or placed in the magnetic induction field of a macroscopic permanent magnet. Magnetic transport (Figure 5b) is more difficult, as it requires stronger and long-range magnetic forces to move the magnetic beads within the liquid, without the need of a microfluidic flow. The use of magnetic beads as labels for detection is shown in Figure 5c: here, a magnetic bead is bound to the surface of the microchannel, and a magnetic field sensor monitors its stray field, when the particle is placed in an external magnetic induction. A particularly interesting property of magnetic beads is that they can be magnetically suspended in a microfluidic channel using magnetic forces, without the requirement of having a supporting substrate. Such trapping of beads or SPS can be advantageous, if one wants to have a high exposure of the beads to a liquid flow. Also, when locally alternating

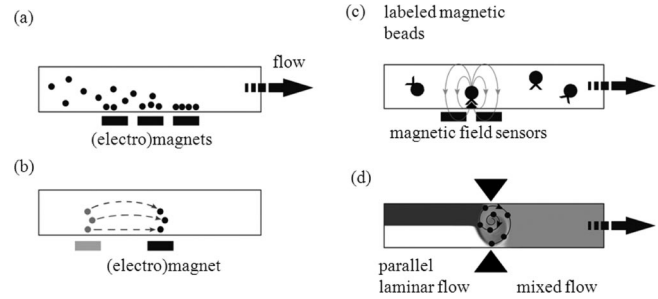

Figure 5. Schematics of basic manipulations of magnetic beads in a microfluidic channel. (a) Separation of magnetic beads from a flow by actuation of electromagnets or positioning of magnets. (b) Transport of magnetic beads using long-range magnetic forces provided by an electromagnet or magnet. (c) Detection of the stray field of a bead by a magnetic field sensor, after specific binding of the labeled bead on the sensor surface. (d) Mixing of two laminar streams by dynamic agitation of a supraparticle structure using a locally applied alternating magnetic field between two soft magnetic tips.

magnetic fields are applied, for example, via soft magnetic field focusing structures, a dynamic agitation of the magnetic beads is possible that can be used to mix the essentially laminar flow patterns within a microfluidic channel (Figure 5d).

4.1. Retention and Separation

4.1.1. Systems with Macroscopic Magnets

Separation of magnetic bead-labeled biomolecules or cells from a liquid solution is a well-documented and a widely practiced application today. Many types of magnetic particles have been developed for use in separation processes, including purification processes and immuno-assays.[105−109] Magnetic separator design can be as simple as the application and removal of a permanent magnet to the wall of a test tube to cause particle aggregation, followed by removal of the supernatant. However, it is preferable to increase the separator efficiency by producing regions with a high magnetic field gradient to capture the magnetic beads as they float or flow by in the carrier medium. Magnetic cell sorting (MACS) is a commonly used magnetic cell sorting technology,[78,110] in which cells bound to superparamagnetic particles are retained in a high-gradient magnetic field, generated by placing a porous magnetic column in the field of external magnets. After flowing the sample solution through the column, the latter is removed from the separator, and the retained particles can be analyzed using flow cytometry or microscopy. For such application, it is necessary to loosely pack a flow column with a stationary magnetizable matrix of thin wires or beads.[111,112] Such approach has the drawback that close monitoring of the separation process is difficult due to the nature of the filter geometry. Continuous flow separation in microfluidic devices was reviewed by Pamme (not restricted to magnetic beads).[113] Considering magnetic beads, separation in a microfluidic capillary without magnetic stationary phase has been demonstrated.[114] In this separation technique, also known under the name magnetic field-flow fractionation,[115] a magnetic force acts on the magnetic beads, forcing them toward the capillary wall. The magnetic retention force is opposed by diffusion back into the flow stream, so that a steady-state particle distribution and an ensemble of beads of specific height is formed at the capillary surface. Hydrodynamic forces act perpendicular to the applied field and laterally displace the magnetic plugs along the capillary wall. Less-magnetic species will be less closely packed, extend more to the center of the capillar, and will therefore experience larger hydrodynamic forces. Hence, less-magnetic species will move faster and "elute" first from the capillary.

Continuous flow magnetic particle and cell separation systems have been intensively studied by groups at The Ohio State University and The Cleveland Clinic Foundation.[116] These systems have a macroscopic dimension from the magnet point of view, but, from a liquid transport point of view, they may be called "microfluidic", as their functioning is based on the presence of laminar flow patterns. Figure 6a is a schematic diagram of a so-called quadrupole magnet configuration, where four magnets are arranged to induce a maximum magnetic field gradient toward the outer side of a liquid carrying tube, inserted in the free space between the magnets.[117] Williams et al. described how such a quadrupole magnet can be combined with an annular fluidic circuit.[118] The separation takes place within a laminar flow of the carrier fluid along a thin annular channel. A magnetic field gradient is imposed across the thin dimension of the channel, perpendicular to the direction of the flow. The sample mixture is arranged to enter the system close to one of the channel walls, and, as the sample is carried along the channel by the flow of the fluid, those components that interact more strongly with the field gradient are carried transverse across the channel thickness. A division of the flow at the channel outlet using a stream splitter completes the separation into two fractions. The radial particle separation velocity is induced by the field gradient and can be calculated using eq 7. The technique was given the name split-flow thin

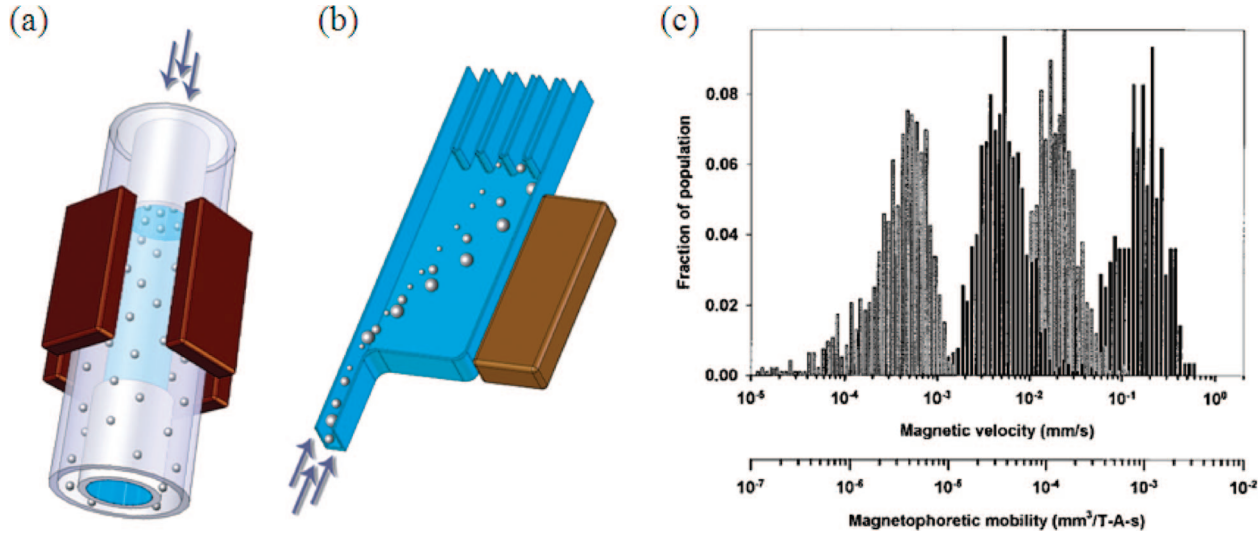

Figure 6. (a) Schematic diagram of a magnetic quadrupole separator. The magnetic force increases linearly in the radial direction. A magnetic particle suspension is injected from the top in the inner annular flow channel, while a buffer solution flows within the outer annular flow channel. As the magnetic particle suspension flows through the separator, the magnetic particles are deflected in the radial direction. If sufficiently deflected, the particles are caught in the lower outer annular flow channel. Undeflected or weakly deflected particles follow the inlet streamlines and are collected in the inner annular waste flow channel. (b) Schematic diagram of a magnetic dipole separator. A magnetic force directed to the right is created, and a magnetic particle suspension injected in the bottom port migrates to the right. Different types of magnetic particles will be deflected into different outlet ports. (c) Distribution of the magnetically induced velocity and magnetophoretic mobility of four different types of magnetic beads in a magnetic dipole separator. (c) Reprinted with permission from ref 124. Copyright 2001 Springer.

(SPLITT) fractionation, a derivative of field flow fractionation, as separation is obtained within a mobile phase without the use of a stationary phase.[119,120] This separation is essentially a binary one, in the sense that the input sample stream is split into a first exit stream of highly magnetic and a second stream of less or nonmagnetic particles. Besides annular liquid flow channels, SPLITT fractionation devices with rectangular geometry[121,122] and a magnetic field-flow fractionation device with helical microfluidic channel placed in a quadrupole magnetic field[123] have been proposed.

Permanent magnets arranged in a dipole configuration have been used for separation of magnetic beads as well. Figure 6b is a schematic diagram of a magnetic dipole separator. Magnetic beads migrate perpendicular to the direction of the flow at a rate proportional to their magnetic content. This permits separation of the injected sample into multiple outlet streams on the basis of the magnetic properties of each bead species. By combining a separator design with a constant magnetic energy gradient, an optical monitoring of the beads (or bead-labeled cells), and a theoretical model for interpretation, it is possible to trace back the linear bead trajectories to basic magnetic properties of the magnetic beads. This technique was coined "cell tracking velocimetry".[124−126] Figure 6c is a histogram of the distribution of four different types of magnetic beads with different magnetically induced velocities, as measured by cell tracking velocimetry, together with the derived magnetophoretic mobilities. In this case, the magnetic energy gradient of the dipole separator was designed to be $(1/\mu_0)(\mathbf{B}\cdot\nabla)\mathbf{B} = 198$ T A/mm^2 in the region of interest (see eq 7). In other work, the combination of magnetic dipole separation with microfluidics has been proposed,[127] experimentally demonstrated on-chip[128] and analytically modeled.[129] Other permanent magnet configurations have been proposed for separation as well.[130−133]

4.1.2. Systems with Microscopic Magnets: Magnetic Templates

While the separation systems discussed so far have a macroscopic dimension from the magnet point of view, an interesting option for generating a local and strong magnetic field gradient is to bring micropatterned soft magnetic material into the field generated by a larger permanent magnet (as done in a MACS column[134]). Because of the high magnetic permeability of the magnetic material, the magnetic flux from the permanent magnet is focused into the magnetic microstructure and will create strong gradients at certain magnetic interfaces, at which magnetic beads can be separated from a passing solution. Magnetic induction gradients of 0.1−1 T/mm have typically been realized in microfluidic channels using soft magnetic structures combined with permanent magnets.[135,136] In principle, using arrangements of bulk permanent magnets, 10 T/mm gradients are possible.[137] A first reported magnetic separation structure was based on electrodeposited nickel posts of 7 μm height and 15 μm diameter. Once magnetized by an external neodymium−iron−boron permanent magnet, these nickel post generated the strong magnetic field gradient that efficiently trapped 4.5 μm superparamagnetic beads suspended in water flowing past the posts.[138] This experiment was later confirmed by other authors.[139] Using a similar idea, magnetic separation was demonstrated by evaporating a thin layer of cobalt on a preformed microstructure realized via soft lithography or classical lithography.[140,141] In one case, liquid PDMS polymer mixed with magnetic particles was allowed to polymerize in the presence of a magnetic field, a process during which the magnetic particles can be trapped in the polymerized PDMS microchannel wall. Hereafter, these embedded magnetic beads act as "anchors" that can trap magnetic beads that are flowing in the microchannel. Also, the packing of Ni particles within a channel for the generation of high magnetic field gradients in a nearby microfluidic channel was reported.[142] Several papers exist on the analytical and numerical modeling of the magnetic trapping by a micropatterned magnetic structure.[140,143−146] A magnetic separator consisting of micropatterned permalloy elements adjacent to a microfluidic channel was presented by Smistrup et al.[147] When an external magnetic field is applied transverse to the channel, the elements are magnetized and generate magnetic field gradients within the channel, such that the magnetic beads are attracted to and captured at the channel side walls. Two types of magnetic beads could be selectively placed at either side of the channel, with negligible cross-talk, by use of hydrodynamic focusing. This system also enabled the simultaneous exposure of a DNA sample to two types of DNA probes.[148] A variant of this separation system was presented, in which a staggered herringbone microfluidic mixer was integrated in the microchannel.[149] This proved to increase the capture-and-release efficiency by up to a factor of 2. Simulations of bead trajectories, capture efficiencies, and capture distributions were also presented. Following a similar idea, a system with stainless steel wires placed close to a capillary in the magnetic field of permanent magnets showed magnetic flux focusing at the wire ends and was able to separate magnetic beads from a solution flowing through the capillary.[150]

An original idea for continuous magnetic separation (without accumulation of magnetic beads at certain positions in a microchannel) was presented by Berger et al.[136] It is based on the magnetic force generated by an array of magnetized stripes that are positioned at an angle with respect to a hydrodynamic flow direction. These stripes create a series of magnetic field gradients that trap the magnetic beads and alter their flow direction. Figure 7a is a schematic diagram of the microfluidic chip with indication of the oblique magnetic stripes or wires. The sum of the hydrodynamic force and the magnetic force acting on a magnetic bead creates a resultant force vector, which moves the

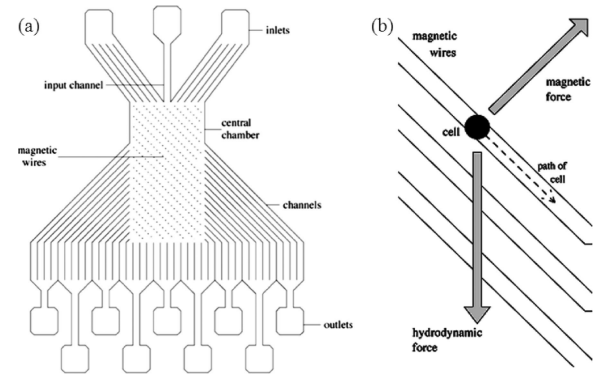

Figure 7. (a) Schematic diagram of the microfluidic chip with magnetic wires at an angle with respect to the hydrodynamic flow direction. (b) Because of the vector sum of hydrodynamic and magnetic force, a magnetic bead or magnetically labeled cell will move along the direction of the magnetic stripe, while nonmagnetic objects will move along the hydrodynamic force direction. Reprinted with permission from ref 136. Copyright 2001 Wiley−VCH, Weinheim.

magnetic bead or cell labeled with beads out of the main sample stream,[151] as illustrated in Figure 7b. A similar separation principle was later presented by others.[152−154]

4.1.3. Systems Using Microelectromagnets

An important difference between the use of a permanent magnet and an electromagnet is the much lower magnetic induction generated by the latter. A permanent magnet easily generates a magnetic induction of 0.5−1 T, while the magnetic induction of a simple planar coil is typically in the mT range. Following the discussion in section 3.1, one understands that a microelectromagnet will produce a much smaller magnetic force (in the fN range for a simple spiral coil and the chosen parameters for the magnetic beads), so that fluidic flow in the microchannels needs to be strongly limited or that magnetic beads need to pass at an extremely close distance to the planar coil. On the other hand, coils offer flexibility, as the magnetic field can be simply switched off by setting the coil current to zero. The group of C. H. Ahn has pioneered the use of microelectromagnets for the separation of magnetic beads.[155−157]

Figure 8a presents a schematic diagram of a microelectromagnet consisting of a planar coil and a soft magnetic yoke structure. Copper spiral coils were electroplated into photoresist molds on a Si substrate, and, when actuated by currents in the order of 0.3 A, could effectively retain and separate micrometer-size superparamagnetic beads from a flow. The integrated fluidic microchannel was realized by anodically bonding a microstructured Pyrex wafer to the Si substrate. For enhancing the generated magnetic field (by about a factor of 2 with respect to a simple coil, as half of the space with $\mu_r = 1$ around the coil is replaced by a soft magnetic material with high magnetic permeability), the spiral coil is combined with an electroplated permalloy magnetic yoke microstructure (Figure 8b), leading to effective magnetic bead separation from a flow (Figure 8c). Such soft magnetic microstructures have also been used in combination with micropatterned current-carrying wires for magnetic field enhancement.[158] However, the spiral design results in stronger magnetic fields and forces as compared to other current-carrying geometries.[159] Similar work exists on the separation of magnetic beads by microelectromagnets made of copper spiral coils and various wire microstructures in combination with nickel soft magnetic yokes.[160−163] Magnetic bead capture by current-carrying wires also has been studied theoretically, and optimum separation conditions, as influenced by parameters like microchannel dimension, magnetic field magnitude, and flow speed, were determined.[164,165] Besides separation via electromagnets realized directly underneath a microfluidic channel, also "external" microelectromagnets or magnetic tweezers have been proposed to trap magnetic beads in a liquid solution. The tweezers were made by winding 25 μm thick copper wire around a 50 μm diameter soft magnetic needle and can be scanned to effectively displace the magnetic beads in a fluidic reservoir.[166]

Coils offer flexibility, but only relatively small magnetic forces can be generated. Combining a coil with a soft magnetic yoke structure can, at maximum, increase the force by a factor of 2 with respect to the simple coil. Also, ohmic heating of a coil can pose problems and require active cooling of the microfluidic system.[167] An interesting option to generate larger forces is to combine a current-carrying coil or wire for local magnetic field gradient generation with a uniform external magnetic field for imposing a large magnetic moment to the superparamagnetic beads (see eq 1).[168−170] Such setup allowed for the application of relatively strong pN forces (100× enhancement) for magnetic beads in the micrometer range and on a spatial scale corresponding to the microfluidic channel width.

4.2. Magnetic Transport

Magnetic separation is different from magnetic transport in the sense that, in separation, the beads are retained (separated) by action of a magnetic field, but transported using a liquid flow. In magnetic transport, magnetic forces effectively transport the particle, which is a bigger challenge: it requires magnetic fields and magnetic forces that act on a longer range than necessary for separation, where magnetic

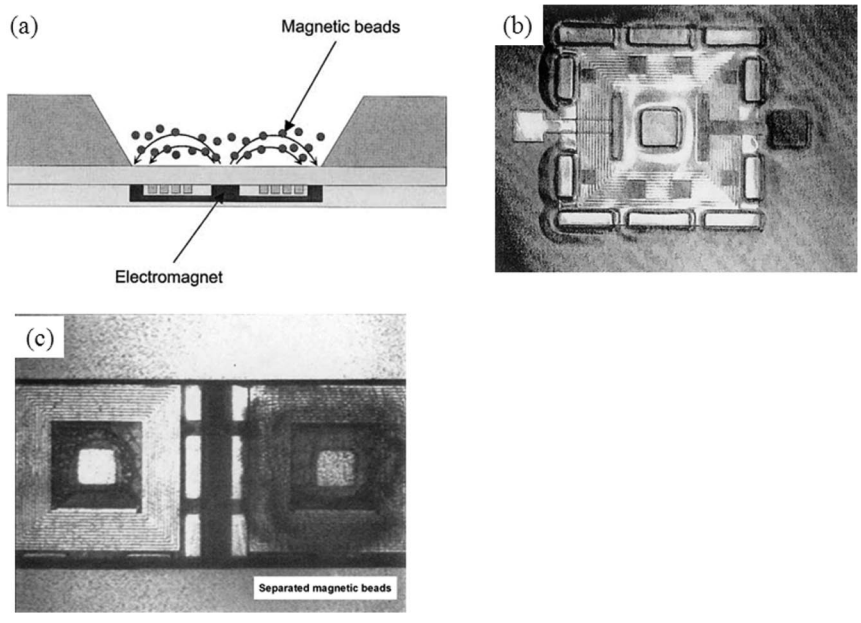

Figure 8. (a) Schematic diagram of a microelectromagnet used for separation of magnetic beads. (b) Micrograph of the fabricated electromagnet (coil width = 50 μm). (c) Separation of 1 μm diameter magnetic beads out of a flow by actuating the second coil with a current of 0.3 A. Reprinted with permission from ref 156. Copyright 2001 Elsevier.

beads approach very closely the magnetic actuation region by the fluid motion. Transport is a difficult task, as the magnetic susceptibility $\Delta\chi$ of the magnetic beads is rather weak (typically ≤ 1), due to small magnetic core volumes and demagnetization effects of the particles (see eq 2). This explains why mostly the large field of permanent magnets has been used for the separation and positioning of magnetic beads.[78]

In an approach toward miniaturization and automation of analytical applications, a system has been proposed in which liquid movement is substituted by magnetically induced movement of magnetic particles.[171] Fluidic channels were realized on a plastic cartridge of centimeter size, and magnetic transport was induced by mechanically moving external permanent magnets. In another approach, magnetic particles have been transported over millimeter distances in a microfluidic channel using an array of electromagnets actuated in a four-phase scheme.[172] Each electromagnet consisted of a 0.3 mm diameter magnetic needle core with a wire-wound coil of 300 turns. For coil currents of the order of 0.5 A, forces of 0.1 pN were possible. Also, alginate microdroplets with encapsulated magnetic particles have been transported using this method.[173]

Besides these still "macroscopic" fluidic transport systems, also miniaturized solutions have been proposed for bead transport, thereby taking advantage of batch microfabrication technologies. Typically, the size of the (micropatterned) magnets determines the spatial range, where appreciable magnetic forces act on the microbeads. Serpentine gold wires micropatterned on silicon substrates have been combined with microfluidic structures realized in PDMS to transport 4.5 μm polystyrene-coated magnetic beads.[170] By engineering the magnetic field generated by different current-carrying wires, a microsystem was realized that could generate local magnetic field maxima able to trap the magnetic beads (see Figure 9). When the field maxima change location, the beads followed those maxima. The device allowed precise positioning and transport over a distance of 100 μm in a single actuation event, which is partly due to the presence of a permanent magnet placed in proximity of the microfluidic chip. The main role of this magnet was to enhance the magnetic force by inducing a magnetic moment in the magnetic beads. A microelectromagnet wire matrix, based on two layers of mutually orthogonal arrays of linear wires, has demonstrated magnetic transport of $1-2$ μm size magnetic particles over 20 μm distances in a single actuation event.[174] This is a typical working range for the magnetic force, generated by a current-carrying conductor, when no external permanent magnet is used to induce a magnetic moment in the beads. A transporting device consisting of a set of two tapered conductors shifted linearly over half a period was demonstrated by Wirix-Speetjens et al.[91,175] This device was fabricated using standard semiconductor technology and photolithography techniques. Current conductors (TiW 10 nm/Au 150 nm/TiW 10 nm) were evaporated and patterned using a lift-off process on an oxidized Si wafer. A 250 nm thick SiO_2 layer was then sputtered onto the wafer for passivation. By sending a dc current through one of the current conductors, a magnetic field is generated that magnetizes the particles. Once the particles are magnetized, they moved toward the edge of the conductor, where the field is highest. Subsequently, they were attracted to the nearest narrow cross section, driven by the field gradient that is created by tapering the conductor. This way, one-dimensional stepwise transport was realized by applying low frequency nonoverlapping clock pulses to both conductors alternatively. The average speed of a magnetic particle was defined as the distance over which the particle is transported parallel to the conductor edge divided by the minimal time needed to reach the next minimal cross-section and is of the order of several 10 μm/s. In another approach, a planar coil array-based magnetic transport system has been proposed, in which an individual coil is capable of displacing beads over millimeter distances in a liquid-containing capillary.[176] A drastic increase of the magnetic energy and magnetic forces acting on the beads was obtained by placing the complete coil array in a uniform static magnetic field that imposes a permanent magnetic moment onto the beads. The very small magnetic field (gradient) of a simple planar coil proved then to be sufficient to displace 1 μm diameter beads over a distance of the order of the coil size. The coils were realized using simple Printed Circuit Board (PCB) technology (100 μm Cu winding width, 35 μm winding height, 200 μm winding pitch) and had a small number of windings ($N = 4-10$). Arranging adjacent coils with spatial overlap over two layers of the PCB circuit and actuating them in a specific three-phase scheme assured the long-range displacement of the beads. Moreover, it was found that these polarized beads formed cylindrical columns with a length of the order of the microfluidic channel size, due to magnetic dipole interactions. This column formation helped to generate the strong magnetic force. On a smaller length scale, arrays of $50-100$ μm-size microcoils were made on silicon substrates by electroplating soft magnetic NiCoP pillars at the center of electroplated Cu coils.[163,177] These microelectromagnets generated sufficient magnetic force to transport 1 μm diameter beads from coil to coil.

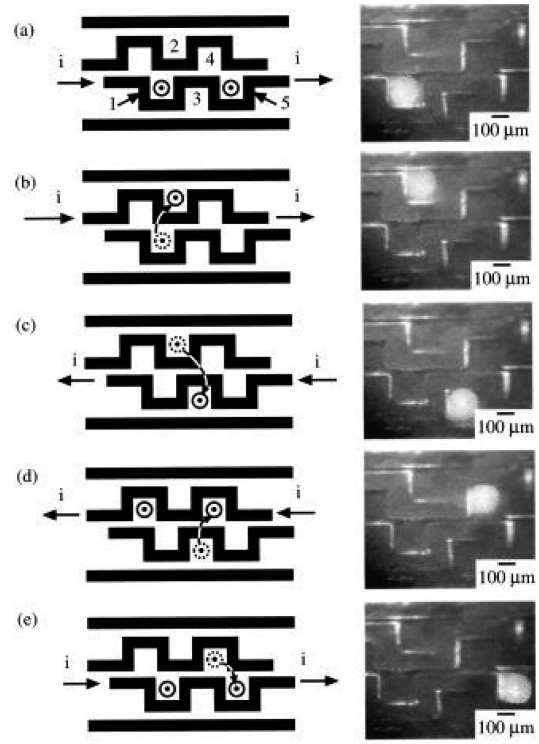

Figure 9. Sequence of schematics and corresponding microscopic images, showing the stepwise transport of magnetic field maxima and magnetic beads, by arranging the relative positions and currents *i* of two serpentine wires. Reprinted with permission from ref 170. Copyright 2001 American Institute of Physics.

Also, a transport system was proposed, which employed a translating periodic potential energy landscape to move magnetic beads horizontally over a substrate. The potential energy landscape was created by superimposing an external rotating magnetic field on top of the local magnetic field distribution of a periodic arrangement of Co micromagnets. At low driving frequencies of the external field rotation (a few Hz), the magnetic beads become locked into the potential energy landscape and move at the same velocity as the traveling magnetic field wave. Therefore, this technique was coined traveling wave magnetophoresis.[178] Also, complex patterns of soft magnetic microstructures placed in a rotating magnetic field were able to trap, transport, and release magnetic particles. The translatable local magnetic field maxima were created here by variations in local radii of curvature at structural edges of the microstructures.[179]

4.3. Magnetic Beads as Labels for Detection

A common approach to detecting biological molecules is to attach a label that produces an externally observable signal. The label may be a radio-isotope, enzyme, fluorescent molecule, or charged molecule, but also magnetic beads can be used as labels for biosensing. Magnetic labeling, detection, and the combination of a sensor chip with microfluidic system integration aspects were reviewed by several authors.[180−182] Magnetic labels have several advantages over other labels. The magnetic properties of the beads are stable over time, especially because the magnetism is not affected by reagent chemistry or subject to photobleaching (a problem with fluorescent labeling). There is also no significant magnetic background present in a biological sample, and magnetic fields are not screened by aqueous reagents or biomaterials. In addition, magnetism can be used to remotely manipulate the magnetic particles. Finally, a number of very sensitive magnetic field detection devices have been developed during recent years, like giant magnetoresistance (GMR)[183] and spin-valve[184,185] magnetic sensors that enable the measurement of extremely weak magnetic fields, such as the magnetic stray field generated by the magnetization of a single magnetic bead. A basic GMR or spin-valve device consists of a pair of magnetic films separated by a nonmagnetic conducting layer.[186] When an external magnetic field rotates the magnetizations of the magnetic layers toward alignment, spin-dependent electron scattering is reduced at the interfaces within the device, thus decreasing its electrical resistance. GMR sensors can be microscopic in size and sensitive to the presence of micrometer and smaller size magnetic particles, when in close proximity; even single micrometer-size particles immobilized down to a few hundred nanometer above the sensor could be detected.[182] Also, magnetic particles passing by in a flow, rather than being immobilized above the sensor area, have been detected.[187] Besides GMR sensors, measurements of single magnetic beads have been demonstrated using miniaturized Hall sensors[188,189] and planar Hall effect sensors based on permalloy thin films.[190] A possible inconvenience of the magnetic sensor-based detection systems for commercial applications, however, is that the cost of such a system can be an issue, due to sensor fabrication (often on a silicon substrate) and integration of the sensor in a microfluidic package.

A research group at the Naval Research Laboratory, Washington, DC,[191−194] followed by others,[195,196] has developed a microsystem for the capture and detection of micrometer-sized, paramagnetic beads on a chip containing an array of GMR sensors, the so-called bead array counter (BARC). Bound beads are detected by the GMR sensors by applying a uniform magnetic field perpendicular to the substrate, and therefore imposing a magnetic moment to the superparamagnetic beads. These induced moments generate an in-plane magnetic field component that is measured by the GMR sensor. Applying the uniform field normal to the plane of the GMR sensor rather than in-plane has the advantage that, due to demagnetization effects, a much larger magnetizing field can be applied to the beads without saturating the sensor.[197] Figure 10 shows optical micrographs that represent a sensor chip with 64 individually addressable GMR sensors and two reference sensors. Each sensor is a serpentine resistor trace that is 1.6 μm wide and with a 4.0 μm pitch (see Figure 10c), with a total length of 8 mm within a 200 μm diameter circular zone. The zone was matched to an arraying system for probe deposition (250 μm spots) to selectively capture beads from a flow. The sensor chips are covered with a silicon nitride passivation layer of about 1 μm thick to protect the circuitry from the corrosive and conductive media and biochemical reagents. This nitride layer was etched down to a final thickness of 250 nm over each sensor zone leading to a larger signal due to the smaller immobilized bead-sensor distance. Using Dynal M-280 2.8 μm diameter beads, the threshold for detection was approximately 10 beads per 200 μm diameter sensing area. The GMR sensor sensitivity increases with decreasing surface area of the sensor; however, the chemical sensitivity, or number of analyte molecules that can bind to the surface, increases with increasing surface area. Theoretical modeling showed that a GMR sensor can detect a single superparamagnetic bead of any size,[197−199] as long as all system dimensions (bead size, sensor size, distance between bead and sensor) scale down proportionally. When the sensor size approaches the size of the bead, it should be possible to detect beads with a radius down to 100 nm or smaller.

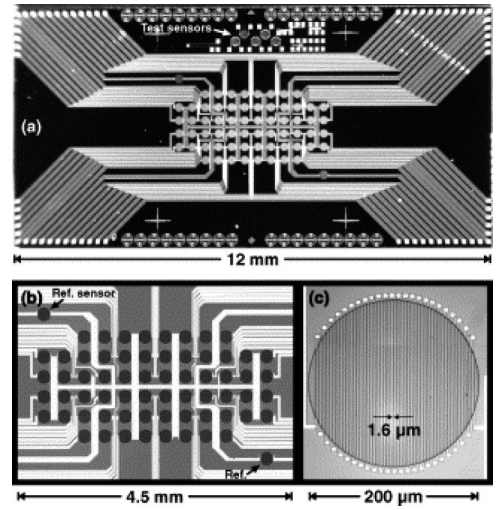

Figure 10. Optical micrographs of a third-generation bead array counter (BARC) sensor chip. (a) Photograph of the 68 pin−out chip, including a central sensing area with 64 sensors and two reference sensors, and a number of test structures. (b) Closer view of the central sensing area. (c) Close-up of one serpentine GMR sensor trace encompassing a 200 μm diameter sensing zone. Reprinted with permission from ref 193. Copyright 2000 Elsevier.

A group at Philips Research has proposed a compact biosensor platform with GMR sensors suited for the detection

of superparamagnetic nanoparticle labels.[200,201] The platform consists of a disposable microfluidic cartridge, a GMR chip, and an electronic reader. Wires integrated in the silicon of the sensor chip are used to generate a well-defined magnetic field on the sensor surface, thus removing the need for mechanical alignment with an external apparatus. To optimize the signal-to-noise ratio, the magnetic labels are excited at high frequency (1 MHz). These wires also apply forces onto the beads to attract the latter toward the sensor surface. A signal modulation scheme is applied to obtain optimal detection accuracy. Experimental results indicated that three beads of 300 nm can be detected on a sensor surface of 1500 μm^2 for a measurement time of 1 s. In an effort of cost optimization, the GMR sensors were deposited on a passive silicon substrate, with the electronic circuitry placed on an external chip.[202] Despite this, the use of comparatively expensive silicon as substrate and the microfluidic packaging of the chip[203] might raise cost issues for a (single-use) diagnostic test, unless this particular approach would prove to outperform others, by, for example, a much higher sensitivity.

A lot of bead-sensing experiments today have been done with micrometer-size beads composed of magnetic γ-Fe_2O_3 and Fe_3O_4 nanoparticles dispersed in a polystyrene matrix. To maximize the sensor response, the magnetic beads should have a magnetization as high as possible and yet remain nonremnant to avoid clustering when suspended in solution. With the goal of achieving larger signals from the magnetic labels, one has developed soft ferromagnetic beads with 100% magnetic content and much higher saturation magnetization.[192] One micrometer diameter NiFe beads showed a susceptibility of ~3, the maximum obtainable value for a uniformly magnetized sphere. Because of this property, smaller solid ferromagnetic beads could effectively be used as biomagnetic labels, which would also increase the dynamic range of biosensor assays by allowing more labels per unit area.

4.4. Enhancing the Bead−Flow Interaction and Mixing

Most of the magnetic bead-related phenomena discussed so far were based on the interaction of individual beads with the magnetic field. An interesting property of magnetic beads is that they can form linear-like chain structures or more complex SPS, when placed in a magnetic field due to the magnetic dipole interaction between beads. When the magnetic induction can be very locally applied, it is possible to have a small-size magnetic SPS or bead "plug" spanning the cross-section of a microchannel, which will be characterized by a strong perfusion by a liquid flow. This is of importance for both biomolecule capture and catalysis applications. Hayes et al.[204] used a varying magnetic field generated by a mechanically moved permanent magnet to create a relatively large magnetic SPS plug composed of 1−2 μm diameter superparamagnetic beads (see Figure 11a). The plug could be rotated through all axes in a microfluidic channel, without loss of structural form, allowing dynamic micrometer-scale movement without direct mechanical, electrical, or photonic interactions.[204] A number of potential applications of this phenomenon were described, such as binding biomolecules on the magnetic particles for immunoassays,[207] studying subcellular biomechanics, and microfluidic mixing in pico- and femtoliter volumes.

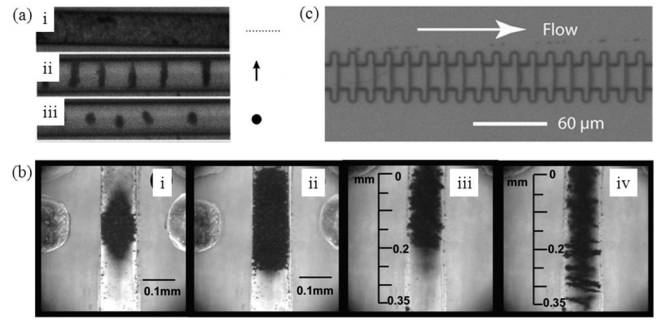

Figure 11. (a) Superparamagnetic particles in a cylindrical microchannel (20 μm diameter), as observed by optical microscopy: (i) High-volume fraction 1−2 μm diameter particles without applied external magnetic field. (ii) Induced column-like structures that form immediately upon application of an external magnetic field in the plane of the page. (iii) Upon rotation of the applied magnetic field perpendicular to the page, the top of the column-like structures is visible. (b) Video microscopy images of (i) a dense SPS kept over the microchannel cross-section in an alternating magnetic field by two soft magnetic tips, at a field oscillation frequency $f = 5$ Hz, a liquid flow velocity $v_0 = 0$ cm/s, and a magnetic field amplitude $B_0 = 100$ mT, (ii) the expanded SPS of (i) for $f = 5$ Hz, $v_0 = 0$ cm/s, and $B_0 = 5$ mT, (iii) a snapshot image of the oscillating SPS at the most downstream position in the channel for $f = 5$ Hz, $v_0 = 0.4$ cm/s, and $B_0 = 25$ mT, and (iv) a snapshot image of the oscillating SPS at the most downstream position in the channel for $f = 5$ Hz, $v_0 = 0.4$ cm/s, and $B_0 = 20$ mT. (c) Optical image of a microchannel showing the retention of 18 self-assembled nanoparticle magnetic chains that are perfectly positioned in the geometrical traps of the microchannel, while applying a flow from the left to the right. (a) Reprinted with permission from ref 204. Copyright 2001 American Chemical Society. (b) Reprinted with permission from ref 205. Copyright 2004 American Institute of Physics. (c) Reprinted with permission from ref 206. Copyright 2008 American Chemical Society.

The shape of a SPS depends on different parameters, like the size of the magnetic moment of the beads and the magnetic dipolar interaction between different beads. These properties are linked to the amplitude and frequency of the applied magnetic field, the shape and magnetic content of the beads, the concentration of the magnetic particles in the fluid, the temperature, etc. Despite the complexity of the aggregation process of a magnetic fluid into a SPS, the physical effects of a magnetic field on such a structure are now very well understood.[208,209] When exposed to a strong, continuous magnetic field, the magnetic fluid will rapidly form a cross-linked network. The continuous-field structure is determined by the kinetics of bead aggregation, and the particles are prohibited from rearranging to minimize energy, as long as the field persists. In contrast, it was found that the application of a pulsed field (square wave alternating between field-on and field-off states) to a magnetic fluid did produce an energetically determined suspension structure.[210,211] By allowing particle diffusion during the field-off state, a pulsed field enables minimization of energy through structural rearrangements, and the SPS consists of one-dimensional periodic patterns composed of high-concentration regions of magnetic particles ("columns"), aligned in the field direction and sharply separated from low-concentration regions.[208,212,213] Qualitatively, the dependence of the structure complexity on the tuning parameters can be understood from the time it takes for the particles to aggregate, which depends on the ratio of the magnetic interaction energy between particles relative to thermal energy. Applying a biaxial rotating magnetic field, produced by two orthogonal pairs of Helmholtz coils in quadrature, induces a rotation of dipolar

chains of superparamagnetic particles and subjects the aggregates to magnetic forces causing them to rotate within the suspending fluid. It has been shown, with both scatterning dichroism[214] and video-microscopy experiments,[215] that magnetic fluids have the capacity of reducing the size of the structures they are composed of, to decrease their viscous drag while rotating synchronously with the field.

For an application where low-concentration biomolecules need to be recovered from a flow by the SPS, it is useful to have only a small amount of magnetic beads in the bead plug, as this will improve the purification or concentration of bound biomolecules per bead. The highest possible number of biomolecules should bind to the lowest possible number of beads, to result in the highest biomolecule concentration per bead. Rida and Gijs[205] applied micromachined soft magnetic tips to focus the magnetic induction generated by an electromagnet very locally over a microchannel. An oscillating and localized magnetic field was applied to study the magnetohydrodynamic transport of a small magnetic SPS consisting of ferromagnetic beads (see Figure 11b). The particles formed open columnar structures that had a strong exposure to the fluid flow. The dynamics of the SPS were analyzed as a function of the flow rate and the frequency and amplitude of the magnetic field. The experimental data were well described by a magnetohydrodynamic model, where the columns in the SPS were represented by cylinders. This type of magnetic particle-driven mixing was also modeled numerically.[216]

Ferromagnetic beads, which form stable rotating chains in an alternating magnetic field, easily form bead clusters and agglomerates after field removal. However, in many bioanalytical applications, individual beads should be released from the plug after analyte capture for further processing. Unfortunately, the dynamic manipulation technique described in the previous paragraph cannot be readily applied to superparamagnetic or low-coercivity beads, as the latter change their magnetic state by Néel relaxation. Rotation of chains of superparamagnetic beads was achieved using macroscopic rotating magnetic fields,[217−219] but such approaches are based on complex systems, making microfluidic integration difficult. Moreover, such a system is not directly suitable for bead retention in a microchannel, as the magnetic field gradients are weak. However, dynamic actuation of superparamagnetic beads in a microchannel could be demonstrated using a quadrupolar magnetic actuation system,[21] where cyclic bead motion was achieved in a confined microchannel volume by superposing a magnetic time-varying field, as induced by two soft magnetic tips connected to an electromagnet, and a static field induced by two permanent magnets.

In other work,[206,220] retention of magnetic beads in a microfluidic channel was achieved, not by focusing the field at a specific location across the channel, but by periodically varying the width of the channel. When brought into a homogeneous magnetic field applied perpendicular to the channel axis, a solution of magnetic beads flowing through the microchannel spontaneously self-assembles in periodic magnetic chains located at the larger cross sections of the microchannel (see Figure 11c). This configuration benefits from the lowest total magnetostatic energy, as originating from magnetic dipole interactions between the individual magnetic beads. These geometrically trapped nanoparticle chains are at the basis of a good fluid perfusion through the magnetic chain structure and a high biomolecule capture efficiency. To enhance the interaction of magnetic beads with molecules present in a flow, magnetic beads were also chemically fixed to a glass surface, either using poly(ethylene glycol) (PEG) hydrogels[221] or by electrostatic assembly on micropatterned silane structures.[222,223]

The dynamic manipulation of magnetic bead aggregates was also investigated for mixing applications. Active fluid mixing was demonstrated in microchannels made in a micromachined microfluidic chip of polymethylmetacrylate (PMMA). Mixing was based on the manipulation by a local alternating magnetic field of self-assembled porous structures of ferromagnetic microbeads that are placed over the section of the channel.[205,224] Using a sinusoidally varying magnetic field ($1\ \text{Hz} < f < 100\ \text{Hz}$), a rotational motion of the SPS was induced, thereby strongly enhancing the fluid perfusion through the SPS that behaved as a dynamic random porous medium. The mixing is the result of the chaotic splitting of fluid streams through the dynamic and randomly porous structure of the SPS and the relative motion of magnetic entities with respect to the fluid flow. It was quantified by monitoring the fluorescent intensity of initially parallel fluorescent and nonfluorescent laminar streams. A 95% mixing efficiency over a channel length as small as the channel width (200 μm) and at flow rates of 0.5 cm/s was obtained. This demonstrates the large lateral mass transfer induced by the SPS as a consequence of the highly heterogeneous and dynamic nature of the SPS. On a smaller length scale, a mixing system consisting of a microfluidic channel integrated with a number of soft magnetic elements at the sides of the channel was demonstrated.[225,226] The elements were magnetized by placing the chip in a homogeneous external alternating magnetic field. This way, dynamic plugs of magnetic beads that spanned the microchannel were created, and 85% mixing efficiency was obtained. Similar mixing efficiencies were reported by other authors using a similar approach.[227] Another type of magnetic force-driven mixer has been fabricated.[228] This mixing device was based on a silicon chip with embedded microconductors as a magnetic field source, and a microchannel guiding the fluid streams. By applying a time-dependent control signal to a row of microconductors, it was found that a two-dimensional serpentine channel geometry with transverse electrodes was able to create the stretching and folding of material lines, resulting in good mixing. In other work, magnetic beads were chemically linked to create permanent chains that subsequently were magnetically actuated by a rotating magnetic field to mix two laminar streams in a microfluidic channel.[217] The mixing via the use of magnetic beads has also been described in detail using numerical simulations.[228−230]

Another technique to realize magnetic bead chains is the magnetic assembly of microbead chains onto a surface.[141,231] It was shown that superparamagnetic particles assemble on a micropattern of thin ferromagnetic islands, acting as ferromagnetic traps; magnetic bead trapping could be controlled by varying the external magnetic field bias. In addition, a programmable self-assembly method for the placement of two or more different types of superparamagnetic colloidal beads onto lithographically defined magnetic microwell templates has been demonstrated.[232] Besides mixing, the agglomeration of magnetic microbeads into a SPS also has shown to play a role in magnetic transport. The large magnetic bead transport velocities (10 mm/s) obtained by actuation via a planar coil array placed in a

uniform magnetostatic field only could be explained by the formation of columnar magnetic objects with a strongly enhanced magnetic moment and corresponding magnetic energy.[176]

4.5. Magnetic Droplets

In contrast to continuous flow microfluidics, where comparatively large liquid volumes are pumped through the microsystem, droplet microfluidics, also called "digital microfluidics", handles only small self-enclosed liquid entities.[233,234] The advantage of droplet handling is the strong reduction of the transported volumes and the possibility of working simultaneously with a plethora of different samples in a common system, which is why the manipulation of small droplets is steadily gaining impact on the development of lab-on-a-chip systems.[234] To perform reactions between the different droplets, the system however needs to be able to execute various droplet manipulation steps, such as transport, merging, mixing, and splitting. Among the solutions presented in recent years, which range from electrowetting over dielectrophoresis to acoustic actuation,[233] magnetic droplet manipulation offers the advantage of long-range magnetic forces, which do not rely on the intrinsic properties of the manipulated medium and do not interact with most biological materials.[235] This noninteraction, on the other hand, requires the introduction of magnetically responsive material into the droplets, where they translate an applied magnetic field gradient into a force pulling the droplet into the direction of the gradient.[236] Such magnetic particles have the advantage that they can serve as functionalized components of the system, such as optical indicators[237] or mobile substrates[238] in addition to being the force mediators.[239] While magnetic particle actuation in droplets allows a nonlabeling, fast, and material-independent controlled droplet manipulation, electrical mechanisms are better compatible with smaller liquid volumes. Electrowetting-on-dielectric (EWOD) is a particularly promising technique, because it uses a simple device configuration and fabrication, generates large forces on the microscale, and consumes little energy. EWOD-based manipulations of aqueous droplets have been demonstrated in parallel-plate devices filled with oil[240] or dry in air.[241]

A challenge in magnetic droplet manipulation is the application of the magnetic field gradient. In some cases, an external magnet was used, which can be moved according to the requirements of the droplet manipulation.[242] In combination with a suitable three-dimensional structuring of the surface to create barrier or gating structures, all droplet manipulation steps, like separation, transport, and fusion, can be implemented (see Figure 12), but at the cost of increasing system complexity and decreasing flexibility.[243] Droplet movement, coalescence, and splitting have also been investigated for droplets moving on an open hydrophobic surface.[244] These processes were actuated by magnetic beads internalized in an oil-coated aqueous droplet using an external magnet. The results were explained theoretically with a simple model that balances magnetic, friction, and capillary-induced drag forces and includes the effects of particle type, droplet size, surrounding oil layer, surface tension, and viscosity.

In other work, magnetic particle concentration and separation was demonstrated in droplets moving in a channel[245,246] or near the bottom of an oil-filled reservoir,[247] by using both permanent magnet-induced forces and EWOD droplet manipulation. Mixing has been demonstrated as well using a rotating magnetic field acting on magnetic bead chains inside an aqueous droplet positioned on a superhydrophobic surface.[248] A different approach was the use of a matrix of coils to generate local magnetic field gradients. In this case, the magnetic particles no longer follow a moving magnet, but are controlled by the changing topology of the applied magnetic field.[249−251] Because the actuating field gradient only acts on the particles enclosed inside the droplet, the magnetic force is transferred onto the droplet via the droplet wall. The moving particles accumulate at the droplet boundary and push the droplet into the desired direction. As a consequence, the droplet will move as long as the magnetic actuation is larger than the friction exerted by the surrounding liquid and surfaces. In case a droplet should stay in place, the local friction can be increased, either by introducing three-dimensional obstacles[252] or by varying the wetting properties of the surface in contact with the droplet.[253]

5. Magnetic Cell Manipulation

5.1. Cell Types

5.1.1. Cells with Magnetic Character

Few cells with intrinsic magnetic properties exist naturally. A first type of cell with magnetic character is a deoxygenated red blood cell (RBC) (see Figure 13a). Hemoglobin is the iron-containing oxygen-transport metallo-protein in the RBCs of vertebrates. In mammals, the protein makes up about 97% of the RBC's dry content, and around 35% of the total content (including water). Oxygenated hemoglobin is diamagnetic due to the presence of paired electrons on its Fe atoms. Oxygenated RBCs have therefore a small relative magnetic susceptibility with respect to that of water: $\Delta\chi_{oxy} \equiv \chi_{RBC,oxy} - \chi_{water} = -0.19 \times 10^{-6}$,[254] with $\chi_{water} = -9.0 \times 10^{-6}$.[255] Deoxyhemoglobin is the form of hemoglobin without the bound oxygen to the Fe atom, resulting in a RBC relative

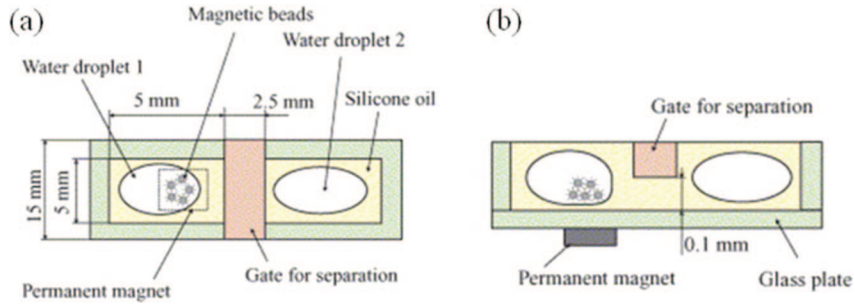

Figure 12. Schematic top view (a) and side view (b) of a magnetic droplet actuation system. Magnetic beads in a first water droplet can be extracted from the droplet using a permanent magnet and a physical barrier (gate), for subsequent merging with a second water droplet. Reprinted with permission from ref 243. Copyright 2006 Elsevier.

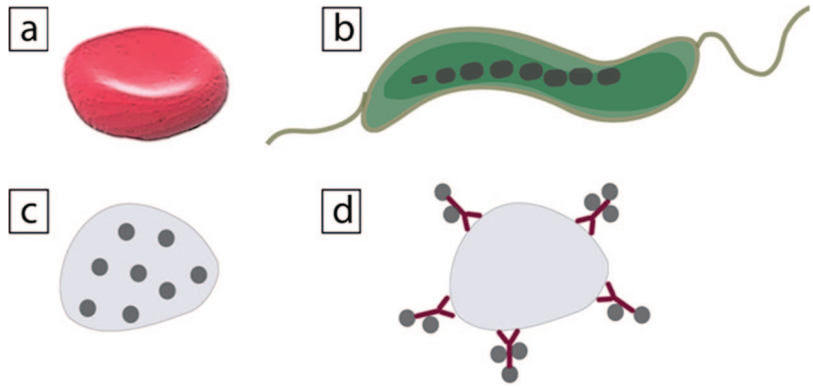

Figure 13. Schematic diagram of (a) a red blood cell, (b) a magnetotactic bacterium, (c) a cell with digested magnetic nanoparticles, and (d) a cell with magnetic nano- or microparticles attached to the surface via a ligand−receptor interaction.

magnetic susceptibility $\Delta\chi_{deoxy} \equiv \chi_{RBC,deoxy} - \chi_{water} = 3.3 \times 10^{-6}$.[256] While this is still a small value, the use of magnetic fields in the tesla range allows one to generate sufficient magnetic force to retain or separate deoxygenated RBCs from a complex matrix.[257] Magnetotactic bacteria form a second category of naturally magnetic cells[258] (see Figure 13b). These mobile bacteria are present in water-based sediments and move along the earth's field lines, a phenomenon called magnetotactism. At the basis of this magnetic interaction is a cluster or row of biogenerated magnetic Fe_3O_4 crystals inside the bacteria.

5.1.2. Nonmagnetic Cells Labeled with Magnetic Beads

Other cell types are essentially nonmagnetic and can be magnetically "activated" with magnetic nano- or microparticles via digestion of the particles by the cell (see Figure 13c) or via a (specific) ligand−receptor interaction at the cell surface (see Figure 13d). The majority of literature data on magnetic bead-based cell separation deal with the separation of white blood cells (WBCs), cancer cells, or bacteria from serum or blood. Blood has two main components, plasma and cells, each representing about one-half of its volume. There are three main types of cells with different functions under different conditions: erythrocytes or RBCs, leukocytes or WBCs, and platelets. RBCs transport oxygen, WBCs defend against disease, platelets promote clotting, while plasma proteins perform a variety of functions. Table 1 gives an overview of the most important type of cells and their abundance in normal blood. Depending on the needs of diagnosis, only some of the blood cells will be of interest, and these need to be isolated and purified from other cell types that are irrelevant or can even compromise good analysis of the selected cells. The WBCs are divided into five classes: neutrophils, lymphocytes, monocytes, eosinophils, and basophils (see Table 1). However, this classification is too general for many applications. The cluster of differentiation (CD) is a protocol used for more precise identification and investigation of cell surface molecules present on WBCs and other cell types.[259] CD molecules are proteins that can act in a variety of ways as receptors or ligands important to the cell behavior. Usually a combination of CD markers is used to classify cells, identify their function, or reveal cellular responses to particular pathological situations. Cell populations are defined using a plus or a minus symbol to indicate whether a certain cell fraction expresses or lacks a CD molecule. For example, a CD34+, CD31− cell is one that expresses CD34, but not CD31. This CD combination typically corresponds to a stem cell, opposed to a fully differentiated endothelial cell. Table 2 presents the CD markers for a few types of cells.

Table 1. Absolute and Relative Number of Cell Populations and Subpopulations in Normal Blood (Adapted from Ref 260)

cell type	quantity/μL	fraction of WBC (%)
red blood cells	5×10^6	
reticulocytes	$(3-7) \times 10^4$	
platelets	$(2-5) \times 10^5$	
white blood cells (total)	$(5-10) \times 10^3$	100
neutrophils	$(4-8) \times 10^3$	40−65
monocytes	$(2-8) \times 10^2$	4−8
eosinophils	50−300	1−3
basophils	0−100	0−1
lymphocytes (total)	1000−4000	20−40
CD4+ T cells	400−1600	15−20
CD8+ T cells	200−800	7−10
B cells	200−800	7−10
natural killer cells	100−500	4−6

Table 2. Cluster of Differentiation (CD) Markers for Several Cell Types

cell type	CD markers
stem cells	CD34+, CD31−
all white blood cells	CD45+
monocytes	CD45+, CD14+
T cells	CD45+, CD3+
B cells	CD45+, CD19+, or CD45+, CD20+
natural killer cells	CD16+, CD56+, CD3−

If an assay is seeking to analyze the DNA from WBCs, a microliter sample volume is sufficient to analyze. However, rare cells in blood, like bacteria, tumor cells, or fetal cells in maternal blood, occur in concentrations of ten to a hundred cells per milliliter. Sampling of 1 μL volume may not provide even one cell of interest for subsequent analysis. Clearly, the large initial sample volume with few numbers of target cells requires a powerful preconcentration or purification step.[261] Here, magnetic beads can play a prominent role, if they specifically bind to CD markers on the cell surface. Also, the intracellular uptake of superparamagnetic iron oxide nanoparticles has been studied.[262] Three different cell types, mesenchymal stem cells, cardiac fibroblasts, and cultured hematopoietic stem cells, were exposed to superparamagnetic nanoparticles treated with a number of different transfection agents. The study was based on the magnetophoretic analysis of live cells and supplemented by cytochemical staining.

5.2. Magnetophoretic Mobility of a Cell

The magnetophoretic mobility of a magnetically tagged cell is a parameter that distinguishes these cells from unlabeled cells. Following eq 8, the magnetophoretic mobility of a simple magnetic particle is the velocity of the particle in a magnetic energy gradient divided by the magnitude of the gradient. This velocity is the result of the magnetic force created on the particle by the interaction of the magnetic material with the imposed magnetic energy gradient. While for a magnetic particle, the part of the magnetic force originating from the particle itself (and not from the external field) is related to the particle volume and the susceptibility ($V\Delta\chi$), the situation for an immuno-magnetically labeled cell is more complex. Indeed, the magnetic force depends on the number of magnetic particles on the cell membrane, while the viscous drag force is due to the complete cell−nanoparticles complex. Therefore, in case of a two-step binding protocol on cells (see Figure 14), five parameters will influence the magnetophoretic mobility of an immunomagnetically labeled cell:[264−266] the antibody binding capacity (ABC) of a cell population, the secondary antibody binding amplification factor (ψ), the number of magnetic particles bound to one antibody n, the particle−magnetic field interaction parameter of the magnetic particles ($V\Delta\chi$), and the cell diameter (D_c). ABC is the number of primary antibodies binding to the cell. This value includes not only the number of antigen molecules per cell, but also variables such as valence of antibody binding, steric hindrance, binding affinities, and nonspecific binding events. The amplification factor ψ is obtained by binding a secondary antibody with multiple magnetic particle interaction sites to the primary antibody, and n is the number of magnetic particles that conjugate to the (second) antibody. Summarizing, the magnetophoretic mobility for a cell can in analogy to eq 8 be written as

$$\xi_{\text{cell}} = \frac{ABC\psi nV\Delta\chi}{3\pi D_c\eta} \tag{14}$$

The influence of each of these parameters on the magnetophoretic mobility has been studied in several papers.[263,267] For example,[267] ABC values in the range of 50 000−100 000 were reported for the CD34 antigen, which is a marker for hematopoietic progenitor cells. These cells are stem cells that give rise to all of the blood cell types and are found in the bone marrow of adults or in umbilical cord's blood, placenta, and mobilized peripheral blood.

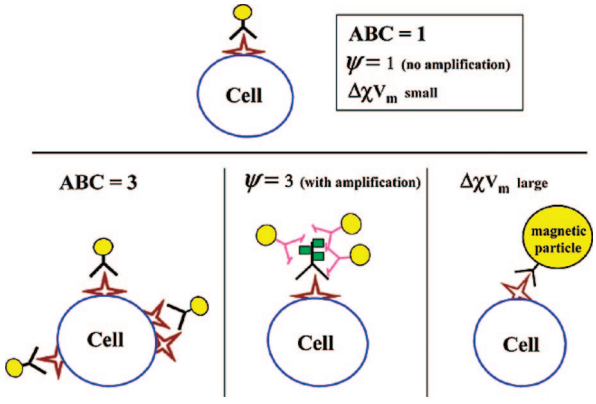

Figure 14. Comparison of immuno-magnetically labeled cells with different values of antibody binding capacities (ABC), secondary antibody amplification (ψ), or magnetic−particle field interaction parameter ($V\Delta\chi$). An increase in any of these parameters will increase the amount of magnetic material bound to the cell and therefore increases the magnetophoretic mobility. Reprinted with permission from ref 263. Copyright 2003 American Chemical Society.

5.3. Cell Separation Methods

Several reviews exist on on-chip separation and analysis of specific cells from a complex matrix.[268−270] Sorting cells, either for subsequent culture or to purify one cell type from a complex sample, is practiced using gravitational, chemical, optical, magnetic, or mechanical methods. The most obvious type of on-chip physical cell separation is a filter structure that selects cells on the basis of differences in size and disparity.[271] Separation based on sedimentation is based on gravitation-induced cell migration across individual fluid lamina with a lateral transport or migration velocity.[272] The driving force of sedimentation is the difference in cell and fluid densities in the gravity field. For a mixture of similar cell types, the cell density, shape, and cell size play a critical role in sedimentation. For cells with similar properties, such as during separation of cancerous cells from healthy tissue, there may not be sufficient difference in sedimentation parameters to achieve efficient separation. However, the main advantages of field-flow sedimentation are the absence of a label, the ability to continuously operate the device for high throughput, and the simplicity of the design. Dielectrophoresis using AC electrical fields is another physical method that has attracted attention.[273] It is most effective when there is a significant size or dielectric difference between cell types. For disparate cell separation, such as separating bacteria from blood cells, there is a strong difference in dielectrophoretic force, and cells physically settle at different locations on a substrate surface. In separation by affinity cell capture, the chemical interaction between cells and a surface is critical for selective adhesion. Various parameters such as association and dissociation constants, the number of bonds between the cell and the surface, or the antibody density influence the adhesion or removal from cells on the surface. In traditional chemical affinity chromatography, the analyte is finally eluted from a column by disrupting the target−capture molecular bond, for example, by changing the pH or ionic strength of the mobile phase. Such approach is less evident, when dealing with the separation of cells. However, the specificity of antibodies to match a desired antigen (CD) on the cell surface has become a cornerstone in cell separation.

Currently, the majority of commercial cell separation systems are based on fluorescent flow cytometers or other complicated instrumentation.[274,275] The most commonly used methods for cell sorting are fluorescence-activated cell sorting (FACS)[274] and magnetic cell sorting (MACS)[110] (see Figure 15). FACS instruments operate in the flow-through regime and use laser-induced fluorescence to count and direct droplet-based cells stained with fluorophore-conjugated antibodies against an appropriate CD on the cell surface. As immunofluorescence is used as the triggering signal or readout, cells need to be labeled with fluorescent markers, which adds up to the cost. Also, immunofluorescence imaging requires higher quality optics, excitation sources, and cameras than normal optical detection. FACS is expensive, voluminous, and requires dedicated and trained staff to operate, but is a high-throughput technique, as up to about a million cells per second can be characterized and separated. However, FACS is time-

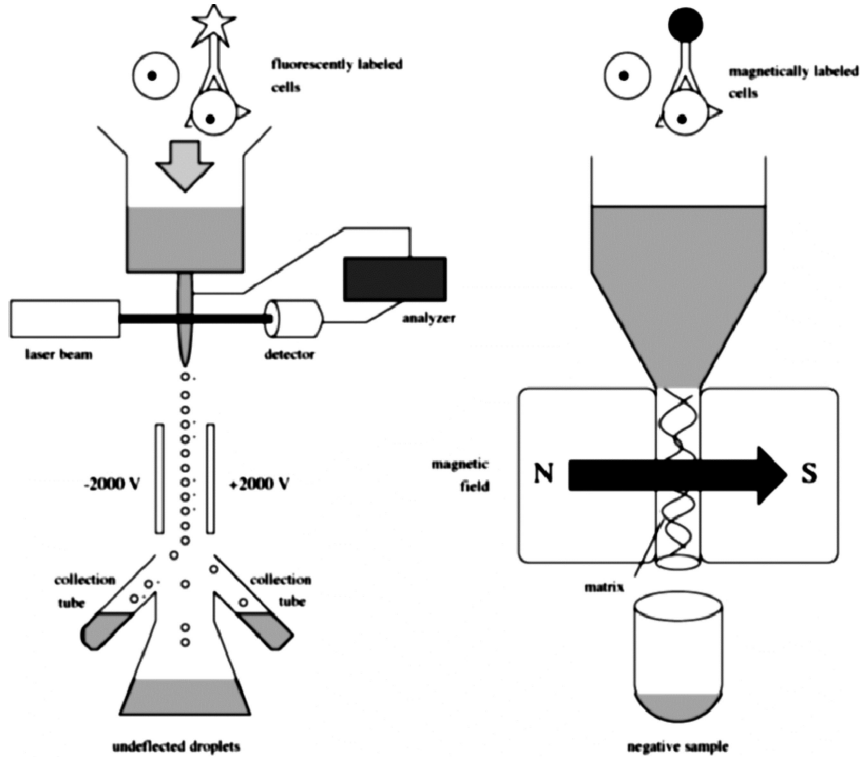

Figure 15. Schematic diagram of the two most commonly used methods for cell sorting. (left) In fluorescence-activated cell sorting, separation is done using the electrostatic deviation of specific fluorescently labeled cell-containing droplets. (right) In magnetic cell sorting, specific magnetic nanoparticle-labeled cells are retained in a high-gradient field magnetic matrix and are eluted from the matrix after removal of the magnetic field for subsequent analysis. Reprinted with permission from ref 136. Copyright 2001 Wiley−VCH.

consuming due to the large number of RBCs, reticulocytes, and platelets in a blood sample. FACS analyses have also been transposed to microfluidic platforms and sorting rates <100 cells/s have been achieved,[276] but the technique still requires high-quality and expensive detection optics and electronics. This explains the interest to look for alternative separation methods. As discussed in section 4.1.2, in MACS, cells labeled with superparamagnetic nanoparticles are retained in a high-gradient magnetic field generated by placing a magnetic column in the field of external magnets. The column is then removed from the separator, and the retained cells are eluted (positive selection). Alternatively, all but the cells of interest are magnetically labeled and are retained in the column, so that only the unlabeled cells of interest pass through the column and are recovered (negative selection). Subsequent cell detection is done using flow cytometry or microscopy. Selectivity of the separation is obtained by grafting the magnetic nanoparticles with antibodies against cell proteins on the surface of specific cells. The MACS method of cell sorting is less expensive and simpler than FACS, but it is important to note that MACS represents only a first sample handling step before additional analysis. Therefore, the idea of performing magnetic separations on a microfluidic platform is attractive, as this will facilitate the direct-reading, separation, and counting of the cells on a single chip. Technical advantages such as the ability to create large magnetic field gradients using only modest magnetic sources and the capability for precise handling of the separated cells make the use of microscale magnetic sorters a very attractive option for point-of-care diagnostic devices.

5.4. Magnetic Cell Separation and Purification

Red Blood Cells

The separation of red blood cells from whole blood was first demonstrated by Melville et al.[257] These authors used a column packed with magnetic wires, which was placed in a magnetic induction of 1.75 T with magnetic gradients close to the wires estimated as 8×10^3 T m^{-1}. After application of whole blood mixed with a reducing agent, the magnetic field was switched off and RBCs "eluted" from the column. Other systems based on a similar retention principle have been used for the separation of RBCs and WBCs from whole blood[277−279] or for the separation of malaria-infected RBCs from whole blood.[280,281] Using a magnetic dipole system, RBCs labeled with several types of transition metal ions were separated by retaining the magnetic beads from a flow at a surface that was close to a magnetic pole.[282] A microfluidic-based permanent magnet assembly, generating a constant magnetic force over a small zone of interest in a microchannel,[124,126] was used to study the magnetophoretic mobilities of oxygenated and deoxygenated RBCs.[254] A continuous separation of RBCs from whole blood or diluted blood was demonstrated in another type of microfluidic device, by passing the blood around thick (40−50 μm) magnetized nickel structures placed in or underneath the microfluidic channel in the presence of an external magnetic field.[153,283,284] The magnetic flux from the external field is attracted toward the nickel, providing a magnetic field gradient in the microfluidic channel that acts differently on a WBC and a RBC. This way, such device proved to separate continuously up to 93% of RBC and 97% of WBCs from whole blood at a volumetric flow rate of 5 μL h^{-1}.[154] This type of separation system has also been modeled theoretically.[285] In other work,

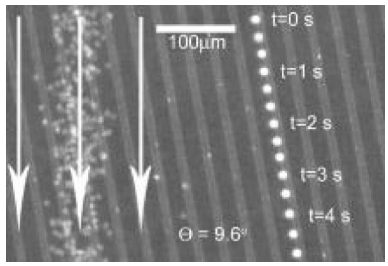

Figure 16. Time lapse image showing a single magnetically tagged fluorescing WBC at different times tracking a magnetic stripe at an angle of 9.6° to the fluid velocity (110 μm/s) indicated by white arrows. Red blood cells on the left are from a single image. All cells entered the chip at the same point approximately 1.5 mm above the field of view. Reprinted with permission from ref 151. Copyright 2004 American Institute of Physics.

nucleated RBCs have been identified in maternal circulation.[286] The detection of these cells provides a potential source for the monitoring and diagnosis of maternal, fetal, and neonatal health and disease. Separation of the nucleated RBCs was done using a two-step enrichment process: (i) a microfluidic separation based on cell size and the cells's ability to deform when moving through an array of posts on the chip, and (ii) a hemoglobin enrichment module followed by a batch-type magnetic separation in a MACS column.

White Blood Cells

As shown in Table 1, WBCs are less abundant, giving high relevance to the separation and purification of this type of cells from whole blood. Several disease conditions can be detected or monitored by counting the number of disease-specific cells. For example, the low concentration of helper T cells (characterized by a surface expression of CD4, or CD4+ cells) and a low ratio of the number of those cells to the number of cytotoxic T cells (CD8+ cells), CD4/CD8, is a practical measure to quantify the progression of the Human Immunodeficiency Virus (HIV).[287] The separation of WBCs from whole blood was demonstrated by Inglis et al.[151] using a continuous flow microfluidic device, consisting of magnetic stripes, magnetized by an externally applied field of 0.08 T and placed at a small angle (9.6°) to the direction of the fluid flow, while a narrow stream of cells was carried by the flow over the stripes. Cells, magnetically labeled using anti-CD45 magnetic beads, were attracted to the stripes and tended to follow the stripe direction, while unlabeled cells did not interact with the stripes and followed the direction of the fluid flow (see Figure 16). It was pointed out[288] that the greatest challenge with this type of system is preventing the magnetically labeled cells from permanently sticking to the stripes.

A microfluidic chip was proposed to separate cultured B cells tagged with 4.5 μm diameter magnetic beads[142] from a flow. The cells were deviated from the fluidic streamlines or trapped by a bed of packed Ni particles within a second nearby channel, the role of which was the generation of high magnetic field gradients in the first microfluidic channel, when the system was placed in an external magnetic field. In other work,[221] magnetic beads were covalently linked to a glass surface using a PEG hydrogel. The beads were completely embedded in the hydrogel and, when placed in an external magnetic field, could separate B cells, which were before incubated with anti-CD19 magnetic beads. The same authors also reported the direct capture of B cells from a flow when the anti-CD19 magnetic beads were linked to the glass with their active surface exposed to the flow. In another study,[289] enrichment of human T cells from a blood sample was demonstrated. First, anti-CD3 magnetic beads were introduced in a chip and captured in a field generated by a permanent magnet. A blood sample was then introduced, T cells were captured and rinsed clean, collected at the chip outlet, and moved off-chip for subsequent analysis. T cell capture efficiencies up to 37% were demonstrated.

WBCs have also been separated from buffy coats or raw blood samples using the magnetic quadrupole and bipole flow sorters developed by The Ohio State University and The Cleveland Clinic Foundation groups, discussed in section 4.1.1. A buffy coat is the fraction of an anticoagulated blood sample after density gradient centrifugation that contains most of the white blood cells and platelets. A typically used procedure is described in ref 290. Human peripheral leukocytes are collected from healthy donors, and the mononuclear cell fraction (MNC) is isolated by centrifugation. The typical composition of the MNC fraction is 90−95% lymphocytes, with the remainder of the cells identified as monocytes and a small fraction of erytrhocytes. The lymphocytes are targeted using mouse antihuman anti-CD45 monoclonal antibody conjugated to fluorescein isothiocyanate (FITC) and magnetized by a secondary rat antimouse polyclonal antibody conjugated to dextran-coated magnetic beads, as used in a MACS-type system. To simulate a real cell sample to be sorted, a small number of magnetically labeled lymphocytes was used to spike unlabeled lymphocytes, at a final fractional concentration of a few % of labeled cells. The binding of the magnetic beads to the target cells increases their susceptibility and makes them sensitive to an external magnetic field. At the same time, the use of FITC conjugated to the primary antibody sensitizes the target cells to UV light and makes them appear as bright cells in FACS analysis, while the unlabeled cells are simply part of the cell autofluorescence background. It was shown that there is a one-to-one correspondence between fluorescent and magnetic cell populations,[291,292] so that FACS analysis of the separated cell fractions allows one to investigate the efficiency of the magnetic separation. An example of cell fluorescence histograms of the original sample and the two sorted fractions is shown in Figure 17. These histograms essentially correlate with the magnetophoretic mobility histograms (of the type shown in Figure 6c), as determined by cell tracking velocimetry in a continuous flow microfluidic magnetic sorter.[293,294]

A quadrupolar magnetic cell sorter was also used to deplete peripheral blood leukocytes of T cells.[295,296] For an average initial number of 2×10^8 total cells, a 4 $\log_{10}$ depletion of CD3+CD45+ T cells was achieved at a sorting speed of 10^6 cells/s. This technique is of interest for allogeneic CD34+ hematopoietic stem cell transplantation, which is the only curative option for many patients with hematological malignancies. A high-level depletion of donor T cells (4−5 $\log_{10}$) from the graft can effectively limit the risk of graft versus host disease. While a high level of depletion of T cells on a clinical scale was indeed obtained, the level of CD34+ stem cells recovered for transplantation was still suboptimal, as shown by FACS analysis. So, still, large samples (2×10^{10} total cells) to be sorted, to obtain a sufficient number of CD34+ cells for a transplant, are required. A dipole magnetic flow sorter was used by the same group[297] to separate CD4+ and CD8+ T cells labeled with primary antibody−FITC conjugate and anti-FITC-magnetic colloid secondary antibody. Postseparation FACS analysis

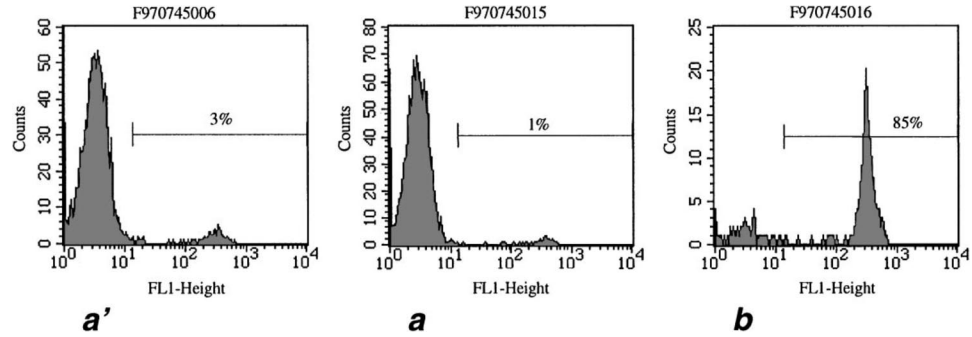

Figure 17. Histograms of labeled human CD45 lymphocytes as a function of cell fluorescent intensity. The cells are separated from a mixture of unlabeled lymphocytes in a magnetic quadrupole flow sorter and subsequently analyzed in a FACS system. Bars and numbers indicate targeted cell fraction (CD45+ cells). (a′) Original sample with a 3% fraction of positive cells, (a) nonmagnetic cell fraction with a 1% fraction of positive cells, and (b) magnetic cell fraction with an 85% fraction of positive cells. This shows the significant enrichment of target cells in the magnetic cell fraction (b) and the depletion of the target cells in the nonmagnetic cell fraction (a). Reprinted with permission from ref 290. Copyright 1999 Elsevier.

showed that, for CD4+ cells, a 3-fold increase in the total marker number per cell is observed, when comparing the highest to the lowest fluorescence fractions. Similarly, a 4-fold increase in total marker number is observed for the CD8+ cells. Also, CD56+ human natural killer cells were separated from human peripheral blood using a two-step antibody sandwich approach and a commercial batch-type MACS system.[298] The sorted cell fractions were subsequently analyzed by FACS, and histograms of the magnetophoretic mobilities of the sorted cell fractions, determined using a microfluidic magnetic cell sorter, were presented.

To reduce the problem of cell loss due to adhesion to the microchannel walls, a droplet-based magnetically activated cell separator was presented.[299] The system consists of a slide with a pending droplet, from which magnetically labeled constituents are retained to the slide surface by a magnet positioned above the slide. The system was tested using CD45+ cells that were separated from bone marrow cells of mice and passed through a 30 μm Nylon mesh prior to separation. The efficiency of cell separation was comparable to that of commercial batch-type systems.

Stem Cells

Cell separation can also be used for the isolation of rare hematopoietic progenitor cells from human umbilical cord blood and mobilized peripheral blood with the subsequent use of the cell isolates as a substitute for bone marrow transplantation in patients having undergone irradiation and high-dose chemotherapy.[300,301] Because these cells are typically rare (0.1−3%), a commercial batch immunomagnetic cell retention system was initially used to enrich the cells prior to cell tracking velocimetry analysis.[302] Within the positive eluents from the MACS column, the range of the magnetophoretic mobility was 50-fold, representing a plausible 50-fold range in expression of surface CD34 antigen, a marker for hematopoietic progenitor cells expression. It was pointed out that monocytes could phagocytose the magnetic nanobeads and become sufficiently magnetized to be retained within the magnetic column, reducing the purity of the positive eluent. A quadrupole magnetic separator was used to determine a $4 \times 10^4-10^5$ ABC range of the CD34 antigen.[267] These values were determined from a number of clinical apheresis samples, obtained from patients that were treated with a granulocyte-macrophage colony-stimulating factor, a cytokine that functions as a white blood growth factor. CD34+ progenitor cells could be separated to 64−95% purities and with a throughput of 10^7 cells/s in a quadrupole magnetic flow sorter.[303]

Cancer Cells

The presence of circulating tumor cells (CTCs) in blood is an indicator of metastatic disease in cancer patients. The concentration of these cells in the blood has been shown to correlate with the prognosis following treatment of breast cancer.[304] A count of one CTC per milliliter of whole blood is related to a lower incidence of relapse following chemotherapy. Tissue-specific markers for these cells are often missing, and the expression patterns of tumor- and epithelial-specific antigens (Ags) as well as the cell size differ, making it difficult to find a single reliable method for the isolation of CTCs.[305] As a result, detecting these rare disease-specific cells from whole blood is an important challenge in cellular separation technology. Several batch-type commercial systems have been used for the immunomagnetic separation of CTCs from whole blood. However, there are concerns about the limited load capacity and potential irreversible entrapment of cells inside the magnetic column.[298] Recoveries of target cells in the 10−90% range were reported (see Table 1 of ref 306 for an overview). Typically, breast cancer tumor cells spiked in human[307] or mouse[308] blood were used as target cells, labeled with both fluorescent markers and magnetic nanoparticles for fluorescent microscopy or FACS analysis after MACS separation.

Besides the batch-type magnetic separation systems, also continuous flow magnetic separation systems have been used to isolate rare (spiked) cancer cells from a blood sample. MCF-7 human breast cancer cells were immunomagnetically labeled by a two-step labeling protocol, similar to what was discussed before.[294,309] Briefly, first a primary mouse antibody (Ab) against a cell surface Ag was allowed to bind to the cell. This Ab can be conjugated to a fluorescent label to allow FACS analysis after magnetic separation. Next, the cells are labeled with a secondary rat antimouse polyclonal Ab conjugated to magnetic nanoparticles. Both a magnetic field[294] and gravitation[309] have been used to separate the cancer cells from their matrix, due to differences in magnetic susceptibility or cellular hydrodynamic diameter of the target cells, respectively. A quadrupole magnetic flow sorter was used to separate HCC1954 breast carcinoma cells overexpressing the HER-2/*neu* gene from peripheral blood leukocytes.[310] Labeled HCC1954 cells were mixed with unlabeled (only fluorescent) leukocytes to form the spiked sample that

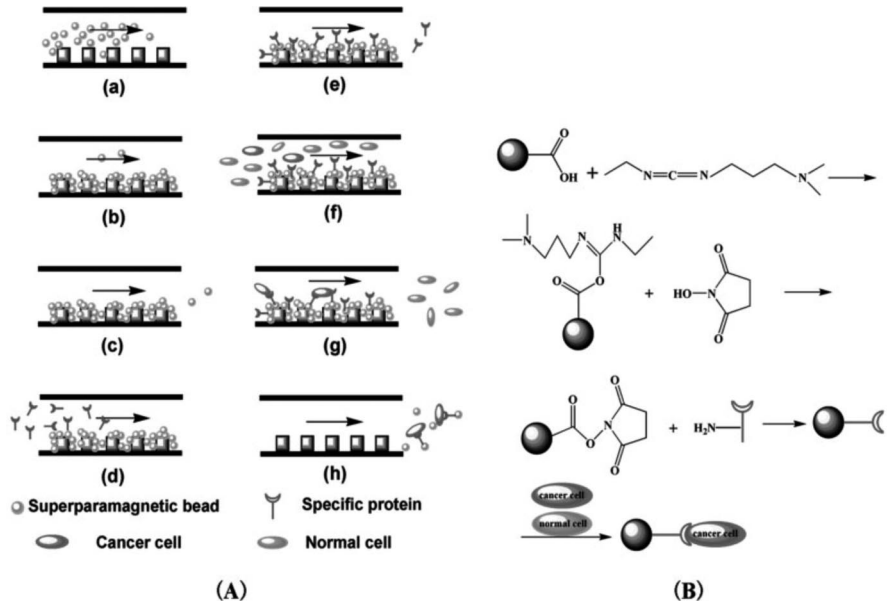

Figure 18. (A) Schematic representation of the experimental protocol for cell capture and sorting. (a) The channel was initially filled with a suspension of superparamagnetic beads. (b) The external magnetic field was applied, and the beads were trapped by the Ni micropillars. (c) Flow of buffer solution, which activates carboxyl groups on the surface of the beads and washes out any untrapped beads simultaneously. (d) Protein solution was then introduced into the flow stream. (e) Proteins were attached to the beads, and any unbound protein was washed out of the channel. (f) Cells were introduced into the channel. (g) Cancer cells were captured by specific protein-functionalized beads anchored to the nickel micropillars. (h) The cancer cells captured by the beads were eluted from the channel, when the external magnetic field was removed. (B) Covalent attachment of specific proteins to a magnetic bead and its capturing of a cancer cell. Reprinted with permission from ref 313. Copyright 2007 Wiley−VCH.

was analyzed by cell tracking velocimetry. High-throughput (3×10^5 cells/s) separations with 89% recovery of the HCC1954 cells were reported. In a very detailed study,[306] the same magnetic separator was used to separate MCF-7 cells from blood using a negative depletion protocol. The protocol consisted of a red cell lysis step, immunomagnetically staining leukocytes with an anti-CD45-phycoerythrin (PE) Ab to provide them with a fluorescent label, binding with the secondary anti-PE-magnetic nanoparticle-conjugated Ab, immunomagnetic sorting using the flow-through system, and a final cell analysis step using an automated cell counter. The process produced an enrichment of the rare cancer cells of 5 $\log_{10}$ and an average final recovery of 46%. This study continued with the analysis of the peripheral blood of head and neck cancer patients.[311] After optimization, the process was able to reduce the number of normal blood cells in a cancer patient's blood from 4×10^9 to 8×10^3 cells/mL and still recover, on average, 2.3 CTC per mL of blood. Spiking studies of a cancer cell line into normal blood and subsequent enrichment using the optimized protocol indicated an average recovery of 83%. The interesting thing of negative depletion is that the rare cancer cells themselves are not labeled, so that further molecular analysis of the nonmanipulated cell is still possible.

Other types of microfluidic devices have been proposed to separate rare cancer cells from a blood sample, based on immunomagnetic labeling. Human cervical cancer cells (HeLa) were internally labeled with magnetic nanoparticles following the endocytosis pathway, and fluorescence was obtained by concomitantly labeling with rhodamine albumin.[312] First, the magnetic particle uptake by the cells over different incubation periods was studied. Cell populations were subsequently sorted according to their acquired magnetic moment using a free-flow microfluidic magnetophoresis device. Another type of integrated microfluidic device consisting of nickel micropillars, microvalves, and microchannels was developed for specific capture and sorting of cancer cells.[313] A regular hexagonal array of micropillars was integrated on the bottom of a microchannel. The Ni generated a strong induced magnetic field gradient in the presence of an external magnetic field to efficiently trap superparamagnetic beads from a flowing stream. These beads were first in situ biofunctionalized by covalent attachment of specific proteins directly to their surface. Because of the microfluidic approach, only submicroliter volumes of reagents and protein solutions needed to be used. Figure 18 shows the experimental protocol to in situ functionalize the superparamagnetic beads in the microchannel and to capture A549 cancer cells (a human lung carcinoma cell line) from a flow. Based on the specific interaction between wheat germ agglutinin and *N*-acetylglucosamine on the cell membrane, A549 cancer cells were effectively captured on the magnetic beads. Before, they were mixed with RBCs at a ratio of 1:10. The cancer cells were sorted with a capture efficiency of 62−74%. For the RBCs, no capture occurred under the same experimental conditions.

HeLa-type and other types of cells were incubated with ferromagnetic beads that were fluorescently labeled prior to use.[314] Because of the ferromagnetic, rather than superparamagnetic, character, magnetic forces on such beads are larger. The cells showed a high uptake with 2−3 μm-size magnetic beads. In other work,[315] incubation and external labeling of oral squamous carcinoma cells with 4.5 μm superparamagnetic beads was reported, followed by microfluidic separation of the labeled cells. Also, apoptopic cells were selectively labeled with magnetic beads and subsequently sorted in a microfluidic device.[316] Apoptosis is the process of programmed cell death that may occur in multicellular organisms. Apoptosis occurs when a cell is damaged beyond repair, infected with a virus, or undergoing stressful conditions such as starvation. As cells, Jurkat cells (a leukemia-derived T-cell-line) were treated with apoptosis-inducing

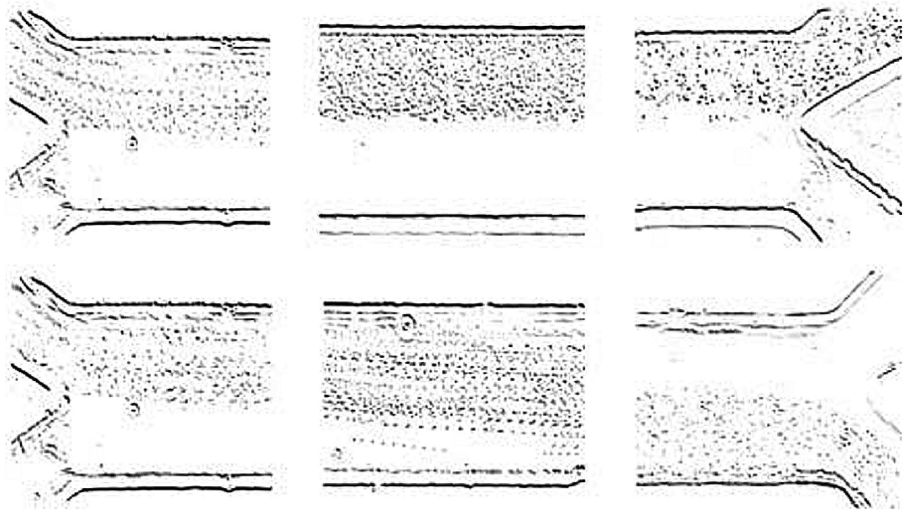

Figure 19. Separation of *E. coli* cells mixed with magnetic nanoparticles in a flow (from left to right) of PBS in a 200 μm wide channel. The composite bright images were generated by overlaying sequential frames of corresponding movies taken at the beginning, middle, and end (left to right) of the microfluidic channel, in the presence or absence of a neodymium disk magnet placed below the channel (bottom and top images, respectively). Reprinted with permission from ref 321. Copyright 2006 Springer.

reagents. Apoptopic cells show expression on their surface of the protein phosphatidylserine. This protein was biotinylated and subsequently bound to magnetic beads grafted with streptavidin molecules. Magnetic-activated cell sorting has also been used to separate dead and apoptotic spermatozoa using colloidal superparamagnetic nanoparticles (~50 nm in diameter) to improve sperm quality for assisted reproductive techniques.[317] Jurkat cells have also been magnetically deposited on the bottom of a microfluidic channel that was held within an assembly of permanent and soft magnets.[318] The Jurkat cells were labeled with both magnetic nanoparticles and fluorescent labels using a two-site sandwich immunoassay. A good magnetic capture efficiency (>99%) and the combination with optical (fluorescent) examination of the cell deposit are the advantageous features[318] of this system.

Bacteria

Magnetic separation and deposition of bacterial cells find application in rapid detection of microbial contamination in solutions such as environmental or industrial water, food, and in clinical microbiology. The previous magnetic deposition system for Jurkat cells reminds of early work on the magnetic deposition, quantitation, and identification of bacteria incubated and reacting with paramagnetic trivalent Er^{3+} lanthanide ions (i.e., not using magnetic beads).[319,320] The magnetic deposition protocol allowed quantitative detection of *Escherichia coli* down to concentrations of 10^5 colony-forming units (CFU) mL^{-1}. This magnetic deposition of the bacterial cells on a microscope slide was examined using dark field microscopy and by light scattering. In more recent work,[321] living *E. coli* bacteria have been separated from flowing fluids in a microfluidic system, either alone or when mixed with RBCs. In this study, 130 nm magnetic beads were used to label *E. coli* bacteria (1×10^7 cells/mL) by incubating the cells with biotinylated anti-*E. coli* Ab, mixing them with the magnetic beads grafted with streptavidin, and then injecting them into the source inlet of a microfluidic circuit equipped with a magnet. Figure 19 shows the separation of *E. coli* cells labeled with the magnetic nanoparticles in a 200 μm wide microfluidic channel. At a flow rate of 30 μL/h, 89% of the *E. coli* cells were separated from phosphate buffered saline (PBS). In the presence of RBCs, the collection efficiency was lower due to the increased viscosity of the RBC containing fluid.

Another microfluidic system, containing a gold interdigitated microelectrode array, was integrated with 145 nm magnetic nanoparticle−Ab conjugates into an impedance biosensor to detect pathogenic bacteria in beef samples.[322] The magnetic nanoparticle−Ab conjugates were prepared by conjugating streptavidin-coated magnetic nanoparticles with biotin-labeled polyclonal goat anti-*E. coli* Abs and were used in the magnetic separation and concentration of the target bacteria near the microelectrode sensor. The impedance sensor was able to detect in a time frame of 35 min as low as 160 or 1200 *E. coli* cells present in a spiked food sample of pure culture and ground beef, respectively. Another microfluidic system with on-chip pumps[323] had a detection limit of 2000 CFU/mL and a maximum capture efficiency from a PBS flow greater than 70% for *E. coli* cells. Off-chip polymerase chain reaction (PCR) and capillary electrophoretic analysis were used to determine the capture efficiencies. Also, a multitarget magnetic activated cell sorter was reported, which made use of microfluidic technology to achieve simultaneous spatially addressable sorting of multiple target cell types in a continuous-flow way.[324] Two types of *E. coli* cells were labeled via target-specific affinity reagents with two different magnetic tags with distinct saturation magnetization and size. The device was engineered so that the combined effect of the hydrodynamic force (F_d) produced from the laminar flow and the magnetophoretic force (F_m) produced from patterned ferromagnetic structures within the microchannel resulted in the selective purification of the differentially labeled target cells into multiple independent outlets. Figure 20 shows the separation architecture. The system had the capability to simultaneously sort multiple magnetic tags with >90% purity and >5000-fold enrichment and multiple bacterial cell types with >90% purity and >500-fold enrichment at a throughput of 10^9 cells/h. Magnetic deposition microscopy, in comparison with conventional blood smear tests, has been used to analyze blood samples of individuals with *Plasmodium falciparum* malaria symptoms.[325] Magnetic deposition microscopy increased detection sensitivity of *P. falciparum*-infected, hemozoin-containing

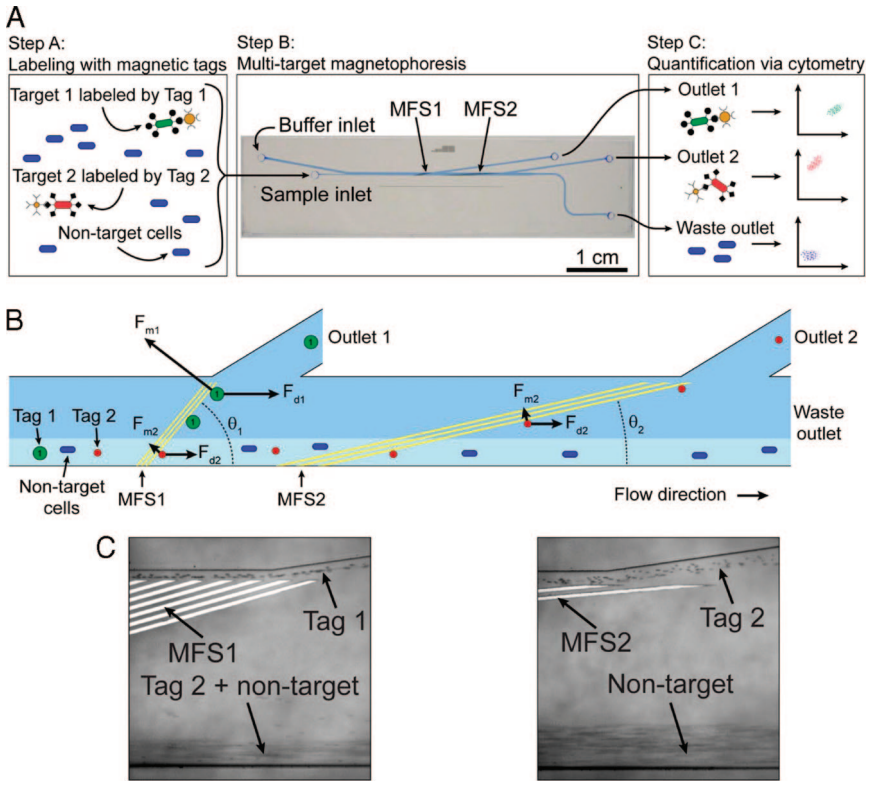

Figure 20. Multitarget magnetic activated cell sorter separation architecture. (A) (Step A) The sample contains an excess of nontarget cells and two different target cells (target 1 and target 2) that are labeled with two different magnetic tags (tag 1 and tag 2) by specific surface markers. (Step B) The sample is continuously pumped into the device where the two target cell types are sorted into spatially segregated independent outlets. Separation occurs in two regions of high magnetic field gradient generated by the microfabricated ferromagnetic strip (MFS) 1 and MFS 2. (Step C) After being sorted, the eluted fractions from each outlet are analyzed via flow cytometry. (B) A free-body diagram showing the balance of forces at the MFS structures. At MFS 1 ($\theta_1 = 15°$), tag 1-labeled target 1 cells are deflected and elute through outlet 1 because $F_{m1} > F_{d1} \sin(\theta_1)$. This is not the case for tag 2-labeled target 2 cells, which are instead deflected at MFS 2 ($\theta_2 = 5°$) because $F_{m2} > F_{d2} \sin(\theta_2)$, and elute through outlet 2. Nontarget cells are not deflected by either MFS and elute through the waste outlet. (C) Optical micrographs (magnification 100×) of the tags being separated at the 2 MFS structures at a total flow rate of 47 mL/h (sample flow = 5 mL/h, buffer flow = 42 mL/h). (Left) Tag 1 is deflected by the steep angled MFS 1. (Right) Tag 2 is deflected by MFS 2. Reprinted with permission from ref 324. Copyright 2008 The National Academy of Sciences of the USA.

RBCs from infected humans, while maintaining detection of ring-stage parasites.

5.5. Cell Biophysics

For applications like magnetic resonance imaging, hyperthermia, and separation, specific binding to or uptake of magnetic beads by a certain cell type is the basis of the magnetically induced contrast. Superparamagnetic particle uptake kinetics of living cells and toxicity aspects of such uptake have been discussed by several authors.[326,327] Also, the incorporation of magnetic beads into cells has provided a new tool to measure cytoskeleton-associated cell functions.[328,329] Superparamagnetic 30 nm beads coated with monovalent ligands and bound to transmembrane receptors of mast cells mediated the cellular signal transduction, when the cell was brought into an external magnetic field.[330] Magnetic particle twisting was used to investigate the mechanical integrity and viscoelastic properties of the cytoskeleton,[331] and, in combination with optical tweezers, superparamagnetic beads were at the basis of force and torque measurement systems on single cells.[332] Recently, cell-bound magnetic microparticles, subjected to 0.1 ms magnetic field pulses, have been used to destruct the targeted cells by penetration of the beads into the cells or by rupturing the cells with the beads,[333] a nonthermal process that is different from hyperthermia.

While one could argue that microfluidic aspects in the studies cited in previous paragraph are not essential, microfluidic chips have been used to handle cells for applications that go beyond the separation and purification of a certain type of cell from a matrix. For example, a microfluidic system has been developed for trapping yeast cells.[334] Single cell analysis of budding yeast cells is required to understand genomic changes that serve as models of human aging and disease. An automated system to capture individual yeast cells in a microfluidic device and to analyze each cell as it buds has been developed. Magnetic capture was chosen to selectively capture old yeast cells because yeast cells that are labeled with magnetic beads retain the beads over multiple divisions and do not pass them onto daughter cells, which form new cell walls. For labeling, the cells were incubated with biotin and thereafter incubated with streptavidin-coated 50 nm superparamagnetic beads. A Ni−Co−B alloy magnetic microstructure was plated into a PDMS chip and used to capture the magnetic bead-labeled yeast cells from a flow. In another study,[335] no labeling with magnetic beads was required to trap yeast cells in a locally weakened magnetic field, obtained by combining an electrical current-induced field with a uniform magnetic field. Trapping of the cells was enabled by placing the latter in a biologically benign ferrofluid matrix with high magnetic susceptibility. An integrated circuit/microfluidic hybrid system[336] was developed to manipulate and concentrate a small number of

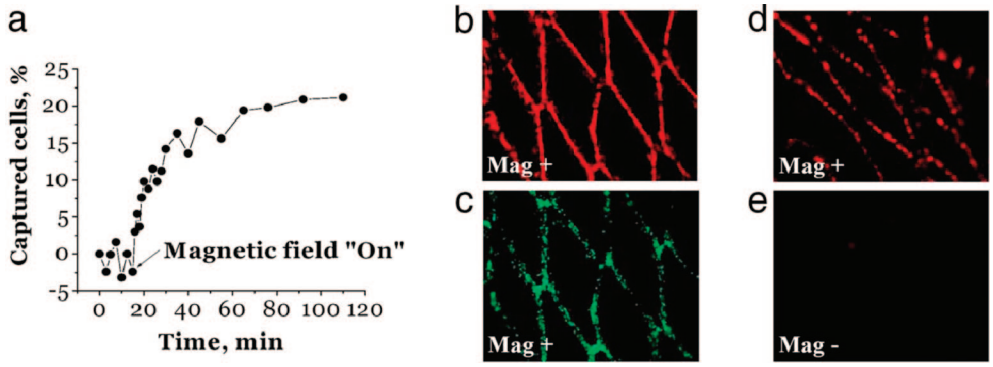

Figure 21. Magnetic targeting of magnetic nanoparticle-preloaded bovine aortic endothelial cells (BAECs) under flow conditions in vitro and in vivo. (a) In vitro capture kinetics of magnetically responsive BAECs onto a 304-grade stainless-steel stent in the presence of a uniform field of 0.1 T and a nonpulsatile flow rate of 30 mL/min. The data were obtained by measuring the fluorescence of the magnetic nanoparticles. (b and c) Magnetically responsive BAECs captured in vitro onto a 304-grade stainless-steel stent as evidenced by the red fluorescence of the magnetic nanoparticles (b) and Calcein green staining of live cells (c). (d) Magnetic nanoparticles-loaded BAECs captured in vivo onto a deployed 304-grade stainless-steel stent in the rat carotid artery. BAECs preloaded with fluorescent magnetic nanoparticles were transthoracically injected into the left ventricular cavity. Animals were exposed to a magnetic field of 0.1 T for 5 min, including the period of injection. The animals were killed 5 min after delivery, and the explanted stents were immediately examined by fluorescence microscopy. (e) Control rats underwent an identical procedure where no magnetic field was used. (Magnification: b−e, ×40.) Reprinted with permission from ref 338. Copyright 2008 The National Academy of Sciences of the USA.

individual cells with tight spatial control, with a potential to study cell−cell interactions at the single cell level. Yeast cells attached to magnetic beads were suspended inside the microfluidic system, and a microcoil array was used to produce spatially patterned microscopic magnetic fields that were reconfigurable in time. Also, bovine capillary endothelial cells containing 250 nm diameter magnetic beads have been manipulated by this hybrid system.[337] These cells were cocultured with peptide-coated magnetic beads, which lead to the uptake of the beads by the cells through endocytosis. In a work aiming at creating tissue on stents using magnetic nanoparticle activation,[338] superparamagnetic nanoparticle-loaded bovine aortic endothelial cells (BAECs) could be magnetically targeted to steel stent wires in an in vitro study. The cells were first preloaded with biodegradable polymeric 290 nm superparamagnetic nanoparticles, having a fluorescent label, and subsequently brought in the proximity of a steel stent placed in an external magnetic field. Figure 21 shows some of the experimental results of this study. Also, in vivo cells transduced with adenoviruses expressing luciferase were targeted to stents deployed in rat carotid arteries. A significantly increased luciferase expression was detected in an external magnetic field with respect to the expression for a nonmagnetic control experiment.

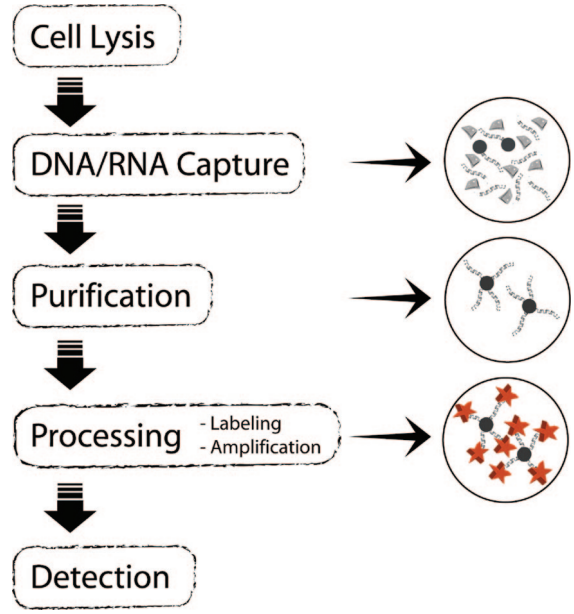

Figure 22. Schematic of the basic steps of an on-chip magnetic nucleic acid assay using magnetic beads as a substrate for the assay.

6. Magnetic Nucleic Acid Assays

An application area where magnetic beads play a standard role in bioanalytical procedures is that of nucleic acid assays. In macroscopic lab-bench protocols, magnetic beads are generally used as mobile substrates for the capture and extraction of nucleic acids.[339,340] With the increasing interest in the combination of microfluidics and magnetic beads, the step toward on-chip processing of nucleic acids was logical. Recent publications demonstrate the feasibility of miniaturizing magnetic nucleic acid assays, while maintaining the procedures and protocols known from batch-type applications. Figure 22 summarizes the steps followed in an assay, where magnetic beads can be applied with differing purposes and at different phases of the assay. The first phase of the protocol involves the specific capture of the molecules of interest and is followed by a washing or purification step to remove the matrix of unbound molecules. Some systems use the magnetic character of the beads in the detection step, where their stray field is measured for example using a magnetoresistive sensor. The processing step, between purification and detection, requires the miniaturization of the labeling or PCR amplification steps and is important for performing a complete on-chip nucleic acid assay. All of these steps are detailed in the following sections.

6.1. DNA Capture and Purification

An important task in on-chip nucleic acid analysis is the capture and purification of the molecules of interest. Using magnetic microbeads in a microfluidic system, the nucleic acids can be brought into contact with the particle surface via different means. A popular solution is the incubation of activated magnetic particles with the sample in a reservoir.[341,342] Here, the capture of the nucleic acids is driven by diffusion, and any subsequent purification step requires the introduction

of a magnetic field to separate the magnetic beads from the sample. Other solutions introduce a relative velocity between the sample and the magnetic particles by either immobilizing the latter and flushing the sample through or over them. Among the published systems, the majority is based on the immobilization of the magnetic particles inside a microchannel before or after the capture step.[343−345] The magnetic particles are hereby held against a flow via a magnetic field perpendicular to the channel, a principle already illustrated in Figure 11. The source of the magnetic field is either a permanent magnet placed underneath the system[342,343,346] or electromagnetic elements integrated into the chip.[344] An inverse approach is the capture of the DNA via the actuation of magnetic beads inside a small sample reservoir.[347] Hereby the particles can be actuated magnetically via either external magnets,[347] electromagnets,[238,348] or passive mixing.[345] The two latter solutions have the advantage of being easily integrated into a system with subsequent DNA processing and detection.

Magnetic beads have also been used in a microfluidic chip for in vitro selection of aptamers from a library.[349] Aptamers are nucleic acid molecules, either RNA or DNA, that bind to molecular targets with high affinity and specificity. Once the nucleic acid sequence of the aptamer is identified for a particular target, it can be produced synthetically, a distinct advantage over traditional affinity reagents such as antibodies, which require biological processes such as cell culture. The starting single-stranded DNA (ssDNA) library consisted of $\sim 10^{14}$ unique sequences, each containing a 60-base internal randomized region flanked by two 20-base PCR primer-specific sequences. The target protein, *Botulinum* neurotoxin type A, was conjugated to the magnetic beads through carbodiimide coupling. Target-conjugated beads were incubated with the heat-treated ssDNA library, and aptamers that bound to the target protein were separated in a microfluidic device. The aptamers bound on the target-coated beads were subsequently amplified via PCR, and single-stranded products are generated. Finally, the binding kinetics of the resulting aptamers was measured.

6.2. DNA Processing

After being captured and purified, the nucleic acids can be subjected to a range of processing steps; they can be hybridized to add labels for a subsequent detection step or amplified via a PCR protocol.[350] The magnetic beads, which carry the captured sample molecules, are hereby usually immobilized in a magnetic field, while primers and labels are added to the system.[351] Generally, such systems combine the capture, purification, and processing of the DNA on-chip, because the magnetic actuation of the particles is the same for the different steps.[352] Alternatively, in systems not employing the particles as a stationary phase, the latter can be used to concentrate and enrich the purified sample via local electromagnets before subsequent processing steps, thus improving the system's sensitivity.[344,353,354] Another interesting approach of using magnetic beads for the hybridization of DNA was presented by Heer et al.,[355] whose system employs the particles solely for accelerating the binding of the target DNA to the capture probes attached to the detection site via magnetic stirring.

In addition to the labeling and enrichment, the captured DNA molecules can be subjected to mechanical forces via the magnetic particles. Chiou et al.[356,357] presented an interesting system where single DNA molecules are rotated and stretched using magnetic tweezers, as demonstrated in Figure 23. One end of the DNA molecules was hereby anchored to the chip surface, while the other end was attached to a magnetic microparticle. Subsequently, any actuation of the particle was translated into a mechanical force acting on the DNA molecule. Thus, the mechanical properties of a single DNA molecule can be easily studied.

Besides being captured at the surface of magnetic microparticles, the DNA can also be processed via a loose interaction with the microparticles. Magnetic SPS within a microfluidic channel were used as a porous separation medium for the separation of long DNA molecules. The structure and porosity of the SPS is a strong function of the microfluidic channel dimension, particle properties, applied magnetic field, etc. Gel electrophoresis is the standard method for separation of DNA by length. However, the efficiency of gel electrophoresis deteriorates seriously for DNA molecules longer than about 40 000 base pairs (40 kbp). This phenomenon was understood in terms of electric field-induced aggregation of the DNA by the electrical dipole−dipole interaction.[358] Slab gel pulsed-field gel electrophoresis or pulsed-field capillary gel electrophoresis, using time-varying drive voltages, can be used to separate the longer chains of DNA.[359] The use of self-assembled magnetic SPS for long DNA separation in microfluidic channels represents a convenient solution, because no microlithography is required to define geometrical constrictions that are simply formed by the porous magnetic matrix.[360] Experimental separations using the SPS stationary phase have been combined with theoretical modeling.[361] This approach has been presented in more detail by Minc et al.,[362−364] in work where a network of columns of magnetic microparticles leads to the length-

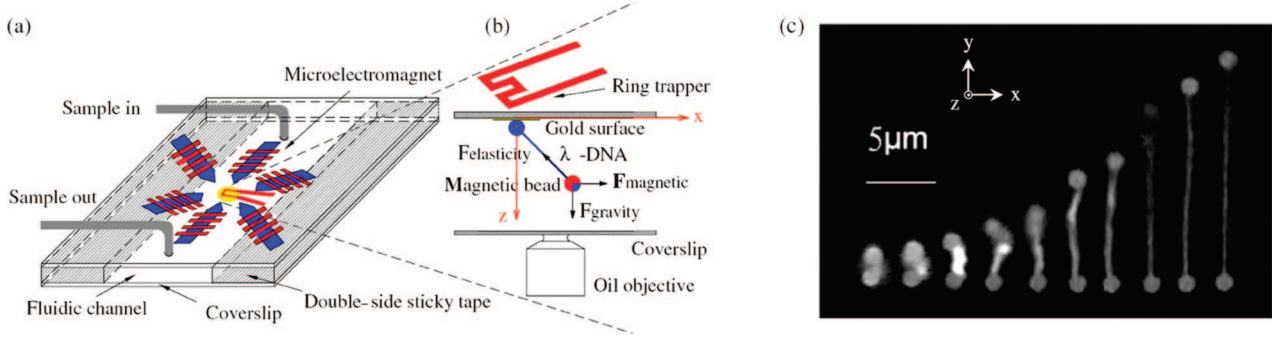

Figure 23. (a) Schematic illustration of magnetic tweezers integrated with microelectromagnets, a ring trapper, a fluidic channel, and a gold-patterned surface. (b) A tethered-DNA magnetic bead is in equilibrium under the action of the magnetic force, DNA elastic force, and the gravitational force. (c) Stretching of a single DNA molecule linked to thiol-modified beads. Reprinted with permission from ref 356. Copyright 2006 The Institute of Physics Publishing.

dependent separation of DNA in the direction of an elektrokinetic flow. Another innovative use of magnetic microparticles for the processing of purified DNA samples has been presented by Park et al.,[365] who use hyperthermia for heating the liquid sample for the different temperature stages of a PCR procedure. Using small aqueous droplets, these authors showed that it is possible to heat a discrete liquid volume to a temperature of 80 °C within 5 min by applying an oscillating magnetic field. The applicability of the heating of small droplets for on-chip PCR has already been presented in the context of magnetic droplet manipulation systems,[366,367] where a self-contained liquid sample is transported toward local heating elements via magnetic particles enclosed in the droplet. The capture of the DNA molecules can be performed before or after the PCR steps, depending on the subsequent detection step.

6.3. DNA Detection

The on-chip detection of nucleic acids offers the advantage of high sensitivity in combination with a high selectivity, depending on the chosen protocols and detection methods. With respect to the latter, two different principles are generally employed: optical and magnetic detection.[368] Optical detection methods are usually based on fluorescent tags, which label the molecules of interest that are captured and concentrated via the magnetic particles.[346,369] Also, a multilayer fluorescent labeling strategy was proposed to amplify the fluorescent intensity: a DNA detection limit of 0.25 fmol/mL was achieved.[370] The detection signals could be amplified using multilayers of biotin−streptavidin conjugated quantum dots based on the binding with a specific biotinylated linker. In contrast, magnetic detection directly uses the magnetic beads as labels[354,371,372] or indirectly for the deformation of small cantilevers.[373] A mixed form relies on the optical detection of the magnetic labels, which can carry fluorescent tags[374] or simply influence the opacity of the detection site.[375]

For the optical detection, the magnetic particles are usually concentrated at the detection site via external magnets or electromagnets. Because the strength of the optical signal indicates the amount of captured molecules, the trapped magnetic particles need to be washed thoroughly. An optical detection of the spatial distribution of magnetically labeled DNA strands, as proposed by Tierno et al.,[376] relies on contrast in the magnetic transport of the labels and would not require washing. Similarly, the direct magnetic detection of the particles also profits from the effect that the sensing element can at the same time act as a trap for the magnetic particles.[354] The magnetic character of the beads allows hereby their detection via integrated sensors, which are based either on the GMR effect[192] or on the Hall effect.[377] Here, the magnetic particles will be detected, either after being bound to the sensor surface by a DNA hybridization step or during the passage over the sensing element. Some publications demonstrate the possibility of detecting single particles using the magnetoresistive method;[198,202,378] see Figure 24, as well as using miniaturized Hall sensors.[377,379] The advantage of these is the possibility of their direct integration into the microfluidic system,[354] which is an important step toward the full on-chip DNA capture and detection.

Detection of PCR-amplified DNA on a GMR sensor was demonstrated using superparamagnetic particles as detection label.[380] The one-step assay was performed on an integrated and miniaturized detection platform suitable for application into point-of-care devices. A double-tagged PCR amplification product of the *LamB* gene of the *Escherichia coli* bacterium was used to investigate binding kinetics of the assay. Biological dose−response curves detecting 4−250 pM amplicon concentrations in a one-step format in total assay times of less than 3 min were presented. Using various tag−antibody combinations specific for one of the individual genes, multianalyte detection was shown for several antibiotic resistance genes of the food pathogen *Salmonella*.

6.4. Integrated DNA Analysis Systems Starting from Cells

Systems have been presented that combine all steps summarized in Figure 22, starting from crude cell samples. The majority of such systems rely on the simple trapping of a plug of magnetic microparticles inside a microchannel via an external magnet.[352,381−383] The sample, washing, and labeling reagents are subsequently passed though the blocked array of particles, and the fluorescent signal can be measured. Alternatively, the magnetic particles can also be separated from the sample solution after the incubation step, as presented by Lien et al.[384,385] and shown in Figure 25. In other work by the same authors, a lysed cell solution was loaded onto a microfluidic chip, which subsequently performed automatic RNA extraction and reverse transcription processes.[386] Total RNA was successfully extracted and purified from the human β-actin gene extracted from T98 cells, while analysis of the PCR products was done off-chip via gel electrophoresis.

Most of the integrated nucleic acid assays, summarized in Table 3, start from samples containing cells or viruses. These are either collected via the magnetic particles and lysed before the amplification step,[385,387,388] which results in free nucleic acids in the solution, or lysed before the capture of the nucleic acids, which are then bound to the magnetic particles and processed further.[83,346,352,382,383,389] Generally,

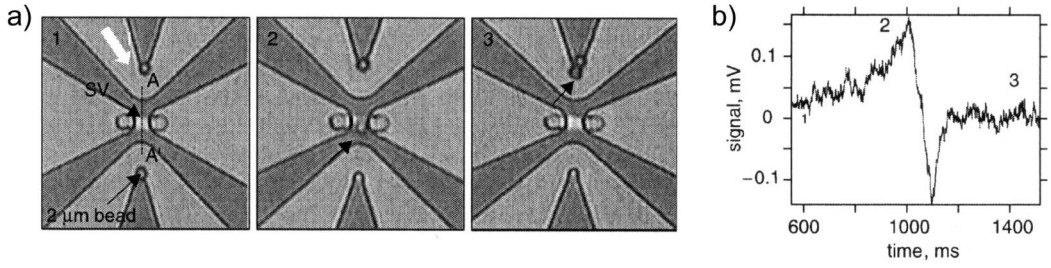

Figure 24. Magnetoresistive detection of the magnetic labels. (a) Micrograph sequence of a single 2 μm bead (indicated by the black arrow) crossing the sensor area. (b) Recorded sensor signal during the passage of a single 2 μm magnetic bead over a spin-valve GMR sensor with 3 mA sense current. The indicated numbers correspond to the sequence numbers in (a). Reprinted with permission from ref 378. Copyright 2005 Institute of Electrical Engineering.

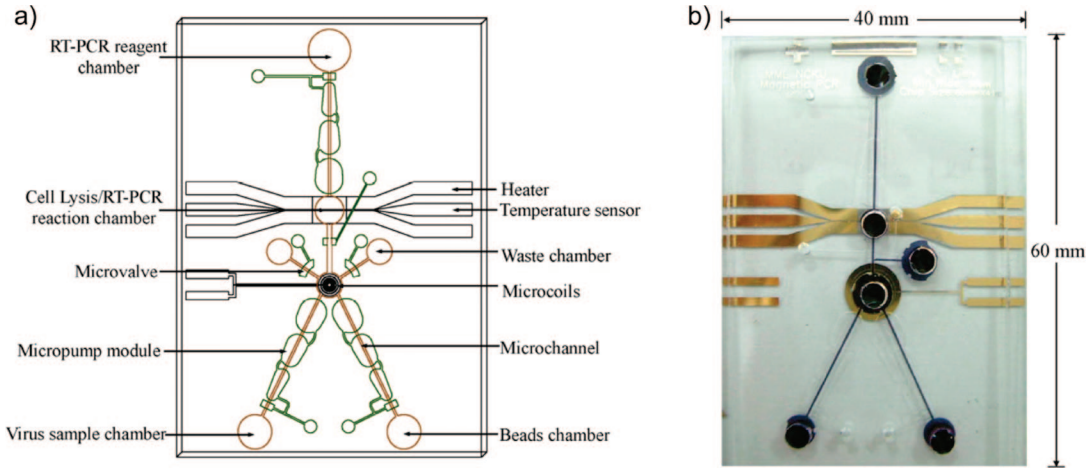

Figure 25. Integrated reverse transcription (RT)-PCR system. (a) Schematic illustration of the integrated RT-PCR chip. Several components including a microtemperature module, a bead collection module, and a microfluidic control module are integrated onto a single chip. (b) Photograph of the RT-PCR chip. The width and length of the chip are 40 and 60 mm, respectively. Note that micropumps, microvalves, electromagnets, microheaters, and microtemperature sensors were integrated on the same chip. Reprinted with permission from ref 385. Copyright 2007 Elsevier.

Table 3. Summary of the Main Characteristics of Representative On-Chip Nucleic Acid Assays Employing Magnetic Beads[a]

	magnetic manipulation step			
detection principle	external magnet	separation after incubation	droplet handling	magnetic assembly for hybridization on detection zone
fluorescent	simultaneous examination of eight DNA samples[383]		10 cells from crude cell sample analyzed in 20 min[83]	high density array, 2×10^8 beads per cm^2 [390]
	liposome label for signal amplification, 10 fmol/mL detection limit[346]			
surface coverage	fluidic shear force against nonspecific binding, 1 pmol/mL detection limit[391]			visualization of hybridization array by specific magnetic particle binding[375]
electrochemical	liposome label containing potassium ferri/ferrohexacyanide and interdigitated electrodes for detection, 10 μmol/mL detection limit[392]	fully integrated system, start from crude cell samples, pathogenic bacteria, and SNP detection[382]		
magneto-resistive	detection limit of 10 μg/mL target DNA[368]			integrated electronics, detection limit10 pmol/mL or 16 pg on surface[378]
	2.5 mmol/mL target DNA detected using MgO-based tunnel junction sensor[393]			10 nmol/mL detection limit, 140 DNA molecules per sensor[394]
PCR	amplification of sample for high sensitivity, detection of SNP[352]	integrated chip, slab-gel electrophoresis analysis, virus detection limit: 100 PFU/mL[385]	500× preconcentration, detection of 1−50 RNA copies[389]	
	electrochemical mRNA detection for viability of *E. coli*, down to 100 CFU/mL[342]	lab-on-a-CD, Hepatitis B virus and *E. coli*, 10 DNA copies/μL detected[388]		
	DNA recovery from 1 *E. coli* cell[395]	34 ng of total mRNA isolated from 10 μg of total RNA[343]		

[a] The systems are categorized on the basis of the magnetic manipulation step and the detection principle. SNP: single nucleotide polymorphism. PFU: plaque-forming unit. CFU: colony-forming unit.

systems employing PCR as the detection step rely on the magnetic capture and purification of cells and viruses with a subsequent lysis step to release the nucleic acids, while systems that use the magnetic particles as labels for the detection perform the capture steps after the cell lysis. Several integrated systems combine the different features; for

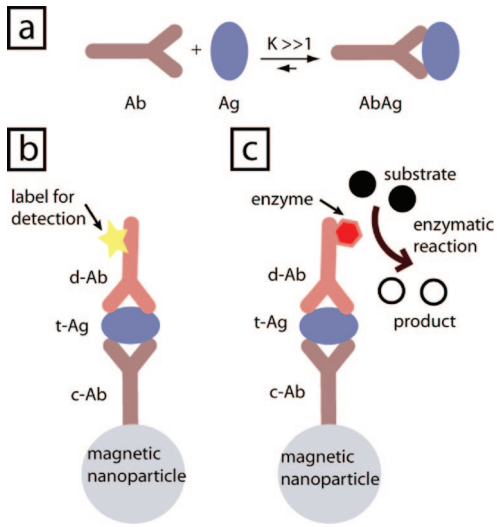

Figure 26. (a) Schematic representation of the reaction between an antibody (Ab) and its specific antigen (Ag) to form an AbAg immunocomplex. (b) Schematic representation of sandwich immunocomplex formation. A surface-linked capture antibody (c-Ab) is reacting with its target antigen (t-Ag). A labeled detection antibody (d-Ab) is then reacting with the t-Ag. (c) Schematic representation of an immunocomplex formed with a d-Ab labeled with an enzyme. The conversion of the enzyme substrate to its product by an enzymatic reaction leads to the formation of a detectable molecule.

example, PCR amplification can be combined with fluorescent detection on the same chip.

7. Magnetic Immunoassays

Magnetic bead-based immunoassays performed in the microfluidic format have attracted particular interest, because of the multiple advantages and promising potential applications.[26,27] Basically, an immunoassay consists of using antibodies (Abs) as chemical reagents to analyze target molecules, called antigens (Ags). The technique is based on the recognition of a target antigen (t-Ag) by its Ab. When brought into contact, Ag and Ab form, due to specific and strong molecular interactions, a stable immunocomplex structure (see Figure 26a). Immunoassays are among the most important techniques used for biological molecule analysis. They are widely used both in research and in analytical sciences and have been explored for many applications, ranging from environmental analysis to clinical diagnosis. The technique can be divided in two subclasses: that of competitive and noncompetitive assays, respectively. In a competitive immunoassay, the t-Ags to be detected compete with known labeled Ags (Ags*) for immunocomplex formation. The detection and quantification of the immunocomplex formed with Ag* permits one to deduce the amount of t-Ag present in the sample. In a noncompetitive immunoassay,

Table 4. Summary of the Different Application Areas for Microfluidic Magnetic Bead-Based Immunoassays and Overview of Literature Results, Quoting the Detection Method, the Type of Assay, the t-Ag That Is Analyzed, and the Detection Limit of the Assay

detection technique	type of assay	target Ag	detection limit	ref
Proof of Concept				
fluorescence	direct	fluorescein isothiocyanate (FITC)	3.9 μg/mL	207
fluorescence	direct	biotin-4-fluorescein	1 μg/mL	381
fluorescence	direct	IgG2a (mouse)	10 μg/mL	381
fluorescence (evanescent field detection)	sandwich	IgG (rabbit)	120 ng/mL	396, 397
fluorescence	sandwich	IgG (goat)	5 ng/mL	398
fluorescence	direct	fluorescently labeled biotin	0.2 μg/mL	399
fluorescence	direct	antistreptavidin IgG (rabbit)	12.5 pg/mL	400
fluorescence	direct	antistreptavidin IgG (rabbit)	100 pg/mL	401
fluorescence	sandwich	mouse IgG	10 pg/mL	402
fluorescence	sandwich	mouse IgG	250 pg/mL	96
luminescence	sandwich	human insulin and interleukin-6	250 pg/mL	403
colorimetric	Ab transport	antimouse IgG (rabbit)	150 ng/mL	404
electrochemical	sandwich	mouse IgG	50 ng/mL	405
electrochemical	sandwich	mouse IgG	16 ng/mL	406
surface coverage	direct	antiovalbumine IgG (rabbit)	10 ng/cm^2	407
magnetic force discrimination	sandwich	mouse IgG	250 pg/mL	408
magnetic force discrimination	sandwich	IgG (rabbit)	15 ng/mL	408
GMR	direct	antimouse IgG (goat)	n.a.	409
agglutination test	direct	protein A	1−2 pg/mL	410
magnetic frequency relaxation	direct	rabbit IgG	n.a.	411
Brownian relaxation	direct	biotinylated T7 phage	n.a.	412, 413
surface coverage	sandwich	streptavidin, IgG	1 fg/mL	414
agglutination test		biotinylated bovine serum albumin (BSA)	100 pg/mL	415
fluorescence	kinetics of chemical reaction			416
agglutination test	kinetics of biomolecular recognition			417
Recombinant Protein Dosing from Cell Culture				
fluorescence	sandwich	IgG (mouse)	1 ng/mL	206
fluorescence of single bead on silicon chip	sandwich	IgG (mouse)	1 ng/mL	418
Disease Marker Detection				
fluorescence	sandwich	parathyroid hormone	1.4 ng/mL	207
fluorescence	sandwich	interleukin-5	2 ng/mL	207
fluorescence (evanescent field detection)	sandwich	interleukin-4	10 ng/mL	397
fluorescence	sandwich	tumor necrosis factor α	45 pg/mL	419
surface coverage and GMR	magneto-sandwich	S100$\beta\beta$ protein	27 pg/mL	420
surface coverage	magneto-sandwich	S100$\beta\beta$ protein	0.2 ng/mL	421
magnetic force discrimination	sandwich	*D. farinae* IgE (human)	85 pg/mL	422
magnetic force discrimination	sandwich	*D. pteronyssinus* IgE (human)	~0.04 ng/mL	422
surface coverage	sandwich	West Nile Virus	700 viral particles	414
surface coverage	sandwich	*Staphylococcus* enterotoxin B	1 fg/mL	423
surface coverage via surface plasmon resonance	sandwich	*Staphylococcus* enterotoxin B	100 pg/mL	424
fluorescence and Hall effect	sandwich	dengue virus IgG	not reported	425
		IgG (mouse)	1 ng/mL	
fluorescence	sandwich	dengue virus	10^3 PFU/mL	426
electrochemical	sandwich	various tumor markers	0.5 ng/mL	427
GMR	sandwich	parathyroid hormone	4 pg/mL	428
inductive	sandwich	Troponin I (cardiac marker)	0.5 ng/mL	429
optical reflection (evanescent field)	sandwich	Troponin I	<20 pg/mL	430
		drugs of abuse	<1 ng/mL	

only the t-Ags of the sample are involved in the immunocomplex formation. The quantitative measure of t-Ag is then directly obtained by measuring the total amount of immunocomplex formed during the experiment. Both immunoassay subclasses have been employed in the microfluidic format. However, due to efficiency and simplicity, microfluidic magnetic bead-based immunoassays have been principally developed in the noncompetitive way.

Depending on the experimental design, the number of Abs involved in the immunocomplex formation reaction is varying. A t-Ag, like a bacteria toxin, can be directly immobilized on a reaction substrate and can be quantified with a labeled detection antibody (d-Ab) in a direct immunoassay, involving a single type of Ab. This technique is however limited, because t-Ags for direct surface immobilization have to be available. A more flexible technique, called sandwich immunoassay, consists of flanking the t-Ag to be detected between a capture antibody (c-Ab) linked to a reaction substrate and a labeled d-Ab (see Figure 26b). In this technique, the t-Ag is specific for both c-Ab and d-Ab. It has to be noted that the t-Ag often is an Ab. Also, an enzyme can be used to label the d-Ab, and, in this case, flowing the enzyme substrate through the magnetic bead reaction chamber leads to the formation of a detectable product (see Figure 26c). An enzyme is a biomolecule able to convert its specific substrate to a product by catalyzing a biochemical reaction. The advantage of this technique is the possibility to generate many detectable molecules with only a few immunocomplexes, increasing thereby the detection sensitivity.

The success of magnetic bead-based immunoassays in the microfluidic format can be explained by their multiple advantages. A recurrent issue in microfluidic immunoassays is to control the surface chemistry of the microchannel wall to allow a reproducible c-Ab surface binding. This drawback is circumvented when using magnetic beads on-chip, because particle surface chemistry can be perfectly controlled off-chip prior to use of the beads. Furthermore, the limited microfluidic reaction chamber volume (in the nL−μL range) permits one to efficiently concentrate a small amount of magnetic beads in a confined space. As a result, the number of captured t-Ag is concentrated at a small defined location, thereby enhancing the detection signal intensity. Finally, the magnetic beads can be easily recovered after analysis for further applications or analysis. Table 4 summarizes the principal microfluidic magnetic immunoassay results reported in literature, categorized by application area and highlighting the detection method, the t-Ag analyzed, and the detection limit. The cited papers are discussed in more detail further in this section.

7.1. Magnetic Beads as Substrate

When magnetic beads are used as a reaction substrate, the immunocomplexes formed during the assay are linked to the particle surface. The particle surface chemistry has to be strictly controlled to allow a reproducible immunocomplex formation. In a direct immunoassay, the t-Ags are attached to the particle surface, and specific d-Abs are linked to the particle via the t-Ags. However, when a sandwich immunoassay is executed, c-Abs have to be linked to the particle surface prior to t-Ag capture. This can be done using a covalent chemical bond between the activated particle surface and a chemical group conjugated to the c-Ab. The use of physicochemical interactions or molecular recognition (for example, forming the biotin/streptavidin complex) are popular techniques for grafting c-Abs to the magnetic particle surface. The immunoassay is then executed by flowing solutions of sample and reagents to the reaction chamber containing the magnetic beads, followed by signal detection. The latter can be done using a d-Ab labeled with a detectable tag (for example, a fluorescent dye). However, when an additional chemical reaction is needed to generate a detectable molecule (for example, in case of an enzymatic reaction), the signal is detected in the bulk solution.

7.1.1. Direct Fluorescent Detection

Direct signal detection is performed by recording the fluorescence generated by the labeled d-Abs. This detection principle benefits from the high sensitivity offered by fluorescence. In early work, a single rare earth permanent magnet positioned at the top of a capillary was used to generate a strong magnetic field gradient within a microcapillary. This led to a magnetic force that retained a densely packed bed of magnetic beads in the microcapillary (see Figure 27a).[207] Flowing appropriate solutions of target sample and reagents resulted in the formation of detectable immunocomplex at the magnetic bead surface. A direct assay was demonstrated by direct interaction of FITC with an immobilized anti-FITC conjugate. Also, heterogeneous sandwich assays were demonstrated for parathyroid hormone and interleukin-5 (IL-5) down to concentrations of a few ng/mL (see Figure 27b). Magnetic bead positioning using external magnets was also used as a reliable solution to trap magnetic beads at a glass surface in a method that was called "magnetically assisted transport evanescent field fluoroimmunoassay". For excitation of the fluorescent labels on the beads, an evanescent wave was generated by total internal reflection of a laser beam at the optical interface between a prism and the sample[396] or at the surface of a planar waveguide.[397] The waveguide was combined with a multichannel microfluidic device for application of sample and reagents. Rabbit-IgG and interleukin-4 were detected with detection limits of 120 and 10 ng/mL, respectively.[397] The evanescent technique may reduce or eliminate washing steps, as interference from fluorescent species in the sample matrix is strongly minimized. Separation and washing steps could also be eliminated by configuring the microfluidic device with an interdigitated electrode microarray for dielectrophoretically moving the various Abs and t-Ag to the detection area.[402] A detection limit of 10 pg/mL was reported using mouse IgG as t-Ag.

Also, pairs of small permanent magnets with opposite poles were positioned close to a microcapillary, to retain magnetic beads injected in the capillary. Such system was used to purify Immunoglobulin E from serum followed by analysis by capillary electrophoresis.[431,432] Also, three different pairs of magnets were used to create three plugs with differently functionalized magnetic beads in an effort toward a multiplex immunoassay.[381] In other work, retention of magnetic beads in a microfluidic channel was achieved, not by focusing the field at a specific location across the channel, but by periodically varying the width of the channel. Upon the action of a constant magnetic field, magnetic beads introduced in the microchannel self-assembled in magnetic chains (see Figure 11c). The self-assembled magnetic chains are then positioned over the entire cross-section of the microchannel, strongly enhancing the liquid−particle interaction, as demonstrated by direct and sandwich immunoassays.

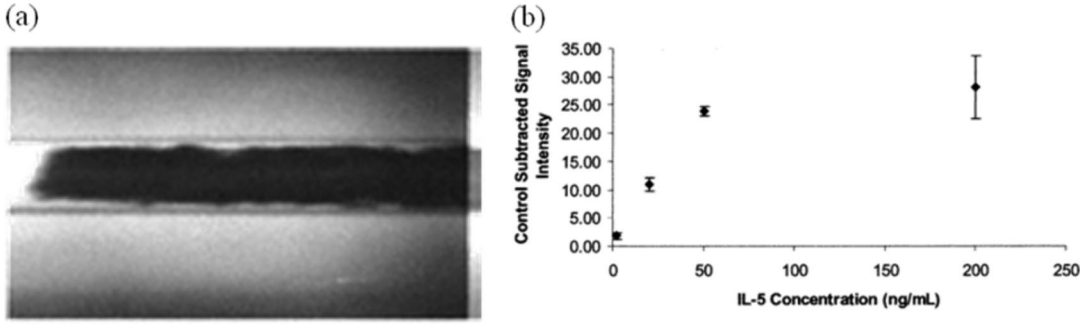

Figure 27. (a) Micrograph of part of a packed bed of 1−2 μm diameter magnetic particles within a 50 μm diameter fused silica capillary in the presence of a 0.236 T magnetic field. The total packed bed is ~1.2 mm in length and has ~2.4 nL volume. (b) Calibration curve of interleukin-5 (IL-5) generated from a sandwich immunoassay performed on the magnetic particles. Biotinylated rat monoclonal antimouse IL-5 was immobilized as c-Ab on the magnetic particles, to bind to a mouse IL-5 t-Ag; FITC-conjugated rat monoclonal antimouse IL-5 was the d-Ab. Reprinted with permission from ref 207. Copyright 2001 American Chemical Society.

A 1 ng/mL detection limit was obtained for mouse IgG. The assay was executed either integrally on-chip while consuming nanoliter volume of sample and reagents,[206,220] or part of the protocol was performed off-chip.[433] Another promising solution to retain magnetic beads was to combine solenoids, for generating a current-activated controlled magnetic field, with a microfluidic device for the execution of a low-volume immunoassay.[398] When placed close to the microchannel, two solenoids (obtained by winding copper wires on a ferromagnetic bar) generated a strong magnetic field gradient that was sufficient to trap the magnetic beads in a flowing stream and execute immunoassay experiments. Goat IgG was analyzed in a sandwich immunoassay with a 5 ng/mL detection limit. In contrast to their use for magnetic bead retention, permanent magnets can also be used to generate a magnetic force to displace magnetic particles perpendicularly to multiple colaminar streams containing sample, washing, and reagent solutions.[399,434] In this way, complete immunocomplex formation or multistep biochemical processes can be implemented. A magnetic bead-based microflow cytometer with integrated sample pretreatment module was used for the purification, concentration, detection, and collection of target viruses (dengue virus serotype 2).[426] Instead of using PCR techniques, the system proposed to detect the target virus by using magnetic bead-based flow cytometry. By sandwich magneto-immunocomplex formation, target viruses in blood or serum could be captured and separated magnetically, followed by a sorting step based on the presence of a fluorescent Ab for identifying the surface t-Ag of the target viruses. Virus samples with a concentration of 13 plaque-forming unit/mL (PFU/mL) could be detected.

Also, a sandwich immunoassay using streptavidin-coated beads as substrate and completely performed on-chip was presented.[96] The beads were electrostatically self-assembled on aminosilane micropatterns at the bottom of a microfluidic channel. Mouse IgG diluted in PBS with 1% bovine serum albumin (BSA) solution was used as t-Ag and detected down to a concentration of 15 ng/mL in stop-flow mode and 250 pg/mL in continuous flow mode, using 1.3 μL of sample volume. In other work, a monolithic and fully integrated complementary metal oxide semiconductor (CMOS) chip was presented for the manipulation and detection of single fluorescent magnetic beads in a PDMS microchannel positioned on top of the chip.[418] Magnetic manipulation was done by current actuation of microcoils on the silicon chip, and detection was achieved using single photon avalanche diodes that are located in the center of each microcoil and count the fluorescent photons originating from a single magnetic bead. This approach permitted microscope-less fluorescence detection with high sensitivity. Detection of murine monoclonal Abs with a limit of 1 ng/mL was reported in a noncompetitive sandwich immunoassay, performed using the bead surface as assay substrate.

7.1.2. Enzyme Reaction-Based Detection

Enzymatically Generated Fluorescence. Important work in miniaturized enzymatic reaction-generated fluorescence detection was reported by Hermann et al.[419] These authors have developed a microfluidic system enabling the execution of parallel ELISA experiments (see Figure 28). In their system, the magnetic beads are trapped in a reaction chamber by an external permanent magnet and capture the t-Ag of interest. This step is followed by the generation of a fluorescent signal during an enzymatic reaction in stop flow conditions. Additionally, the magnet is displaced along microfluidic chambers, dragging the magnetic beads with it and allowing an efficient mixing. To reduce the assay noise due to nonspecific adsorption of Abs to the microchannel wall, a dual network of channels between which the magnetic beads are transferred is used. In a first network, the immunocomplexes are formed by flowing appropriate solutions of sample and reagents, while the enzymatic reaction is performed in the other channel. The networks are linked using fluidic bridges controlled by pressure activated valves, ensuring the complete isolation of the two chambers and avoiding contamination. After the enzymatic reaction, the generated fluorescent solutions are driven away from the magnetic beads (simultaneous stopping all reactions) to parallel microchannels for detection. An off-chip antistreptavidin immunocomplex was formed by direct linking model and detection Ab to streptavidin-coated magnetic nanoparticles.[400] This direct immuno-assay was quantified on-chip using enzymatically generated fluorescence down to an antistreptavidin Ab concentration of 12.5 pg/mL. The same authors have also demonstrated on-chip the formation of an immuno-complex consisting of two antibodies[401] on magnetic particles. Antistreptavidin was used as a model Ab and was detected down to a 100 pg/mL concentration. Detection of tumor necrosis factor-α (TNF-α) was demonstrated down to 45 pg/mL in a complete assay time of less than 1 h.[419] Other authors have presented a droplet-based assay, where magnetic bead manipulation was combined with electrowetting, and showed detection of human insulin and interleukin-6 with a detection limit of ~250 pg/mL using enzymatically generated chemiluminescent detection.[403]

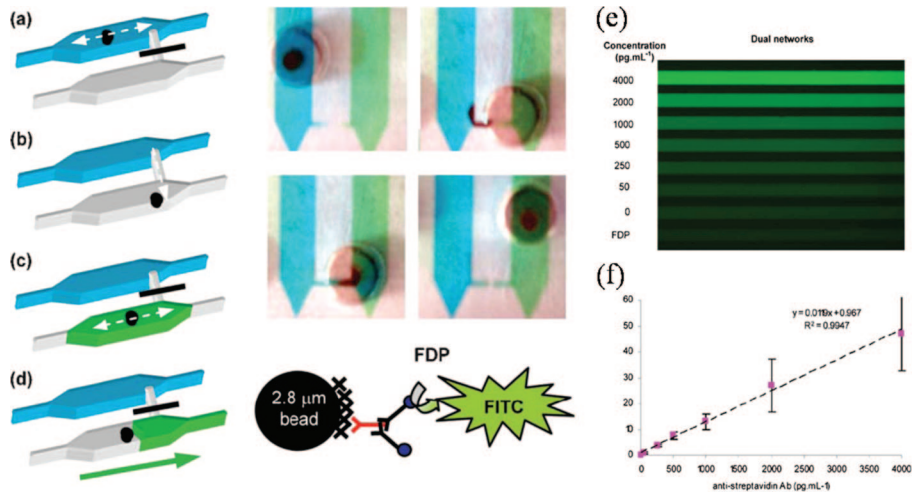

Figure 28. Schematic of the immunocomplex formation and detection in a dual channel network microfluidic system. (a) About 10^6 streptavidin-coated magnetic beads are trapped inside the complexation chamber. The antistreptavidin antibody (t-Ag) binds specifically to the streptavidin-coated beads during a 5 min incubation period with mixing. Similarly, the alkaline phosphatase (AP)-coupled d-Ab is added to form the reactive immunocomplex. (b) The valve is transiently opened, and the reactive beads are magnetically transferred into the reaction chamber. (c) The AP enzyme processes the fluorescein diphosphate (FDP) substrate into the fluorescent molecule FITC. While the reaction takes place, the solution is homogenized by displacing the beads. (d) The reacted solution is then pushed into the detection area. (e) Microfluidic ELISA results obtained without pretreatment of the microfluidic channel against nonspecific adsorption: simultaneous fluorescent detection in all eight channels of the device. (f) Standard curves for the quantification of antistreptavidin antibodies. Each point represents the average obtained in four separate experiments. Reprinted with permission from ref 401. Copyright 2007 The Royal Society of Chemistry.

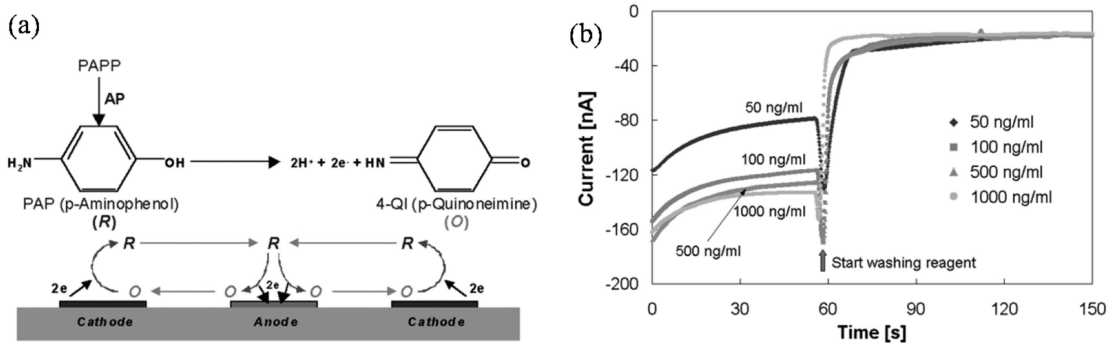

Figure 29. (a) Enzymatic reaction for electrochemical detection: *p*-aminophenyl phosphate (PAPP) is converted by the enzyme AP, which is the label chosen for the d-Ab, to the electrochemical product *p*-aminophenol (PAP). The latter is then converted at the interdigitated electrodes to 4-quinoneimine in a 2-electron oxidation process. (b) Immunoassay results measured by chronoamperometric detection of the conversion of PAP. Reprinted with permission from ref 405. Copyright 2002 The Royal Society of Chemistry.

Colorimetric Detection. In colorimetric detection, the products obtained after enzymatic conversion are chromogen and have negligible fluorescence. This technique is less sensitive than fluorescence, but can be developed using a normal microscope equipped with a camera. Its application for an immunoassay in the microfluidic format was demonstrated by Lehmann et al.[404] in a water-in-oil droplet-based system. The system consisted of a two-dimensional array of coils disposed under an oil bath with a bottom Teflon layer, surrounded by strong permanent magnets to generate a permanent magnetic field perpendicular to the Teflon surface. The latter can be locally hydrophilized by an air plasma to form several 10 μL reaction zones, in which water droplets containing sample and reagent solutions were immobilized. When activating the appropriate coils, the magnetic beads move within an aqueous droplet along the chip surface and between the different droplet reservoirs. This unique displacement technique permits one to bring into contact successively t-Ag (down to a 150 ng/mL concentration) with enzyme labeled d-Ab, and enzyme substrate, without contamination between each of the steps. Another colorimetric reaction in a water-in-oil droplet-based system was the hydrolysis of *p*-nitrophenylphosphate substrate (down to 500 μg/mL) using alkaline phophatase as the enzyme.[435]

Electrochemical Detection. When the enzymatic reaction converts the enzyme substrate to a detectable electrochemical product, the immunoassay can be detected using electrochemistry. The advantage of this technique is the possibility to convert a biological recognition reaction in an electrical parameter that can be directly detected by an electronic sensor and system for further signal analysis. Experimentally, a potential is applied between electrodes soaked in the sample solution, and a current due to the oxidation of the electrochemical product is detected. As the transport of the electrochemical product from the bulk solution to the electrode surface is limited by diffusion, the immunocomplex has to be located close to the electrochemical sensor for good detection efficiency.

An efficient solution to localize c-Ab-coated magnetic particles at the bottom of a microchannel is to use a planar electromagnet constituted of serpentine coils embedded in an electroplated permalloy structure.[405] When activated, the coil generates a magnetic field that magnetizes and traps the magnetic beads. Thereafter, solutions of t-Ag and d-Ab

labeled with the enzyme *p*-aminophenyl phosphate (PAPP) are introduced in the microchannel, and immunocomplexes form. The t-Ag detection is performed by flowing the enzyme substrate through the microchannel. The substrate is converted in an electrochemically detectable product, and electrochemical detection is performed using interdigitated microelectrodes (see Figure 29) placed on top of the coils. This way, the detection limit for mouse IgG, which was chosen as the t-Ag, was <50 ng/mL. Another solution for magnetic bead trapping in a lab-on-a-chip module was to use an electroplated permalloy microarray at the bottom of the microfluidic chip, flanked by two strong permanent magnets.[406] When covered by a microfluidic channel, the beads are trapped at the location of the magnetic posts. Once immunocomplexes were formed, an array of interdigitated microelectrodes disposed at the top of the magnetic pattern was activated for the electrochemical detection (detection limit 16 ng/mL for mouse IgG). Another group proposed an electrochemical immunosensor that pulls t-Ag bound to magnetic nanoparticles from a laminar flow to a gold electrode by applying a local magnetic field gradient.[427] This selectively removes the particles from flowing biological fluids without any washing steps. A set of five disk-shape gold electrodes coated with c-Ab and an Ag/AgCl reference electrode was used to detect changes in electrode potential due to the binding of the t-Ag with the c-Ab. As t-Ag, four different tumor markers were detected in a simultaneous multiple assay (detection limit 0.5 ng/mL), by using four types of magnetic nanoparticles coated with specific Abs. The complex formation between the t-Ag at the magnetic bead surface and the d-Ab immobilized on the gold electrode permits a time-dependent observation of the electrical potential between the electrodes, the response of which is directly related to the tumor marker concentration. Note that no enzyme reaction was necessary in this potentiometric detection approach.

7.2. Magnetic Beads as Label for Detection

Besides the utilization of magnetic particles as reaction substrate in an immunoassay, they have also shown promising results when used as label. The principle of using magnetic particles as detection label in an immunoassay is presented in Figure 30. The method consists of first coating the surface of the biosensor with a c-Ab (using, for example, techniques developed for microtiter plate-based immunoassays) and blocking the remaining sites that are not occupied by c-Ab. Next, the t-Ags are flown through the reaction chamber, and the immunoreaction between c-Ab and t-Ag occurs. A solution of magnetic particles functionalized by the d-Ab that is complementary to the t-Ag is then introduced in the chip, forming a magneto-sandwich. The formation of the immunocomplex, and thereby the presence of t-Ag, is revealed by detecting the presence of the magnetic particles. As the quantity of immobilized particles will depend on the number of formed immunocomplexes, a quantitative assay is possible. Different techniques for detecting the presence of the magnetic particles, essentially of optical and/or magnetic nature, have been investigated.

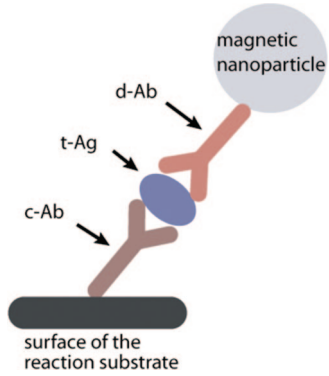

Figure 30. Schematic of immunocomplex labeling with a magnetic nanoparticle. The sandwich immunocomplex with magnetic nanoparticle label is linked to the reaction substrate. The immunocomplex formation is detected by detecting the presence of the particle.

7.2.1. Surface Coverage Measurement

The simplest method to detect surface-linked magnetic particles is to measure optically the fraction of the substrate surface that is covered, and then calculate the number of immuno-magnetosandwich complexes that are formed. Because the number of particles attached to the surface can be, in principle, as low as the number of immunocomplexes, the technique potentially is very sensitive. However, nonspecific surface adsorption of the magnetic particles can pose a problem and asks for strategies to obtain a minimal background signal. A perfect control of the surface chemistry and optimized washing protocols are therefore very important. Parameters like the surface zeta potential were optimized to allow an optimal c-Ab binding, while different types of magnetic particles, which either bind specifically or nonspecifically to the substrate, were studied.[421,436] Techniques to mechanically remove nonspecifically bonded magnetic beads have been investigated.[407,437] This permits one to reduce the background noise during measurements and therefore increases the test sensitivity. Different approaches using liquid flow shear forces, mechanical pulling using a magnet, or centrifugation have been proposed.[407,437] A potential bottleneck is that the transport of highly diluted analytes from the bulk of the solution to the sensor surface due to normal diffusion is slow, so that only a small fraction of the analyte can reach the sensor surface in a reasonable time. This effect strongly limits the sensitivity of the system. To accelerate the molecular transport beyond what is possible by diffusion, external forces can be applied, for example, electrophoretic forces, for analyte concentration near the surface.[414] In other work, 500 nm magnetic beads were specifically attached to an optically transparent and functionalized sensor surface.[430] A specific immunoreaction resulted in a surface coverage with beads that was quantified using the internal reflection of a light beam from the back of the surface. The cardiac marker Troponin I could be detected down to concentrations of the order of 20 pg/mL and drugs of abuse down to a concentration of 1 ng/mL, taking as samples blood plasma and whole saliva. Overall, the most important advantage of the surface coverage measurement technique is the absence of the need for a complex detection system. In principle, a camera mounted on a microscope and connected to a computer equipped with image treatment software is sufficient.

Multiple and parallel immunoassays were demonstrated with good sensitivity.[407,437] The protein S100$\beta\beta$, a marker for stroke and minor head injury, was detected down to 2 pg/mL.[420,421] 300 nm magnetic particles in combination with strong rinsing and a blocking step allowed for the best specific and sensitive detection of S100$\beta\beta$ in serum over a wide concentration range. Also, an ultrasensitive, two-step

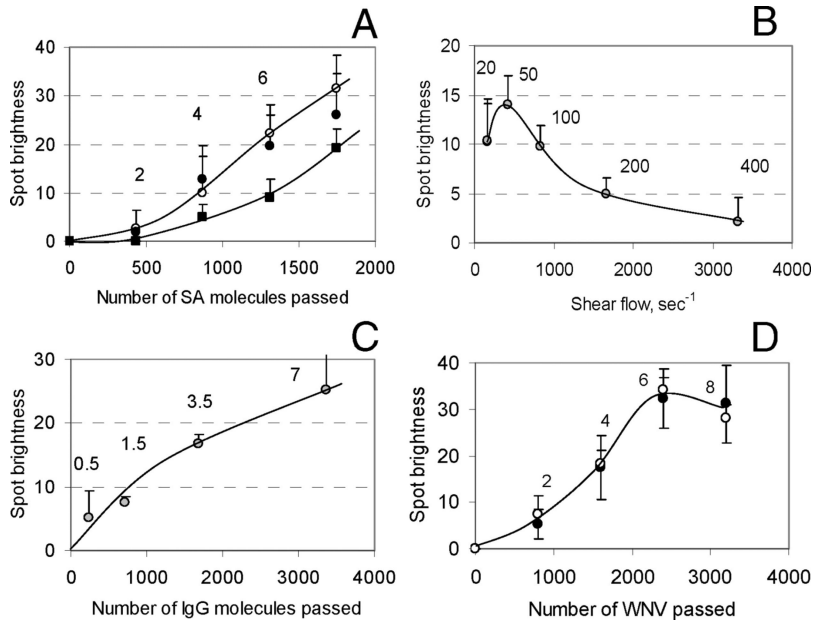

Figure 31. Dependence of spot brightness on the number of analyte molecules passed through the flow cell and on the magnetic bead shear flow. The spot brightness is due to the presence of immobilized magnetic particles and is observed by dark-field optical microscopy. (A) Streptavidin (SA) molecules captured on anti-SA-IgG array from buffer solution (○), from the same buffer containing 1% dialyzed chicken serum (●), and 10% chicken serum (■) at a flow rate of 20 μL/min. (B) Dependence of the signal on the shear flow upon electrophoretic capturing of SA for 4 min. Numbers over points denote flow rate in μL/min. (C) Antiovalbumin-IgG captured on an ovalbumin array at a flow rate of 60 μL/min. (D) Assay of viruses in serum from West Nile virus (WNV)-infected chickens. The serum was dialyzed against water, diluted 1:200 with buffer, and WNV antigens were captured on an array of anti-WNV-IgG (●). The same procedure was followed for a sample purified by exclusion chromatography (○). The flow rate of the sample solution was 20 μL/min. The numbers above the experimental points in panels A, C, and D denote the time of capture in min. Reprinted with permission from ref 414. Copyright 2007 American Chemical Society.

immunoassay method was developed for rapid assay of proteins and viruses using dark-field optical microscopy detection of immobilized magnetic beads.[414] In the first step, electrophoresis was used to quickly bring soluble analytes from a flowing solution to a microarray of probe molecules immobilized on a semipermeable membrane. In a second step, the captured analyte was detected by scanning the microarray with functionalized magnetic beads, which passed over the array surface by shear flow and were pressed to the array surface by a magnetic field. This method routinely detected analytes in concentrations as low as 20 aM (1 fg/mL) (500−1000 molecules detected) within 2−3 min in the presence of a 10^{11}-fold excess of other protein molecules in the sample (see Figure 31), which is a truly impressive result! In the same line, other authors described a semihomogeneous implementation of a fluidic force discrimination assay, detecting in 10 min the toxin RCA (*Ricinus communis* agglutinin) and a staphylococcal enterotoxin B with a 35 aM (1 fg/mL) detection limit.[423] In a pure sequential assay,[391] the c-Abs, which are immobilized on a surface, capture t-Ag, a secondary Ab, and Ab-conjugated magnetic bead labels. In the mentioned semihomogeneous assay, the t-Ag, secondary Ab, and the beads are first mixed in solution, and then applied to the substrate covered with c-Ab. Nonspecifically bound beads were removed by controlled laminar flow fluidic forces, and the remaining beads were counted to determine the t-Ag concentrations.

7.2.2. Magnetic Properties Measurement

Manipulating and positioning functionalized magnetic beads in microfluidic devices and monitoring the surface coverage is clearly very interesting for high-sensitivity immunoassays. An alternative way of detecting the presence of the beads on a surface, rather than optically observing them, is to probe the changes in the magnetic environment due to the presence of the beads. This is an interesting approach, because magnetic sensors can be integrated in the chips, and the detection signal can be converted on-chip for analysis using electronics. Furthermore, the magnetic properties of the particles are, in most cases, independent from the immunoassay protocol. A disadvantage for disposable applications, however, is that this will add cost to the system, when comparing with the surface coverage method, due to sensor fabrication (often on a silicon substrate) and integration of the sensor in a microfluidic package.

Magnetic Force Discrimination. A first approach to use the magnetic properties of the magnetic beads is to link a fluorescent polystyrene microparticle (1−5 μm diameter) coated with c-Ab in an immunoreaction via a t-Ag, to magnetic nanoparticles (10−50 nm diameter) functionalized with d-Ab. Applying then a magnetic field gradient into a microfluidic device induces a displacement of the microparticle−nanoparticles complex. The trajectory of such complex can be measured by fluorescent microscopy and directly correlated to the presence of t-Ag in the sample. Without t-Ag, no displacement of the fluorescent particle is observed. This concept was exploited to detect the presence of rabbit IgG and mouse IgG with a detection limit of 250 pg/mL and 15 ng/mL, respectively, in a microfluidic device.[408] The latter consisted of a microchannel (connected to a sample inlet and particles inlet), to which a magnetic field gradient is applied using a permanent magnet placed at the side of the microchannel. This measurement principle was further implemented by integrating a nickel electroplated magnetic core to enhance the particle deviation. The detection of human Immunoglobulin E involved in allergen reactions was

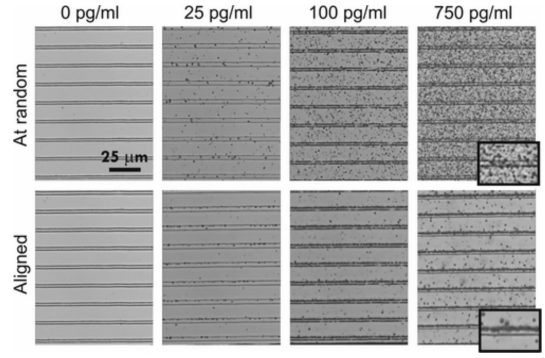

Figure 32. Optical micrographs showing the presence of magnetic particles on the sensor surface for different concentrations of the protein S100$\beta\beta$. The positioning of the magnetic particles before (at random) and after (aligned) release and alignment with the edges of the GMR sensors is illustrated. A scale bar is shown in the top left image. Reprinted with permission from ref 420. Copyright 2007 American Chemical Society.

performed in clinical samples from patients down to a concentration of 40 pg/mL.[422]

Detection with a Giant Magnetoresistance (GMR) Sensor. A sensitive magnetic particle detection technique is to use the GMR effect.[191,409] When a magnetic bead is positioned over or near a GMR sensor, the resistance of the magnetoresistor decreases due to the stray field of the magnetic bead, and the presence of the particle can be directly correlated to the detected signal.[191,372,391,409,420] This detection technique can also be associated with surface coverage measurements and can benefit from all advances made with the surface coverage technique, such as surface chemistry control, or nonspecific magnetic bead removal. For example, a GMR chip of the type shown in Figure 10 has been used to detect 312 pM (10 ng/mL) RCA in serum. De Palma et al.[420] have demonstrated a highly sensitive biosensor by executing immunoassay experiments in a two-step protocol. In a first step, magnetic beads are used to label an optimized magneto-sandwich immunoassay at the surface of a biosensor. After nonspecific bonded magnetic beads are removed, the number of remaining beads is proportional to the t-Ag concentration. Next, in a second step, the remaining beads are released from the substrate using a NaOH solution and concentrated using magnetic forces to a GMR sensor array. This magnetic attraction permits one to relocate the magnetic beads on the most sensitive parts of the GMR sensors (see Figure 32). This technique has allowed the development of an immunoassay for S100$\beta\beta$ proteins with a two-decade dynamic range and a detection limit of 27 pg/mL. Other authors proposed a compact GMR biosensor system that uses actuated magnetic bead labels incorporated in an immunosandwich.[428] For the measurement of parathyroid hormone, a detection limit in the 10 pM range (40 pg/mL) was achieved with a total assay time of 15 min, when 300 nm diameter magnetic beads were used. For 500 nm particles (with a longer-range magnetic stray field), the detection sensitivity was 4 pg/mL.

Other Magnetic Bead Detection Principles. An array of Hall sensors has also been used to measure the presence of magnetic particles that were substrate-linked via an immunocomplex. The Hall chip was realized in CMOS technology and contained 120 sensor elements.[425] A sensitivity of 1 ng/mL was obtained for the detection of mouse IgG, and also the detection of human antidengue virus IgG in serum was reported. Another possibility for detecting substrate-linked magnetic particles is by placing detection coils underneath the substrate.[429] When the magnetic particles were present and magnetized, the inductive load of a coil changes, and the coil inductance or resonance frequency of the coil circuit (around 7 MHz) provided a measure for the concentration of a t-Ag. As model system, Troponin I, a cardiac marker, was detected down to 0.5 ng/mL.

In other work, the frequency dependence of the imaginary part of the magnetic susceptibility of magnetic nanoparticles suspended in a liquid allowed measurement of the rotational Brownian relaxation for 40 nm diameter magnetite particles covered with an avidin layer. This concept was used to demonstrate experimentally the correlation between the peak shift of the AC imaginary part of the nanoparticle susceptibility and its hydrodynamic radius, after binding biotinylated proteins anchored to T7 bacteriophage particles on the avidin shell.[412,413] The nanoparticle hydrodynamic diameter could also be optically measured by monitoring the frequency-dependent magnetic relaxation signal.[411] When biomolecules are bonded to the nanoparticle surface, an increase of hydrodynamic diameter is observed. This diameter change was observed in an iron oxide ferrofluid exposed to goat IgG.

A portable system for rapid purification, concentration, and detection via surface plasmon resonance (SPR) of target analytes from complex matrixes was presented using antibody-coated superparamagnetic nanoparticles.[424] The SPR signal due to surface-bound *Staphylococcus* enterotoxin B was dramatically increased when superparamagnetic particles were used as detection amplifiers: a concentration of 100 pg/mL was easily detected in both buffer and stool samples.

7.3. Agglutination Tests

Agglutination tests exploit the fact that dispersed particles that are grafted with c-Ab form aggregates when they are mixed with a t-Ag-containing fluid. This liquid medium can be serum or blood, and agglutination tests are therefore generally simple, cheap, and do not require sophisticated equipment, nor highly specialized skills. A number of agglutination protocols and grafting techniques have been presented, including the use of magnetic particles.[56] In a magnetic colloid, the particles have a repulsive interaction, which in principle precludes formation of doublets or larger clusters. However, when a magnetic field is applied, the particles can approach each other and form chains. Irreversible and specific particle clustering or doublet formation is observed after switching off the magnetic field. Detection of these formed clusters, when the agglutination test is performed in a microtiter plate (i.e., a nonmicrofluidic format), is by turbidimetry.[438] For example, a limit of detection of 1 pmol/L (45 pg/mL) was reported for ovabulmine in phosphate buffer.[439] The method also leads to kinetic information on immunoreactions. A magnetic microparticle agglutination test in a PDMS microfluidic channel was reported for the detection of biotinylated Protein A.[410] Although dose−response curves were not provided, the first experiments suggested that analytical sensitivities in the ~1−2 pg/mL range are achievable. This interesting result is due to the fact that, by forcing the analyte through a limited number of magnetic particles using microfluidic flow, sample capture is much more efficient than when operating the agglutination assay in the batch format. Other work presents the dynamic actuation of a confined plug of functionalized magnetic beads in a microchannel allowing for analyte

capture with improved efficiency.[415] Here, an original diffusion-based detection method of the aggregated particles was presented. The feasibility of an on-chip agglutination assay was demonstrated by means of the streptavidin/biotinylated-BSA model system. A detection limit of 100 pg/mL confirms the high potential of this approach.

Other authors presented a laminar-flow based device for separation of individual magnetic nanoparticles (5 nm) from agglutinated clusters.[440] The isolated 5 nm magnetic nanoparticles did not exhibit significant magnetophoretic velocities, but did exhibit high magnetophoretic velocities when aggregated by the action of a pH-responsive polymer coating. A simple external magnet is used to magnetophorese the aggregated particles that have captured a t-Ag (streptavidin) from a lower pH laminar flowstream (pH 7.3) to a second higher pH flowstream (pH 8.4) that induces rapid disaggregation of the clusters, after which the individual magnetic nanoparticles are transported to the output chamber. This stimuli-responsive reagent system has been shown to transfer 81% of the streptavidin from an input flowstream to a second flowstream in a continuous flow mode.

8. Catalytic Applications

8.1. Homogenizing Heterogeneous Catalysis Using Magnetic Particles

A field where magnetic particles have potential to play an important role is catalysis. Introduced in small quantity as compared to other reagents in the system, the catalyst is a substance that enhances the reactivity between reagents, but is not consumed during the chemical reaction. Catalysis is generally separated into two subclasses: homogeneous catalysis, where the catalysts are totally spread (dissolved) in the reaction media, and heterogeneous catalysis, where they are attached to a supporting matrix or surface. Homogenous catalysis is the most efficient, as all catalytic sites are easily accessible to reagents. However, homogeneous catalysis suffers from an important drawback: it is difficult to separate the catalyst from reaction products at the end of the reaction process.[441] Separation methods like distillation require high temperature, which may cause thermal stress that degrades the catalyst molecules, while other separation processes (for example, solvent extraction or chromatography) result in catalyst loss. Also, final reaction products are often contaminated by catalysts. As the last ones are in general toxic (for example, a heavy metal), contamination has to be strictly limited.

Heterogeneous catalysis partially overcomes these drawbacks. Here, the catalysts are immobilized at the surface of a supporting (and when possible soluble) matrix and are recovered after reaction by separation (for example, precipitation and/or filtration) from the reaction products. However, a subsequent decrease of catalytic activity and selectivity is generally observed during reactions. It is due to steric effects from the support, which limits reagent diffusion to the surface-anchored catalysts. Also, the bonds between the catalyst and the ligand are often broken and reformed during catalytic reactions. If this happens, the catalyst may break away from the support and become dissolved. This "leaching" problem leads to loss of activity of the catalyst, when it is used with a continuous liquid flow. Reduced leaching has been observed when the catalyst was anchored inside the pores of zeolites or of mesoporous solids.[441]

Magnetic nanoparticles can be used as the support for catalysts and can facilitate their separation from the reaction media.[442−446] However, the low surface energy and easy aggregation of magnetic nanoparticles can hinder their practical applications. To overcome these drawbacks, magnetic nanoparticles have also been introduced in various mesoporous silica structures.[447,448] These types of magnetic nanoparticle-based materials, which combine the advantages of both mesoporous silicas and magnetic particles, are potentially very interesting supports for the immobilization of catalysts. Table 5 presents typical applications of magnetic nanoparticles in catalysis. The cited papers are discussed further in more detail, but here we will not give an exhaustive overview of the use of magnetic nanoparticles in catalysis, as most of the work deals with the application of a permanent magnet to recover the magnetic nanoparticle-supported catalyst from the reaction mixture. The role of microfluidics in this field is still minor.[449,450]

8.2. Transition Metal Catalysts

In many catalysis applications, a transition metal is used as catalyst to transform or bind reagents. The good catalysis activity of those elements is due to their ability to have various oxidation states helping electron transfer or, in the case of metals, to adsorb other substances onto their surface and activate them in the process. Palladium (Pd) is employed to catalyze various chemical reactions, such as hydrogenation,[456,457] Heck,[445,453,454] Suzuki,[445,446,463] or Sonagashira[445] cross-coupling reactions. When using magnetic nanoparticles, different strategies are employed to link Pd atoms to the magnetic nanoparticle surface. The metal can be either complexed using ligands, chemically bonded, or directly immobilized or incorporated to the nanoparticle surface using a supporting matrix. The functionalized magnetic nanoparticles demonstrate a high conversion yield in the reported

Table 5. Application of Magnetic Nanoparticles as Support for the Catalysis of Typical Chemical Reactions

reaction	catalyst	ref
atom transfer radical polymerization	CuBr	451
epoxidation	Mo	452
Heck	Pd	445, 453, 454
hydroformylation	Rh	442, 455
hydrogenation	Pd	456, 457
hydrogenation	Pt	458
hydrogenation	Ru	443
hydrolysis (biocatalyse)	*Candida rugosa* lipase	459, 460
hydrolysis (biocatalyse)	pair of amino acid residues	461
hydrolysis (biocatalyse)	2-pralidoxime	462
Sonagashira	Pd	445
Suzuki	Pd	446, 463
PenicilinV degradation	β-lactamase	464

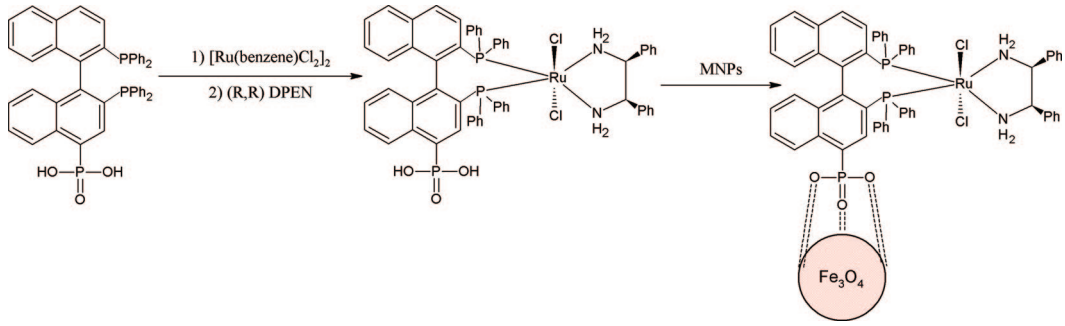

Figure 33. Schematic representation of the immobilization of chiral Ru catalyst on magnetic nanoparticles. Reprinted with permission from ref 443. Copyright 2005 American Chemical Society.

applications, with a minor loss of catalysis efficiency after several runs. An interesting approach was demonstrated by Zheng et al.,[446] who have used functionalized 4 nm magnetic particles to transport and immobilize the catalyst into a conventional solid-phase resin. After reaction, the catalysts are recycled from the solid phase reaction support using magnetic forces, while reaction products are chemically separated from the resin. Chiral catalysis, using ruthenium atoms complexed to the magnetic nanoparticle surface, was demonstrated for the hydrogenation of aromatic ketones.[443] Heterogenized asymmetric catalysts were synthesized by immobilizing preformed Ru catalysts on magnetite nanoparticles via the phosphonate functionality (see scheme of Figure 33). The immobilized catalysts were easily recycled by magnetic decantation and reused for up to 14 times without loss of activity and enantioselectivity.

Rhodium (Rh) is also a well suitable transition metal that can be used for catalysis. Complexed to the surface of magnetic nanoparticles using appropriate ligands[455] or dendrons grown on silica-coated nanoparticles,[442] Rh was used to catalyze hydroformylation reactions. The advantage of using dendrons is the increase of the solubility of the catalysis body in the reaction medium. Excellent reaction yield and enantioselectivity were observed for both immobilization methods. To fully exploit the large surface area of magnetic nanoparticles, a magnetic cobalt core surrounded by a shell of Pt metal was used for the hydrogenation of several compounds.[458] The catalytic activity of the particles demonstrated high efficiency, except for reagents with unfavorable steric interactions with the magnetic nanoparticle surface. Under favorable conditions, the catalytic activity still reached a yield of 100% after seven cycles of reaction and recycling. Used, for example, in olefin epoxidation, molybdenum is another transition metal involved in many catalysis reactions. Using a mesoporous matrix generated by the calcination of sol−gel polymerization products, Mo atoms were attached to a magnetic nanoparticle surface.[452] The catalytic activity of the composite nanoparticles was demonstrated by the epoxidation of several alkenes with high yield, even after six cycles of recycling. Besides the use of functionalized magnetic nanoparticles for small molecule reactions, the polymerization of methyl methacrylate by atom transfer radical polymerization was investigated using magnetite nanoparticles to support a copper(I) bromide (CuBr) catalyst.[451] Under optimized conditions, the catalytic activity of the functionalized nanoparticles was kept at a high level. Furthermore, adjusting the experimental conditions permitted one to synthesize a block copolymer with controlled molecular weight and low polydispersity.

8.3. Biocatalysts

Thanks to advances in magnetic nanoparticle functionalization with organic molecules or proteins, magnetic particles have the potential to support biocatalysts and enzymes. Biocatalysis can be highly selective and permits one to transform organic compounds. Different biocatalysts are available to functionalize magnetic nanoparticles. *Candida rugosa* lipase has been investigated as biocatalyst for the hydrolysis of *p*-nitrophenolbutyrate.[459] Results have shown a lower enzymatic activity for the immobilized enzyme, as compared to the free one. However, the enzymatic activity of the functionalized magnetic nanoparticle was kept constant during several runs (with a slight activity decrease of 2% due to enzyme denaturation after a period of 14 days) and found to be higher as compared to lipase immobilized on standard micrometer-size polymeric microbeads. To exploit the selectivity of *Candida rugosa* lipase enzyme, the resolution of racemic carboxylates was demonstrated on molecules substituted by different alkyl chains.[460] The enantiometric excess was systematically superior to 99%, as measured by gas chromatography (comparable to those found for the free solution enzyme). In other work, the immobilization of β-lactamase by chemical linkage to a magnetic nanoparticle surface was used for the degradation of PenicilinV in phosphate buffered water.[464] The enzyme activity was found to be 54% as compared to the free enzyme in solution, with a slight decrease in efficiency after catalysis reaction.

An interesting approach for the use of magnetic nanoparticles as biocatalyst support was developed by Zheng et al.[461] These authors have used the nanoparticles to support pairs of amino acid residues for the hydrolysis of pesticides. The crucial choice of the biomolecular pair permits one to mimic natural biocatalysts for the cleavage of phosphor ester and carboxylic ester bonds, without using severe pH or transition metal-based catalysis. Furthermore, the functionalized particles kept their catalytic activity after several months of synthesis. In the same area, the immobilization of common antidote, 2-pralidoxime, to a magnetic nanoparticle surface permitted it to degrade by hydrolysis organophosphorus pesticides responsible for serious diseases.[462] With an activity comparable to that found for transition metal-based catalysts, this method permits one to develop a safe and nonpolluting alternative for the destruction of pesticides, without the use of extreme pH or experimental conditions. Other authors have electrochemically detected the pesticide carbofuran, by investigating the inhibition by this pesticide of the enzyme acetylcholinesterase immobilized on magnetic beads. Carbofuran could be detected down to a few ppb thanks to this on-chip enzymatic inhibition reaction.[465]

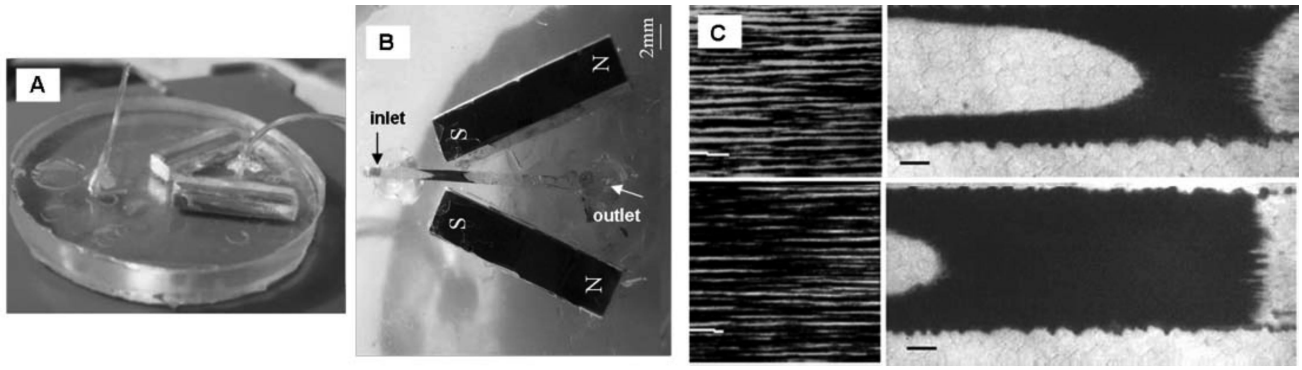

Figure 34. Experimental setup used for the protein digestion experiments. (A) Picture of the PDMS chip with the microchannel (0.25 × 20 × 1 mm^3) and its two inlet−outlet plastic tubings. (B) Expanded view of the magnetic beads immobilized between the two magnets in the microchannel. (C, left) Details of the magnetic beads arrangement at an early and late stage of microplug formation. The orientation of the bead arrays parallel to the channel's axis, providing a low flow resistance and uniform pore size, is visible (white scale bar, 5 μm). (C, right) View of the whole plug at the beginning and end of the plug's formation at a lower magnification (black scale bar, 200 μm). Reprinted with permission from ref 468. Copyright 2008 The Royal Society of Chemistry.

8.4. Magnetic Particle-Based Protein Digestion

A field of activity, where microfluidics has clearly gained a stronghold, is that of proteolysis or protein digestion. Proteolysis is the directed degradation (digestion) of proteins by cellular enzymes, called proteases, or by intramolecular digestion. For example, trypsin is a serine protease found in the digestive system, which predominantly cleaves peptide chains at the carboxyl side of the amino acids lysine and arginine, except when either is followed by proline. It is used for numerous biotechnological processes. Trypsin is commonly used in biological research to digest proteins into peptides for mass spectrometry analysis. It can also be used to dissociate dissected cells (for example, prior to cell fixing and sorting). A promising field, in which magnetic particles in combination with microfluidics can play a determinant role, is the development of microreactors for proteomic applications.[466] Magnetic particles that are grafted with enzyme very efficiently proteolyze the proteins of interest, by simply flowing the latter through the porous magnetic plug. The practical advantage of the microfluidic magnetic particle-based digestion system is that the magnetic matrix can be easily replaced by flushing out the beads and loading new beads into the same channel. Also, grafting on particles can be performed ex situ in large quantities, allowing for reduced cost and better reproducibility.

Grafted trypsin magnetic beads were used in a microfluidic channel for performing protein digestion. Retained as self-assembled magnetic particle chains in a microchannel, thereby forming a porous matrix, the particles are used to digest several types of protein samples from a flow for subsequent analysis.[467] Figure 34 shows the experimental microfluidic channel with the porous magnetic particle plug. Kinetics studies of the hydrolysis of a model peptide show a 100-fold increase in digestion speed obtained by the microfluidic system when compared to a batch-type system. High performance and reproducibility for digesting recombinant human growth hormone are confirmed by analyzing the digested products by both capillary electrophoresis and matrix-assisted laser desorption/ionization time-of-flight mass spectrometry (MALDI-TOF).[467] Anhydrotrypsin, an inactive form of trypsin, with an affinity for certain peptides was grafted on magnetic microparticles to digest a model peptide, human neurotensin, for subsequent mass spectrometry analysis.[467] The same system was used for proteinase K-mediated protein digestion as a step toward the elaboration of a fully integrated device for the detection of pathological prion protein.[468] Reaction kinetics were typically accelerated 100-fold as compared to conventional batch reactions. The proteolytic microsystem was also applied to the digestion of prion protein from brain tissues, and the difference in digestion efficiency between the normal and pathological form was very significant. Other authors reported on the use of trypsin-functionalized magnetic particles of various size (50−300 nm diameter) to digest cytochrome c, BSA, and myoglobin as model proteins, followed by MALDI-TOF analysis.[469−471] In contrast to the conventional digestion approach of using free trypsin for cytochrome c, with an incubation time of 12 h, proteins can be digested on-chip in a matter of minutes.

An allergenic epitope extraction technique, based on functionalized magnetic microparticles self-organized under a magnetic field in a microfluidic channel, was applied for the isolation and identification of prospective allergen epitopes.[472] Ovabulmin, the major protein of egg white and a typical representative of food allergens was selected as the model molecule. In a supplementary step after digestion, capture of allergenic epitopes from the mixture of peptides was performed by a second magnetic immunoaffinity carrier with immobilized antiovalbumin IgG molecules. Captured peptides were eluted subsequently and analyzed with MALDI-TOF.

9. Conclusions and Outlook

We have reviewed advances in the fabrication, manipulation, detection, and application of magnetic particles in microfluidic systems. This research area is highly multidisciplinary, requiring scientific knowledge, ranging from inorganic chemistry involved in the preparation of the magnetic beads, through biochemistry and medical science to allow for their functionalization, to the basic physics of magnetism and magnetic materials. Today many reaction processes are known for the synthesis of magnetic micro- and nanoparticles of various size and composition. These particles can be very reproducibly obtained from a number of suppliers with a tremendous choice in chemical functionalization of the particle surface. Nearly all important functions in a bioassay can be realized using magnetic beads: raw sample purification, providing a solid substrate to the sample, mixing, labeling, manipulation, transport, and sepa-

ration. Magnetic labeling is more universal and robust than, for example, fluorescent labeling, in the sense that the magnetism of the particles cannot be quenched at normal working temperatures. Ultrasmall magnetic nanoparticles can be of the same size as the biomolecules attached to them, thereby providing minimum disturbance to chemical and biological processes and benefit from decreased diffusion times. We have discussed the forces acting on such magnetic particles and the physics of magnetic actuation. Probably the most prominent advantage of magnetic beads over other solid supports is that these particles can be magnetically probed and manipulated using permanent magnets or electromagnets, independent of normal chemical or biological processes.

Introducing these particles in miniaturized fluidic or lab-on-a-chip systems provides further advantages: (i) the reduced volume of a microfluidic chip with respect to a batch-type reaction vial strongly limits the consumption of samples and reagents and results in faster reaction times, as the latter are less compromised by slow diffusion processes over long distances, (ii) microfluidic flow patterns can be engineered by geometrical microchannel design of the chip to generate very controlled space- and time-dependent hydrodynamic forces acting on the particles, and (iii) miniaturized systems that completely integrate various processes, from raw sample pretreatment until specific biomolecular detection, are achievable, which qualifies these systems for point-of-care or in-field testing.

We have identified four important biological application areas for magnetic particle handling in microfluidic systems: cell handling and separation, nucleic acid processing and detection, immunoassays, and catalysis. We showed that specific magnetic labeling permits one to select or deplete certain cell types from a complex matrix, thanks to the combination of magnetic labeling with magnetic separation principles. When introducing a raw cell sample on a microfluidic chip or cartridge, it is possible to capture the DNA, purify and process it, and detect a specific DNA sequence on-chip. One can also detect, with high sensitivity, various types of proteins and disease markers, by developing immunoassays that combine magnetic particles, microfluidics, antigen−antibody interactions, and using a number of different detection principles. Finally, keeping a magnetically suspended plug of magnetic particles in a microfluidic flow is also of interest for catalytic reactions, as demonstrated for protein digestion.

We foresee a bright future for microfluidic systems that incorporate magnetic micro- and nanoparticle manipulation. For cell handling in a clinical environment and cell therapy, magnetic cell sorting techniques with low complexity have been developed. Today these are still cross-checked using more complex fluorescent cell sorting techniques, but, in the future, will provide stand-alone systems for cell purification. For example, purification of stem or progenitor cells and depletion of white blood cells from the sample will be key in cancer treatment and medical transplantation, if a sufficient number of cells can be processed (sorted) in a reasonable time. Microfluidic chips for nucleic acid detection will be playing an important role for point-of-care diagnosis and in-field testing. While, in a clinical environment, high-throughput robotic systems can detect with high sensitivity and at low cost a large number of samples, due to the use of a minimum of consumables, diagnosis in remote areas, quality testing of food, or monitoring of pollution parameters would exclusively depend on the availability of all-integrated microfluidic systems. Immunoassays based on the use of magnetic particles as reaction substrate or as label have been very successful and will further increase in importance. Biomolecules labeled with magnetic nanoparticles will be magnetically driven to a reaction surface, leading to antigen−antibody binding reactions that are much faster than obtainable via normal molecular diffusion. This activated magnetic transport is especially advantageous for detecting very low antigen concentrations (~1 fg/mL or smaller). The combination with precisely engineered microfluidic flow patterns on-chip will allow developing finely tuned washing protocols to remove unspecifically adsorbed particles on the substrate. Optimized chemical reaction/washing protocols have been developed for magnetoresistive sensors, where the magnetic particles need to be immobilized specifically over the most sensitive part of the sensor area. Yet even more attractive is the use of these protocols for optical surface coverage detection of magnetic particles, as there is just a substrate with capture antibodies needed in the microfluidic chip. The method requires only an optical microscope for observation and image processing. As demonstrated, sensitivities obtained with this technique are impressive, and due to its simplicity, a great future can be expected for this type of microfluidic force flow discrimination assays. Also, stand-alone integrated systems, which are comprised of sample pretreatment, processing, and on-chip detection, will have a bright future. The use of catalysts deposited on magnetic nanoparticles for catalyst separation will also be increasingly developed in microfluidic systems. This approach has found application for protein digestion as a preparation step for other analytical techniques, but more work is to be expected from the positioning of a suspension of catalyst-bearing magnetic particles in a microfluidic flow, especially for pharmaceutical or chemical applications. These would strongly benefit from efficient and reusable catalysts during the screening of new synthesis routes for the development of drugs or chemical reagents, with interesting potential for up-scaling by parallelization of the microfluidic circuits. It is clear that the convergence of nanotechnologies and biosciences will be one of the leading and most promising areas of research and development in the 21st century. Magnetic beads certainly will play an important role in these developments.

10. Acknowledgments

We gratefully acknowledge Rana Afshar, Jean Baudry, Jérôme Bibette, Edoardo Charbon, Emile Dupont, Victor Fernandez, Smail Hadjidj, Heinrich Hofmann, Thomas Lehnert, Hicham Majd, Yves Moser, Virendra Parashar, Qasem Ramadan, Amar Rida, Venkataragavalu Sivagnanam, Cumhur Tekin, and Caroline Vandevyver for helpful discussions and collaboration. This work is part of the research programs supported by the Swiss National Science Foundation and the Commission for Technology and Innovation. We also acknowledge the European Commission funded project DETECTHIV (# 037118, Sensitive nanoparticle assay for the detection of HIV).

11. References

(1) Manz, A.; Graber, N.; Widmer, H. M. *Sens. Actuators, B: Chem.* **1990**, *1*, 244.
(2) Auroux, P. A.; Iossifidis, D.; Reyes, D. R.; Manz, A. *Anal. Chem.* **2002**, *74*, 2637.
(3) Vilkner, T.; Janasek, D.; Manz, A. *Anal. Chem.* **2004**, *76*, 3373.

(4) West, J.; Becker, M.; Tombrink, S.; Manz, A. *Anal. Chem.* **2008**, *80*, 4403.
(5) *Encyclopedia of Microfluidics and Nanofluidics*; Li, D., Ed.; Springer: New York, 2008; Vols. *1*−*3*.
(6) Song, H.; Chen, D. L.; Ismagilov, R. F. *Angew. Chem., Int. Ed.* **2006**, *45*, 7336.
(7) Squires, T. M.; Quake, S. R. *Rev. Mod. Phys.* **2005**, *77*, 977.
(8) Whitesides, G. M. *Nature* **2006**, *442*, 368.
(9) Madou, M. J. *Fundamentals of Microfabrication: The Science of Miniaturization*, 2nd ed.; CRC Press: Boca Raton, FL, 2002.
(10) Reyes, D. R.; Iossifidis, D.; Auroux, P. A.; Manz, A. *Anal. Chem.* **2002**, *74*, 2623.
(11) Harrison, D. J.; Manz, A.; Fan, Z. H.; Ludi, H.; Widmer, H. M. *Anal. Chem.* **1992**, *64*, 1926.
(12) Duffy, D. C.; McDonald, J. C.; Schueller, O. J. A.; Whitesides, G. M. *Anal. Chem.* **1998**, *70*, 4974.
(13) McDonald, J. C.; Duffy, D. C.; Anderson, J. R.; Chiu, D. T.; Wu, H. K.; Schueller, O. J. A.; Whitesides, G. M. *Electrophoresis* **2000**, *21*, 27.
(14) Becker, H.; Gartner, C. *Electrophoresis* **2000**, *21*, 12.
(15) Kawaguchi, H. *Prog. Polym. Sci.* **2000**, *25*, 1171.
(16) Kruis, F. E.; Fissan, H.; Peled, A. *J. Aerosol Sci.* **1998**, *29*, 511.
(17) Verpoorte, E. *Lab Chip* **2003**, *3*, 60N.
(18) Becker, R. *Electromagnetic Fields and Interactions*; Dover: New York, 1982.
(19) Chikazumi, S. *Physics of Magnetism*; Robert E. Krieger Publishing Co.: Malabar, FL, 1964.
(20) Häfeli, U.; Schütt, W.; Teller, J.; Zborowski, M. *Scientific and Clinical Applications of Magnetic Carriers*; Plenum Press: New York, 1997.
(21) Moser, Y.; Lehnert, T.; Gijs, M. A. M. *Appl. Phys. Lett.* **2009**; 022505.
(22) Shevkoplyas, S. S.; Siegel, A. C.; Westervelt, R. M.; Prentiss, M. G.; Whitesides, G. M. *Lab Chip* **2007**, *7*, 1294.
(23) Sometimes the equation $\mathbf{F}_m = \mu_0^{-1}\nabla(\mathbf{m}\cdot\mathbf{B})$ is taken as the basic equation for the magnetic force, instead of eq 1. However, this is correct only when **m** has no spatial dependence. Also, we use here the definition of force, where the moment has units of [tesla m^3]. An alternative dimension in literature for the moment is [A m^2], but, in this case, the factor μ_0 in the denominator of eq 1 needs to be replaced by 1.
(24) Jackson, J. *Classical Electrodynamics*; Wiley: New York, 1998.
(25) Pankhurst, Q. A.; Connolly, J.; Jones, S. K.; Dobson, J. *J. Phys. D: Appl. Phys.* **2003**, *36*, R167.
(26) Gijs, M. A. M. *Microfluid. Nanofluid.* **2004**, *1*, 22.
(27) Pamme, N. *Lab Chip* **2006**, *6*, 24.
(28) Lu, A. H.; Salabas, E. L.; Schüth, F. *Angew. Chem., Int. Ed.* **2007**, *46*, 1222.
(29) Horák, D.; Babič, M.; Macková, H.; Beneš, M. J. *J. Sep. Sci.* **2007**, *30*, 1751.
(30) Landfester, K.; Ramírez, L. P. *J. Phys.: Condens. Matter* **2003**, *15*, S1345.
(31) Bergemann, C.; Müller-Schulte, D.; Oster, J.; à Brassard, L.; Lübbe, A. S. *J. Magn. Magn. Mater.* **1999**, *194*, 45.
(32) Grüttner, C.; Rudershausen, S.; Teller, J. *J. Magn. Magn. Mater.* **2001**, *225*, 1.
(33) Grüttner, C.; Teller, J. *J. Magn. Magn. Mater.* **1999**, *194*, 8.
(34) Latham, A. H.; Williams, M. E. *Acc. Chem. Res.* **2008**, *41*, 411.
(35) Grieve, K.; Mulvaney, P.; Grieser, F. *Curr. Opin. Colloid Interface Sci.* **2000**, *5*, 168.
(36) Trindade, T.; O'Brien, P.; Pickett, N. L. *Chem. Mater.* **2001**, *13*, 3843.
(37) Murray, C. B.; Kagan, C. R.; Bawendi, M. G. *Annu. Rev. Mater. Sci.* **2000**, *30*, 545.
(38) Swihart, M. T. *Curr. Opin. Colloid Interface Sci.* **2003**, *8*, 127.
(39) Grasset, F.; Labhsetwar, N.; Li, D.; Park, D. C.; Saito, N.; Haneda, H.; Cador, O.; Roisnel, T.; Mornet, S.; Duguet, E.; Portier, J.; Etourneau, J. *Langmuir* **2002**, *18*, 8209.
(40) Sun, S. H.; Zeng, H. *J. Am. Chem. Soc.* **2002**, *124*, 8204.
(41) Park, S. J.; Kim, S.; Lee, S.; Khim, Z. G.; Char, K.; Hyeon, T. *J. Am. Chem. Soc.* **2000**, *122*, 8581.
(42) Puntes, V. F.; Krishnan, K. M.; Alivisatos, A. P. *Science* **2001**, *291*, 2115.
(43) Shevchenko, E. V.; Talapin, D. V.; Rogach, A. L.; Kornowski, A.; Haase, M.; Weller, H. *J. Am. Chem. Soc.* **2002**, *124*, 11480.
(44) Sun, S. H.; Murray, C. B.; Weller, D.; Folks, L.; Moser, A. *Science* **2000**, *287*, 1989.
(45) Lee, W. B.; Weng, C. H.; Cheng, F. Y.; Yeh, C. S.; Lei, H. Y.; Lee, G. B. *Biomed. Microdevices* **2009**, *11*, 161.
(46) Chu, L. Y.; Utada, A. S.; Shah, R. K.; Kim, J. W.; Weitz, D. A. *Angew. Chem., Int. Ed.* **2007**, *46*, 8970.
(47) Hwang, D. K.; Dendukuri, D.; Doyle, P. S. *Lab Chip* **2008**, *8*, 1640.
(48) Papell, S. S. U.S. Patent 3215572, 1965.
(49) Reimers, G. W.; Khalfalla, S. E. U.S. Patent 3843540, 1974.
(50) Kelley, J. R. U.S. Patent 4019994, 1977.
(51) Sun, S. H.; Zeng, H.; Robinson, D. B.; Raoux, S.; Rice, P. M.; Wang, S. X.; Li, G. X. *J. Am. Chem. Soc.* **2004**, *126*, 273.
(52) Jana, N. R.; Chen, Y. F.; Peng, X. G. *Chem. Mater.* **2004**, *16*, 3931.
(53) Park, J.; An, K. J.; Hwang, Y. S.; Park, J. G.; Noh, H. J.; Kim, J. Y.; Park, J. H.; Hwang, N. M.; Hyeon, T. *Nat. Mater.* **2004**, *3*, 891.
(54) Dumestre, F.; Chaudret, B.; Amiens, C.; Renaud, P.; Fejes, P. *Science* **2004**, *303*, 821.
(55) Daniel, J.-C.; Schuppiser, J.-L.; Tricot, M. U.S. Patent 4358388, 1982.
(56) Bibette, J.; Charmot, D.; Schorsch, G. U.S. Patent 5242964, 1993.
(57) Bibette, J. *J. Magn. Magn. Mater.* **1993**, *122*, 37.
(58) Cornell, R. M.; Schertmann, U. *The Iron Oxides: Structure, Properties, Reactions, Occurrence and Uses*; VCH: Weinheim, 1996.
(59) Petri-Fink, A.; Chastellain, M.; Juillerat-Jeanneret, L.; Ferrari, A.; Hofmann, H. *Biomaterials* **2005**, *26*, 2685.
(60) Lawaczeck, R.; Bauer, H.; Frenzel, T.; Hasegawa, M.; Ito, Y.; Kito, K.; Miwa, N.; Tsutsui, H.; Volger, H.; Weinmann, H. J. *Acta Radiol.* **1997**, *38*, 584.
(61) Kim, D. K.; Zhang, Y.; Kehr, J.; Klason, T.; Bjelke, B.; Muhammed, M. *J. Magn. Magn. Mater.* **2001**, *225*, 256.
(62) Liu, Q. X.; Xu, Z. H.; Finch, J. A.; Egerton, R. *Chem. Mater.* **1998**, *10*, 3936.
(63) Ban, Z. H.; Barnakov, Y. A.; Golub, V. O.; O'Connor, C. J. *J. Mater. Chem.* **2005**, *15*, 4660.
(64) Nikitenko, S. I.; Koltypin, Y.; Palchik, O.; Felner, I.; Xu, X. N.; Gedanken, A. *Angew. Chem., Int. Ed.* **2001**, *40*, 4447.
(65) Stöber, W.; Fink, A.; Bohn, E. *J. Colloid Interface Sci.* **1968**, *26*, 62.
(66) Graf, C.; Vossen, D. L. J.; Imhof, A.; van Blaaderen, A. *Langmuir* **2003**, *19*, 6693.
(67) Lu, Y.; Yin, Y. D.; Mayers, B. T.; Xia, Y. N. *Nano Lett.* **2002**, *2*, 183.
(68) Ulman, A. *Chem. Rev.* **1996**, *96*, 1533.
(69) Molday, R. S. U.S. Patent 4452773, 1984.
(70) Rembaum, A. U.S. Patent 4267234, 1981.
(71) Lee, J. W.; Isobe, T.; Senna, M. *Colloids Surf., A* **1996**, *109*, 121.
(72) Suzuki, M.; Shinkai, M.; Kamihira, M.; Kobayashi, T. *Biotechnol. Appl. Biochem.* **1995**, *21*, 335.
(73) Dynal product catalogue (http:/www.invitrogen.com).
(74) Ugelstad, J.; Berge, A.; Ellingsen, T.; Schmid, R.; Nilsen, T. N.; Mork, P. C.; Stenstad, P.; Hornes, E.; Olsvik, O. *Prog. Polym. Sci.* **1992**, *17*, 87.
(75) Ugelstad, J. U.S. Patent 4774265, 1988.
(76) Kleiber, J.; Walter, T.; Harttig, H.; Lesniak, C.; Mennig, M.; Riedling, M.; Schmidt, H. U.S. Patent 6255477B1, 2001.
(77) Undisclosed inventors. European patent 1154443A1, 2001.
(78) Miltenyi, S.; Muller, W.; Weichel, W.; Radbruch, A. *Cytometry* **1990**, *11*, 231.
(79) Häfeli, U. O.; Pauer, G. J. *J. Magn. Magn. Mater.* **1999**, *194*, 76.
(80) Häfeli, U. O.; Sweeney, S. M.; Beresford, B. A.; Sim, E. H.; Macklis, R. M. *J. Biomed. Mater. Res.* **1994**, *28*, 901.
(81) Olsvik, O.; Popovic, T.; Skjerve, E.; Cudjoe, K. S.; Hornes, E.; Ugelstad, J.; Uhlen, M. *Clin. Microbiol. Rev.* **1994**, *7*, 43.
(82) Jung, Y. W.; Kang, H. J.; Lee, J. M.; Jung, S. O.; Yun, W. S.; Chung, S. J.; Chung, B. H. *Anal. Biochem.* **2008**, *374*, 99.
(83) Lehmann, U.; Vandevyver, C.; Parashar, V. K.; Gijs, M. A. M. *Angew. Chem., Int. Ed.* **2006**, *45*, 3062.
(84) LesliePelecky, D. L.; Rieke, R. D. *Chem. Mater.* **1996**, *8*, 1770.
(85) Hancock, J. P.; Kemshead, J. T. *J. Immunol. Methods* **1993**, *164*, 51.
(86) Tarn, M. D.; Hirota, N.; Iles, A.; Pamme, N. *Sci. Technol. Adv. Mater.* **2009**, *10*, 014611.
(87) Winkleman, A.; Gudiksen, K. L.; Ryan, D.; Whitesides, G. M.; Greenfield, D.; Prentiss, M. *Appl. Phys. Lett.* **2004**, *85*, 2411.
(88) Gassner, A. L.; Abonnenc, M.; Chen, H. X.; Morandini, J.; Josserand, J.; Rossier, J. S.; Busnel, J. M.; Girault, H. H. *Lab Chip* **2009**, *9*, 2356.
(89) White, F. M. *Fluid Mechanics*; McGraw-Hill: New York, 1999.
(90) Faxen, H. *Ann. Phys.* **1922**, *68*, 89.
(91) Wirix-Speetjens, R.; Fyen, W.; Xu, K. D.; De Boeck, J.; Borghs, G. *IEEE Trans. Magn.* **2005**, *41*, 4128.
(92) Gregory, J. *J. Colloid Interface Sci.* **1981**, *83*, 138.
(93) Visser, J. *Adv. Colloid Interface Sci.* **1981**, *15*, 157.
(94) Kar, G.; Chander, S.; Mika, T. S. *J. Colloid Interface Sci.* **1973**, *44*, 347.
(95) Hunter, R. *Zeta Potential in Colloid Science*; Academic Press: New York, 1981.
(96) Sivagnanam, V.; Song, B.; Vandevyver, C.; Gijs, M. A. M. *Anal. Chem.* **2009**, *81*, 6509.
(97) Einstein, A. *Investigations on the Theory of Brownian Movement*; Dover: New York, 1956.
(98) Schaller, V.; Kraling, U.; Rusu, C.; Petersson, K.; Wipenmyr, J.; Krozer, A.; Wahnstrom, G.; Sanz-Velasco, A.; Enoksson, P.; Johansson, C. *J. Appl. Phys.* **2008**, *104*, 093918.

(99) van Ommering, K.; Nieuwenhuis, J. H.; van Ijzendoorn, L. J.; Koopmans, B.; Prins, M. W. J. *Appl. Phys. Lett.* **2006**, *89*, 142511.
(100) Janssen, X. J. A.; Schellekens, A. J.; van Ommering, K.; van Ijzendoorn, L. J.; Prins, M. W. J. *Biosens. Bioelectron.* **2009**, *24*, 1937.
(101) Liu, C. X.; De Palma, R.; Reekmans, G.; Laureyn, W.; Stakenborg, T.; Lagae, L. *Biosens. Bioelectron.* **2009**, *24*, 2294.
(102) Huke, B.; Lucke, M. *Rep. Prog. Phys.* **2004**, *67*, 1731.
(103) Derks, R. J. S.; Dietzel, A.; Wimberger-Friedl, R.; Prins, M. W. J. *Microfluid. Nanofluid.* **2007**, *3*, 141.
(104) Derks, R. J. S.; Frijns, A. J. H.; Prins, M. W. J.; Dietzel, A. H. *Appl. Phys. Lett.* **2008**, *92*, 024104.
(105) Dunnill, P.; Lilly, M. D. *Biotechnol. Bioeng.* **1974**, *16*, 987.
(106) Mosbach, K.; Andersson, L. *Nature* **1977**, *270*, 259.
(107) Kondo, A.; Kamura, H.; Higashitani, K. *Appl. Microbiol. Biotechnol.* **1994**, *41*, 99.
(108) Koneracka, M.; Kopcansky, P.; Timko, M.; Ramchand, C. N. *J. Magn. Magn. Mater.* **2002**, *252*, 409.
(109) Kourilov, V.; Steinitz, M. *Anal. Biochem.* **2002**, *311*, 166.
(110) Manz, R.; Assenmacher, M.; Pfluger, E.; Miltenyi, S.; Radbruch, A. *Proc. Natl. Acad. Sci. U.S.A.* **1995**, *92*, 1921.
(111) Rheinlander, T.; Kotitz, R.; Weitschies, W.; Semmler, W. *J. Magn. Magn. Mater.* **2000**, *219*, 219.
(112) Ebner, A. D.; Ritter, J. A. *AIChE J.* **2001**, *47*, 303.
(113) Pamme, N. *Lab Chip* **2007**, *7*, 1644.
(114) Latham, A. H.; Freitas, R. S.; Schiffer, P.; Williams, M. E. *Anal. Chem.* **2005**, *77*, 5055.
(115) Giddings, J. C.; Yang, F. J. F.; Myers, M. N. *Science* **1976**, *193*, 1244.
(116) Chalmers, J. J.; Zborowski, M.; Sun, L. P.; Moore, L. *Biotechnol. Prog.* **1998**, *14*, 141.
(117) Hatch, G. P.; Stelter, R. E. *J. Magn. Magn. Mater.* **2001**, *225*, 262.
(118) Williams, P. S.; Zborowski, M.; Chalmers, J. *Anal. Chem.* **1999**, *71*, 3799.
(119) Carpino, F.; Moore, L. R.; Zborowski, M.; Chalmers, J. J.; Williams, P. S. *J. Magn. Magn. Mater.* **2005**, *293*, 546.
(120) Hoyos, M.; Moore, L. R.; McCloskey, K. E.; Margel, S.; Zuberi, M.; Chalmers, J. J.; Zborowski, M. *J. Chromatogr., A* **2000**, *903*, 99.
(121) Fuh, C. B.; Chen, S. Y. *J. Chromatogr., A* **1998**, *813*, 313.
(122) Fuh, C. B.; Chen, S. Y. *J. Chromatogr., A* **1999**, *857*, 193.
(123) Williams, P. S.; Carpino, F.; Zborowski, M. *J. Magn. Magn. Mater.* **2009**, 1446.
(124) Nakamura, M.; Zborowski, M.; Lasky, L. C.; Margel, S.; Chalmers, J. J. *Exp. Fluids* **2001**, *30*, 371.
(125) Zhang, H. D.; Moore, L. R.; Zborowski, M.; Williams, P. S.; Margel, S.; Chalmers, J. J. *Analyst* **2005**, *130*, 514.
(126) Moore, L. R.; Zborowski, M.; Nakamura, M.; McCloskey, K.; Gura, S.; Zuberi, M.; Margel, S.; Chalmers, J. J. *J. Biochem. Biophys. Methods* **2000**, *44*, 115.
(127) Blankenstein, G.; Larsen, U. D. *Biosens. Bioelectron.* **1998**, *13*, 427.
(128) Pamme, N.; Manz, A. *Anal. Chem.* **2004**, *76*, 7250.
(129) Nandy, K.; Chaudhuri, S.; Ganguly, R.; Puri, I. K. *J. Magn. Magn. Mater.* **2008**, *320*, 1398.
(130) Nedelcu, S.; Watson, J. H. P. *Miner. Eng.* **2002**, *15*, 355.
(131) Hoffmann, C.; Franzreb, M. *IEEE Trans. Magn.* **2004**, *40*, 462.
(132) Todd, P.; Cooper, R. P.; Doyle, J. F.; Dunn, S.; Vellinger, J.; Deuser, M. S. *J. Magn. Magn. Mater.* **2001**, *225*, 294.
(133) Haik, Y.; Pai, V.; Chen, C. J. *J. Magn. Magn. Mater.* **1999**, *194*, 254.
(134) Miltenyi Biotec product catalogue (http://www.miltenyibiotec.com).
(135) Afshar, R.; Moser, Y.; Lehnert, T.; Gijs, M. A. M. *Sens. Actuators, B: Chem.* **2009**, DOI: 10.1016/j.snb.2009.08.044.
(136) Berger, M.; Castelino, J.; Huang, R.; Shah, M.; Austin, R. H. *Electrophoresis* **2001**, *22*, 3883.
(137) Lyuksyutov, I. F.; Naugle, D. G.; Rathnayaka, K. D. D. *Appl. Phys. Lett.* **2004**, *85*, 1817.
(138) Deng, T.; Prentiss, M.; Whitesides, G. M. *Appl. Phys. Lett.* **2002**, *80*, 461.
(139) Guo, S. S.; Deng, Y. L.; Zhao, L. B.; Chan, H. L. W.; Zhao, X. Z. *J. Phys. D: Appl. Phys.* **2008**, *41*, 105008.
(140) Forbes, Z. G.; Yellen, B. B.; Barbee, K. A.; Friedman, G. *IEEE Trans. Magn.* **2003**, *39*, 3372.
(141) Yellen, B.; Friedman, G.; Feinerman, A. *J. Appl. Phys.* **2003**, *93*, 7331.
(142) Lin, Y. A.; Wong, T. S.; Bhardwaj, U.; Chen, J. M.; McCabe, E.; Ho, C. M. *J. Micromech. Microeng.* **2007**, *17*, 1299.
(143) Smistrup, K.; Bu, M. Q.; Wolff, A.; Bruus, H.; Hansen, M. F. *Microfluid. Nanofluid.* **2008**, *4*, 565.
(144) Mikkelsen, C.; Hansen, M. F.; Bruns, H. *J. Magn. Magn. Mater.* **2005**, *293*, 578.
(145) Furlani, E. P. *J. Appl. Phys.* **2006**, *99*, 024912.
(146) Furlani, E. P.; Ng, K. C. *Phys. Rev. E* **2006**, *73*, 061919.
(147) Smistrup, K.; Lund-Olesen, T.; Hansen, M. F.; Tang, P. T. *J. Appl. Phys.* **2006**, *99*, 08P102.
(148) Smistrup, K.; Kjeldsen, B. G.; Reimers, J. L.; Dufva, M.; Petersen, J.; Hansen, M. F. *Lab Chip* **2005**, *5*, 1315.
(149) Lund-Olesen, T.; Bruus, H.; Hansen, M. F. *Biomed. Microdevices* **2007**, *9*, 195.
(150) Chen, H. T.; Kaminski, M. D.; Rosengart, A. J. *Med. Eng. Phys.* **2008**, *30*, 1.
(151) Inglis, D. W.; Riehn, R.; Austin, R. H.; Sturm, J. C. *Appl. Phys. Lett.* **2004**, *85*, 5093.
(152) Han, K. H.; Frazier, A. B. *J. Appl. Phys.* **2004**, *96*, 5797.
(153) Han, K. H.; Frazier, A. B. *J. Microelectromech. Syst.* **2005**, *14*, 1422.
(154) Han, K. H.; Frazier, A. B. *Lab Chip* **2006**, *6*, 265.
(155) Choi, J. W.; Ahn, C. H.; Bhansali, S.; Henderson, H. T. *Sens. Actuators, B: Chem.* **2000**, *68*, 34.
(156) Choi, J. W.; Liakopoulos, T. M.; Ahn, C. H. *Biosens. Bioelectron.* **2001**, *16*, 409.
(157) Ahn, C. H.; Allen, M. G.; Trimmer, W.; Jun, Y. N.; Erramilli, S. *J. Microelectromech. Syst.* **1996**, *5*, 151.
(158) Do, J.; Choi, J. W.; Ahn, C. H. *IEEE Trans. Magn.* **2004**, *40*, 3009.
(159) Ramadan, Q.; Samper, V.; Poenar, D.; Yu, C. *J. Magn. Magn. Mater.* **2004**, *281*, 150.
(160) Smistrup, K.; Hansen, O.; Bruus, H.; Hansen, M. F. *J. Magn. Magn. Mater.* **2005**, *293*, 597.
(161) Smistrup, K.; Tang, P. T.; Hansen, O.; Hansen, M. F. *J. Magn. Magn. Mater.* **2006**, *300*, 418.
(162) Ramadan, Q.; Samper, V.; Poenar, D. P.; Yu, C. *Biosens. Bioelectron.* **2006**, *21*, 1693.
(163) Ramadan, Q.; Yu, C.; Samper, V.; Poenar, D. P. *Appl. Phys. Lett.* **2006**, *88*, 032501.
(164) Furlani, E. P.; Sahoo, Y.; Ng, K. C.; Wortman, J. C.; Monk, T. E. *Biomed. Microdevices* **2007**, *9*, 451.
(165) Mikkelsen, C.; Bruus, H. *Lab Chip* **2005**, *5*, 1293.
(166) Barbic, M.; Mock, J. J.; Gray, A. P.; Schultz, S. *Appl. Phys. Lett.* **2001**, *79*, 1897.
(167) Song, S. H.; Kwak, B. S.; Park, J. S.; Kim, W.; Jung, H. I. *Sens. Actuators, A: Phys.* **2009**, *151*, 64.
(168) Tondra, M.; Granger, M.; Fuerst, R.; Porter, M.; Nordman, C.; Taylor, J.; Akou, S. *IEEE Trans. Magn.* **2001**, *37*, 2621.
(169) Pekas, N.; Granger, M.; Tondra, M.; Popple, A.; Porter, M. D. *J. Magn. Magn. Mater.* **2005**, *293*, 584.
(170) Deng, T.; Whitesides, G. M.; Radhakrishnan, M.; Zabow, G.; Prentiss, M. *Appl. Phys. Lett.* **2001**, *78*, 1775.
(171) Ostergaard, S.; Blankenstein, G.; Dirac, H.; Leistiko, O. *J. Magn. Magn. Mater.* **1999**, *194*, 156.
(172) Joung, J.; Shen, J.; Grodzinski, P. *IEEE Trans. Magn.* **2000**, *36*, 2012.
(173) Yapici, M. K.; Zou, J. *Microsyst. Technol.: Micro- and Nanosystems-Information Storage Process. Syst.* **2008**, *14*, 881.
(174) Lee, C. S.; Lee, H.; Westervelt, R. M. *Appl. Phys. Lett.* **2001**, *79*, 3308.
(175) Wirix-Speetjens, R.; Fyen, W.; De Boeck, J.; Borghs, G. *J. Appl. Phys.* **2006**, *99*, 103903.
(176) Rida, A.; Fernandez, V.; Gijs, M. A. M. *Appl. Phys. Lett.* **2003**, *83*, 2396.
(177) Ramadan, Q.; Poenar, D.; Yu, C. *Microfluid. Nanofluid.* **2009**, *6*, 53.
(178) Yellen, B. B.; Erb, R. M.; Son, H. S.; Hewlin, R.; Shang, H.; Lee, G. U. *Lab Chip* **2007**, *7*, 1681.
(179) Conroy, R. S.; Zabow, G.; Moreland, J.; Koretsky, A. P. *Appl. Phys. Lett.* **2008**, *93*, 203901.
(180) Megens, M.; Prins, M. *J. Magn. Magn. Mater.* **2005**, *293*, 702.
(181) Graham, D. L.; Ferreira, H. A.; Freitas, P. P. *Trends Biotechnol.* **2004**, *22*, 455.
(182) Tamanaha, C. R.; Mulvaney, S. P.; Rife, J. C.; Whitman, L. J. *Biosens. Bioelectron.* **2008**, *24*, 1.
(183) Baibich, M. N.; Broto, J. M.; Fert, A.; Vandau, F. N.; Petroff, F.; Eitenne, P.; Creuzet, G.; Friederich, A.; Chazelas, J. *Phys. Rev. Lett.* **1988**, *61*, 2472.
(184) Dieny, B.; Speriosu, V. S.; Metin, S.; Parkin, S. S. P.; Gurney, B. A.; Baumgart, P.; Wilhoit, D. R. *J. Appl. Phys.* **1991**, *69*, 4774.
(185) Freitas, P. P.; Silva, F.; Oliveira, N. J.; Melo, L. V.; Costa, L.; Almeida, N. *Sens. Actuators, A: Phys.* **2000**, *81*, 2.
(186) *Magnetic Multilayers and Giant Magnetoresistance*; Hartmann, U., Ed.; Springer Verlag: Berlin-Heidelberg, 1999.
(187) Lagae, L.; Wirix-Speetjens, R.; Das, J.; Graham, D.; Ferreira, H.; Freitas, P. P. F.; Borghs, G.; De Boeck, J. *J. Appl. Phys.* **2002**, *91*, 7445.
(188) Besse, P. A.; Boero, G.; Demierre, M.; Pott, V.; Popovic, R. *Appl. Phys. Lett.* **2002**, *80*, 4199.
(189) Lee, W.; Joo, S.; Kim, S. U.; Rhie, K.; Hong, J.; Shin, K. H.; Kim, K. H. *Appl. Phys. Lett.* **2009**, *94*, 153903.
(190) Ejsing, L.; Hansen, M. F.; Menon, A. K.; Ferreira, H. A.; Graham, D. L.; Freitas, P. P. *Appl. Phys. Lett.* **2004**, *84*, 4729.

(191) Baselt, D. R.; Lee, G. U.; Natesan, M.; Metzger, S. W.; Sheehan, P. E.; Colton, R. J. *Biosens. Bioelectron.* **1998**, *13*, 731.
(192) Miller, M. M.; Sheehan, P. E.; Edelstein, R. L.; Tamanaha, C. R.; Zhong, L.; Bounnak, S.; Whitman, L. J.; Colton, R. J. *J. Magn. Magn. Mater.* **2001**, *225*, 138.
(193) Rife, J. C.; Miller, M. M.; Sheehan, P. E.; Tamanaha, C. R.; Tondra, M.; Whitman, L. J. *Sens. Actuators, A: Phys.* **2003**, *107*, 209.
(194) Edelstein, R. L.; Tamanaha, C. R.; Sheehan, P. E.; Miller, M. M.; Baselt, D. R.; Whitman, L. J.; Colton, R. J. *Biosens. Bioelectron.* **2000**, *14*, 805.
(195) Coehoorn, R.; Prins, M. W. J. European patent 1456658, 2004.
(196) Graham, D. L.; Ferreira, H. A.; Freitas, P. P.; Cabral, J. M. S. *Biosens. Bioelectron.* **2003**, *18*, 483.
(197) Tondra, M.; Porter, M.; Lipert, R. J. *J. Vac. Sci. Technol., A* **2000**, *18*, 1125.
(198) Li, G. X.; Joshi, V.; White, R. L.; Wang, S. X.; Kemp, J. T.; Webb, C.; Davis, R. W.; Sun, S. H. *J. Appl. Phys.* **2003**, *93*, 7557.
(199) Li, G. X.; Wang, S. X. *IEEE Trans. Magn.* **2003**, *39*, 3313.
(200) de Boer, B. M.; Kahlman, J.; Jansen, T.; Duric, H.; Veen, J. *Biosens. Bioelectron.* **2006**, 2366.
(201) Thilwind, R. E.; Megens, M.; van Zon, J.; Coehoorn, R.; Prins, M. W. J. *J. Magn. Magn. Mater.* **2008**, *320*, 486.
(202) Janssen, X. J. A.; van Ijzendoorn, L. J.; Prins, M. W. *Biosens. Bioelectron.* **2008**, *23*, 833.
(203) Wimberger-Friedl, R.; Nellissen, T.; Weekamp, W.; van Delft, J.; Ansems, W.; Prins, M.; Megens, M.; Dittmer, W.; de Witz, C.; van Iersel, B. *J. Micromech. Microeng.* **2009**, *19*, 015015.
(204) Hayes, M. A.; Polson, N. A.; Garcia, A. A. *Langmuir* **2001**, *17*, 2866.
(205) Rida, A.; Gijs, M. A. M. *Appl. Phys. Lett.* **2004**, *85*, 4986.
(206) Lacharme, F.; Vandevyver, C.; Gijs, M. A. M. *Anal. Chem.* **2008**, *80*, 2905.
(207) Hayes, M. A.; Polson, N. A.; Phayre, A. N.; Garcia, A. A. *Anal. Chem.* **2001**, *73*, 5896.
(208) Liu, J.; Lawrence, M.; Wu, A.; Ivey, M. L.; Flores, G. A.; Javier, K.; Bibette, J.; Richard, J. *Phys. Rev. Lett.* **1995**, *74*, 2828.
(209) Flores, G. A.; Liu, J.; Mohebi, M.; Jamasbi, N. *Int. J. Mod. Phys. B* **1999**, *13*, 2093.
(210) Promislow, J. H. E.; Gast, A. P. *Langmuir* **1996**, *12*, 4095.
(211) Promislow, J. H. E.; Gast, A. P. *Phys. Rev. E* **1997**, *56*, 642.
(212) Wirtz, D.; Fermigier, M. *Langmuir* **1995**, *11*, 398.
(213) Wirtz, D.; Fermigier, M. *Phys. Rev. Lett.* **1994**, *72*, 2294.
(214) Melle, S.; Fuller, G. G.; Rubio, M. A. *Phys. Rev. E* **2000**, *61*, 4111.
(215) Melle, S.; Calderon, O. G.; Rubio, M. A.; Fuller, G. G. *J. Non-Newton. Fluid Mech.* **2002**, *102*, 135.
(216) Wang, Y.; Zhe, J.; Chung, B. T. F.; Dutta, P. *Microfluid. Nanofluid.* **2008**, *4*, 375.
(217) Biswal, S. L.; Gast, A. P. *Anal. Chem.* **2004**, *76*, 6448.
(218) Kang, T. G.; Hulsen, M. A.; Anderson, P. D.; den Toonder, J. M. J.; Meijer, H. E. H. *Phys. Rev. E* **2007**, *76*, 066303.
(219) Petousis, I.; Homburg, E.; Derks, R.; Dietzel, A. *Lab Chip* **2007**, *7*, 1746.
(220) Lacharme, F.; Vandevyver, C.; Gijs, M. A. M. 21st IEEE International Conference on Micro Electro Mechanical Systems MEMS 2008, Tucson, AZ, 2008; p 184.
(221) Pregibon, D. C.; Toner, M.; Doyle, P. S. *Langmuir* **2006**, *22*, 5122.
(222) Sivagnanam, V.; Sayah, A.; Gijs, M. A. M. *Microelectron. Eng.* **2008**, 1355.
(223) Sivagnanam, V.; Sayah, A.; Vandevyver, C.; Gijs, M. A. M. *Sens. Actuators, B: Chem.* **2008**, *132*, 361.
(224) Rida, A.; T., L.; Gijs, M. A. M. 7th International Conference on Miniaturized Chemical and Biochemical Analysis Systems, October 5−9, 2003, Squaw Valley, CA, 2003; p 579.
(225) Lund-Olesen, T.; Buus, B. B.; Howalt, J. G.; Hansen, M. F. *J. Appl. Phys.* **2007**, *103*, 07E902.
(226) Lund-Olesen, T.; Buus, B. B.; Howalt, J. G.; Hansen, M. F. *J. Appl. Phys.* **2008**, *103*, 07E902.
(227) Lee, S. H.; van Noort, D.; Lee, J. Y.; Zhang, B. T.; Park, T. H. *Lab Chip* **2009**, *9*, 479.
(228) Suzuki, H.; Ho, C. M.; Kasagi, N. *J. Microelectromech. Syst.* **2004**, *13*, 779.
(229) Zolgharni, M.; Azimi, S. M.; Bahmanyar, M. R.; Balachandran, W. *Microfluid. Nanofluid.* **2007**, *3*, 677.
(230) Calhoun, R.; Yadav, A.; Phelan, P.; Vuppu, A.; Garcia, A.; Hayes, M. *Lab Chip* **2006**, *6*, 247.
(231) Yellen, B.; Friedman, G.; Feinerman, A. *J. Appl. Phys.* **2002**, *91*, 8552.
(232) Yellen, B. B.; Friedman, G. *Langmuir* **2004**, *20*, 2553.
(233) Mukhopadhyay, R. *Anal. Chem.* **2006**, *78*, 1401.
(234) Jensen, K.; Lee, A. *Lab Chip* **2004**, *4*, 31N.
(235) Garcia, A. A.; Egatz-Gomez, A.; Lindsay, S. A.; Dominguez-Garcia, P.; Melle, S.; Marquez, M.; Rubio, M. A.; Picraux, S. T.; Yang, D. Q.; Aella, P.; Hayes, M. A.; Gust, D.; Loyprasert, S.; Vazquez-Alvarez, T.; Wang, J. *J. Magn. Magn. Mater.* **2007**, *311*, 238.
(236) Mukhopadhyay, R. *Anal. Chem.* **2005**, *77*, 55A.
(237) Dorvee, J. R.; Derfus, A. M.; Bhatia, S. N.; Sailor, M. J. *Nat. Mater.* **2004**, *3*, 896.
(238) Shikida, M.; Nagao, N.; Imai, R.; Honda, H.; Okochi, M.; Ito, H.; Sato, K. *J. Micromech. Microeng.* **2008**, *18*, 035034.
(239) Buriak, J. M. *Nat. Mater.* **2004**, *3*, 847.
(240) Pollack, M. G.; Fair, R. B.; Shenderov, A. D. *Appl. Phys. Lett.* **2000**, *77*, 1725.
(241) Lee, J.; Moon, H.; Fowler, J.; Schoellhammer, T.; Kim, C. J. 14th IEEE International Conference on Micro Electro Mechanical Systems (MEMS 2001), Interlaken, Switzerland, 2001; p 259.
(242) Egatz-Gomez, A.; Melle, S.; Garcia, A. A.; Lindsay, S. A.; Marquez, M.; Dominguez-Garcia, P.; Rubio, M. A.; Picraux, S. T.; Taraci, J. L.; Clement, T.; Yang, D.; Hayes, M. A.; Gust, D. *Appl. Phys. Lett.* **2006**, *89*, 129902.
(243) Shikida, M.; Koyama, M.; Nagao, N.; Imai, R.; Honda, H.; Okochi, M.; Tsuchiya, H.; Sato, K. *Sens. Actuators, B: Chem.* **2009**, *137*, 774.
(244) Long, Z.; Shetty, A. M.; Solomon, M. J.; Larson, R. G. *Lab Chip* **2009**, DOI: 10.1039/b819818g.
(245) Wang, Y.; Zhao, Y.; Cho, S. K. *J. Micromech. Microeng.* **2007**, *17*, 2148.
(246) Shah, G. J.; Kim, C. J. *J. Microelectromech. Syst.* **2009**, *18*, 363.
(247) Ohashi, T.; Kuyama, H.; Suzuki, K.; Nakamura, S. *Anal. Chim. Acta* **2008**, *612*, 218.
(248) Roy, T.; Sinha, A.; Chakraborty, S.; Ganguly, R.; Puri, I. K. *Phys. Fluids* **2009**, *21*, 027101.
(249) Lehmann, U.; Hadjidj, S.; Parashar, V. K.; Vandevyver, C.; Rida, A.; Gijs, M. A. M. *Sens. Actuators, B: Chem.* **2006**, *117*, 457.
(250) Beyzavi, A.; Nguyen, N. T. *J. Phys. D: Appl. Phys.* **2009**, *42*, 015004.
(251) Nguyen, N. T.; Beyzavi, A.; Ng, K. M.; Huang, X. Y. *Microfluid. Nanofluid.* **2007**, *3*, 571.
(252) Shikida, M.; Inouchi, K.; Honda, H.; Sato, K. 17th IEEE International Conference on Micro Electro Mechanical Systems (MEMS 2004), Maastricht, The Netherlands, 2004; p 359.
(253) Lehmann, U.; Parashar, V.; Hadjidj, S.; Rida, A.; Gijs, M. A. M. Digest of Technical Papers of Transducers 2005, Seoul, Korea, 2005; p 77.
(254) Zborowski, M.; Ostera, G. R.; Moore, L. R.; Milliron, S.; Chalmers, J. J.; Schechter, A. N. *Biophys. J.* **2003**, *84*, 2638.
(255) Spees, W. M.; Yablonskiy, D. A.; Oswood, M. C.; Ackerman, J. J. H. *Magn. Reson. Med.* **2001**, *45*, 533.
(256) The susceptibility values are expressed here in SI units. In the cgs system, they are a factor of 4π smaller.
(257) Melville, D.; Paul, F.; Roath, S. *Nature* **1975**, *255*, 706.
(258) Blakemore, R. P. *Annu. Rev. Microbiol.* **1982**, *36*, 217.
(259) Zola, H.; Swart, B.; Banham, A.; Barry, S.; Beare, A.; Bensussan, A.; Boumsell, L.; Buckley, C. D.; Buhring, H. J.; Clark, G.; Engel, P.; Fox, D.; Jin, B. Q.; Macardle, P. J.; Malavasi, F.; Mason, D.; Stockinger, H.; Yang, X. F. *J. Immunol. Methods* **2007**, *319*, 1.
(260) Greer, J. P.; Foerster, J.; Lukens, J. N.; Rodgers, G. M.; Paraskevas, F.; Glader, B. E. *Wintrobe's Clinical Hematology*, 11th ed.; Lippincott Williams & Wilkins: Philadelphia, PA, 2003.
(261) Grodzinski, P.; Yang, J.; Liu, R. H.; Ward, M. D. *Biomed. Microdevices* **2003**, *5*, 303.
(262) Jing, Y.; Mal, N.; Williams, P. S.; Mayorga, M.; Penn, M. S.; Chalmers, J. J.; Zborowski, M. *FASEB J.* **2008**, *22*, 4239.
(263) McCloskey, K. E.; Chalmers, J. J.; Zborowski, M. *Anal. Chem.* **2003**, *75*, 6868.
(264) McCloskey, K. E.; Chalmers, J. J.; Zborowski, M. *Cytometry* **2000**, *40*, 307.
(265) McCloskey, K. E.; Comella, K.; Chalmers, J. J.; Margel, S.; Zborowski, M. *Biotechnol. Bioeng.* **2001**, *75*, 642.
(266) McCloskey, K. E.; Zborowski, M.; Chalmers, J. J. *Cytometry* **2001**, *44*, 137.
(267) McCloskey, K. E.; Moore, L. R.; Hoyos, M.; Rodriguez, A.; Chalmers, J. J.; Zborowski, M. *Biotechnol. Prog.* **2003**, *19*, 899.
(268) Pappas, D.; Wang, K. *Anal. Chim. Acta* **2007**, *601*, 26.
(269) Yi, C. Q.; Li, C. W.; Ji, S. L.; Yang, M. S. *Anal. Chim. Acta* **2006**, *560*, 1.
(270) Toner, M.; Irimia, D. *Ann. Rev. Biomed. Eng.* **2005**, *7*, 77.
(271) VanDelinder, V.; Groisman, A. *Anal. Chem.* **2007**, *79*, 2023.
(272) Springston, S. R.; Myers, M. N.; Giddings, J. C. *Anal. Chem.* **1987**, *59*, 344.
(273) Das, C. M.; Becker, F.; Vernon, S.; Noshari, J.; Joyce, C.; Gascoyne, P. R. C. *Anal. Chem.* **2005**, *77*, 2708.
(274) Bonner, W. A.; Sweet, R. G.; Hulett, H. R.; Herzenbe, L. *Rev. Sci. Instrum.* **1972**, *43*, 404.
(275) Shapiro, H. H. *Practical Flow Cytometry*; Wiley-Liss: New York, 2003.
(276) Fu, A. Y.; Chou, H. P.; Spence, C.; Arnold, F. H.; Quake, S. R. *Anal. Chem.* **2002**, *74*, 2451.
(277) Graham, M. D. *J. Appl. Phys.* **1981**, *52*, 2578.

(278) Melville, D.; Paul, F.; Roath, S. *IEEE Trans. Magn.* **1982**, *18*, 1680.
(279) Takayasu, M.; Kelland, D. R.; Minervini, J. V. 16th International Conference on Magnet Technology, Ponte Vedra Beach, FL, 1999; p 927.
(280) Paul, F.; Melville, D.; Roath, S.; Warhurst, D. C. *IEEE Trans. Magn.* **1981**, *17*, 2822.
(281) Paul, F.; Roath, S.; Melville, D.; Warhurst, D. C.; Osisanya, J. O. S. *Lancet* **1981**, *2*, 70.
(282) Fuh, C. B.; Su, Y. S.; Tsai, H. Y. *J. Chromatogr.* **2004**, *1027*, 289.
(283) Jung, J.; Han, K. H. *Appl. Phys. Lett.* **2008**, *93*, 223902.
(284) Qu, B. Y.; Wu, Z. Y.; Fang, F.; Bai, Z. M.; Yang, D. Z.; Xu, S. K. *Anal. Bioanal. Chem.* **2008**, *392*, 1317.
(285) Furlani, E. P. *J. Phys. D: Appl. Phys.* **2007**, *40*, 1313.
(286) Huang, R.; Barber, T. A.; Schmidt, M. A.; Tompkins, R. G.; Toner, M.; Bianchi, D. W.; Kapur, R.; Flejter, W. L. *Prenatal Diagn.* **2008**, *28*, 892.
(287) Yu, L. M.; Easterbrook, P. J.; Marshall, T. *Int. J. Epidemiol.* **1997**, *26*, 1367.
(288) Inglis, D. W.; Riehn, R.; Sturm, J. C.; Austin, R. H. *J. Appl. Phys.* **2006**, *99*, 08K101.
(289) Furdui, V. I.; Harrison, D. J. *Lab Chip* **2004**, *4*, 614.
(290) Zborowski, M.; Sun, L. P.; Moore, L. R.; Williams, P. S.; Chalmers, J. J. *J. Magn. Magn. Mater.* **1999**, *194*, 224.
(291) Zborowski, M.; Williams, P. S.; Sun, L.; Moore, L. R.; Chalmers, J. J. *J. Liq. Chromatogr. Relat. Technol.* **1997**, *20*, 2887.
(292) Leigh, D. R.; Steinert, S.; Moore, L. R.; Chalmers, J.; Zborowski, M. *Cytometry, Part A* **2005**, *66A*, 103.
(293) Chalmers, J. J.; Zhao, Y.; Nakamura, M.; Melnik, K.; Lasky, L.; Moore, L.; Zborowski, M. *J. Magn. Magn. Mater.* **1999**, *194*, 231.
(294) Chalmers, J. J.; Haam, S.; Zhao, Y.; McCloskey, K.; Moore, L.; Zborowski, M.; Williams, P. S. *Biotechnol. Bioeng.* **1999**, *64*, 519.
(295) Lara, O.; Tong, X. D.; Zborowski, M.; Farag, S. S.; Chalmers, J. J. *Biotechnol. Bioeng.* **2006**, *94*, 66.
(296) Tong, X. D.; Xiong, Y.; Zborowski, M.; Farag, S. S.; Chalmers, J. J. *Exp. Hematol.* **2007**, *35*, 1613.
(297) Moore, L. R.; Zborowski, M.; Sun, L. P.; Chalmers, J. J. *J. Biochem. Biophys. Methods* **1998**, *37*, 11.
(298) Comella, K.; Nakamura, M.; Melnik, K.; Chosy, J.; Zborowski, M.; Cooper, M. A.; Fehniger, T. A.; Caligiuri, M. A.; Chalmers, J. J. *Cytometry* **2001**, *45*, 285.
(299) Kim, Y.; Hong, S.; Lee, S. H.; Lee, K.; Yun, S.; Kang, Y.; Paek, K. K.; Ju, B. K.; Kim, B. *Rev. Sci. Instrum.* **2007**, *78*, 074301.
(300) Powles, R.; Mehta, J.; Kulkarni, S.; Treleaven, J.; Millar, B.; Marsden, J.; Shepherd, V.; Rowland, A.; Sirohi, B.; Tait, D.; Horton, C.; Long, S.; Singhal, S. *Lancet* **2000**, *355*, 1231.
(301) Weissman, I. L. *Science* **2000**, *287*, 1442.
(302) Melnik, K.; Nakamura, M.; Comella, K.; Lasky, L. C.; Zborowski, M.; Chalmers, J. J. *Biotechnol. Prog.* **2001**, *17*, 907.
(303) Moore, L. R.; Rodriguez, A. R.; Williams, P. S.; McCloskey, K.; Bolwell, B. J.; Nakamura, M.; Chalmers, J. J.; Zborowski, M. *J. Magn. Magn. Mater.* **2001**, *225*, 277.
(304) Cristofanilli, M.; Budd, G. T.; Ellis, M. J.; Stopeck, A.; Matera, J.; Miller, M. C.; Reuben, J. M.; Doyle, G. V.; Allard, W. J.; Terstappen, L.; Hayes, D. F. *New Engl. J. Med.* **2004**, *351*, 781.
(305) Leitzel, K.; Lieu, B.; Curley, E.; Smith, J.; Chinchilli, V.; Rychlik, W.; Lipton, A. *Clin. Cancer Res.* **1998**, *4*, 3037.
(306) Lara, O.; Tong, X. D.; Zborowski, M.; Chalmers, J. J. *Exp. Hematol.* **2004**, *32*, 891.
(307) Hager, G.; Tong, D. C. C.; Schiebel, I.; Rezniczek, G. A.; Watrowski, R.; Speiser, P.; Zeillinger, R. *Gynecol. Oncol.* **2005**, *98*, 211.
(308) Allan, A. L.; Vantyghem, S. A.; Tuck, A. B.; Chambers, A. F.; Chin-Yee, I. H.; Keeney, M. *Cytometry, Part A* **2005**, *65A*, 4.
(309) Chalmers, J. J.; Haam, S.; Zhao, Y.; McCloskey, K.; Moore, L.; Zborowski, M.; Williams, P. S. *Biotechnol. Bioeng.* **1999**, *64*, 509.
(310) Nakamura, M.; Decker, K.; Chosy, J.; Comella, K.; Melnik, K.; Moore, L.; Lasky, L. C.; Zborowski, M.; Chalmers, J. J. *Biotechnol. Prog.* **2001**, *17*, 1145.
(311) Yang, L. Y.; Lang, J. C.; Balasubramanian, P.; Jatana, K. R.; Schuller, D.; Agrawal, A.; Zborowski, M.; Chalmers, J. J. *Biotechnol. Bioeng.* **2009**, *102*, 521.
(312) Pamme, N.; Wilhelm, C. *Lab Chip* **2006**, *6*, 974.
(313) Liu, Y. J.; Guo, S. S.; Zhang, Z. L.; Huang, W. H.; Baigl, D.; Xie, M.; Chen, Y.; Pang, D. W. *Electrophoresis* **2007**, *28*, 4713.
(314) Mitrelias, T.; Palfreyman, J.; Jiang, Z.; Llandro, J.; Bland, J. A. C.; Sanchez-Martin, R. M.; Bradley, M. *J. Magn. Magn. Mater.* **2007**, *310*, 2862.
(315) Mauk, M. G.; Ziober, B. L.; Chen, Z. Y.; Thompson, J. A.; Bau, H. H. *Oral-Based Diagnostics* **2007**, *1098*, 467.
(316) Kim, H. S.; Son, O. T.; Kim, K. H.; Kim, S. H.; Maeng, S.; Jung, H. I. *Biotechnol. Lett.* **2007**, *29*, 1659.
(317) Said, T. M.; Agarwal, A.; Zborowski, M.; Grunewald, S.; Glander, H. J.; Paasch, U. *J. Androl.* **2008**, *29*, 134.
(318) Nath, P.; Strelnik, J.; Vasanji, A.; Moore, L. R.; Williams, P. S.; Zborowski, M.; Roy, S.; Fleischman, A. *Anal. Chem.* **2009**, *81*, 43.
(319) Zborowski, M.; Tada, Y.; Malchesky, P. S.; Hall, G. S. *Colloids Surf., A* **1993**, *77*, 209.
(320) Zborowski, M.; Tada, Y.; Malchesky, P. S.; Hall, G. S. *Appl. Environ. Microbiol.* **1993**, *59*, 1187.
(321) Xia, N.; Hunt, T. P.; Mayers, B. T.; Alsberg, E.; Whitesides, G. M.; Westervelt, R. M.; Ingber, D. E. *Biomed. Microdevices* **2006**, *8*, 299.
(322) Varshney, M.; Li, Y. B.; Srinivasan, B.; Tung, S. *Sens. Actuators, B: Chem.* **2007**, *128*, 99.
(323) Beyor, N.; Seo, T. S.; Liu, P.; Mathies, R. A. *Biomed. Microdevices* **2008**, *10*, 909.
(324) Adams, J. D.; Kim, U.; Soh, H. T. *Proc. Natl. Acad. Sci. U.S.A.* **2008**, *105*, 18165.
(325) Karl, S.; David, M.; Moore, L.; Grimberg, B. T.; Michon, P.; Mueller, I.; Zborowski, M.; Zimmerman, P. A. *Malar. J.* **2008**, *7*, 66.
(326) Wilhelm, C.; Gazeau, F.; Roger, J.; Pons, J. N.; Bacri, J. C. *Langmuir* **2002**, *18*, 8148.
(327) Tiwari, A.; Punshon, G.; Kidane, A.; Hamilton, G.; Seifalian, A. M. *Cell Biol. Toxicol.* **2003**, *19*, 265.
(328) Valberg, P. A.; Butler, J. P. *Biophys. J.* **1987**, *52*, 537.
(329) Wang, N.; Butler, J. P.; Ingber, D. E. *Science* **1993**, *260*, 1124.
(330) Mannix, R. J.; Kumar, S.; Cassiola, F.; Montoya-Zavala, M.; Feinstein, E.; Prentiss, M.; Ingber, D. E. *Nat. Nanotechnol.* **2008**, *3*, 36.
(331) Moller, W.; Nemoto, I.; Heyder, J. *IEEE Trans. Nanobiosci.* **2003**, *2*, 247.
(332) Romano, G.; Sacconi, L.; Capitanio, M.; Pavone, F. S. *Opt. Commun.* **2003**, *215*, 323.
(333) Ogiue-Ikeda, M.; Sato, Y.; Ueno, S. *IEEE Trans. Nanobiosci.* **2003**, *2*, 262.
(334) Koschwanez, J. H.; Carlson, R. H.; Meldrum, D. R. *Rev. Sci. Instrum.* **2007**, *78*, 044301.
(335) Aki, A.; Ito, O.; Morimoto, H.; Nagaoka, Y.; Nakajima, Y.; Mizuki, T.; Hanajiri, T.; Usami, R.; Maekawa, T. *J. Appl. Phys.* **2008**, *104*, 094509.
(336) Lee, H.; Liu, Y.; Westervelt, R. M.; Ham, D. *IEEE J. Solid-State Circuits* **2006**, *41*, 1471.
(337) Lee, H.; Liu, Y.; Ham, D.; Werstervelt, R. M. *Lab Chip* **2007**, *7*, 331.
(338) Polyak, B.; Fishbein, I.; Chorny, M.; Alferiev, I.; Williams, D.; Yellen, B.; Friedman, G.; Levy, R. J. *Proc. Natl. Acad. Sci. U.S.A.* **2008**, *105*, 698.
(339) Schlaurman, T.; de Boer, R.; Patty, R.; Kooistra-Smid, M.; van Zwet, A. *J. Microbiol. Methods* **2007**, *71*, 238.
(340) Leb, V.; Stocher, M.; Valentine-Thon, E.; Holzl, G.; Kessler, H.; Stekal, H.; Berg, J. *J. Clin. Microbiol.* **2004**, *42*, 585.
(341) Yeung, S. W.; Lee, T. M. H.; Cai, H.; Hsing, I. M. *Nucleic Acids Res.* **2006**, *34*, e118.
(342) Zhao, W. T.; Yao, S. J.; Hsing, I. M. *Biosens. Bioelectron.* **2006**, *21*, 1163.
(343) Jiang, G. F.; Harrison, D. J. *Analyst* **2000**, *125*, 2176.
(344) Lien, K. Y.; Lin, J. L.; Liu, C. Y.; Lei, H. Y.; Lee, G. B. *Lab Chip* **2007**, *7*, 868.
(345) Lund-Olesen, T.; Dufva, M.; Hansen, M. F. *J. Magn. Magn. Mater.* **2007**, *311*, 396.
(346) Kwakye, S.; Baeumner, A. *Anal. Bioanal. Chem.* **2003**, *376*, 1062.
(347) Yeung, S. W.; Hsing, I. M. *Biosens. Bioelectron.* **2006**, *21*, 989.
(348) Rida, A.; Gijs, M. A. M. *Anal. Chem.* **2004**, *76*, 6239.
(349) Lou, X. H.; Qian, J. R.; Xiao, Y.; Viel, L.; Gerdon, A. E.; Lagally, E. T.; Atzberger, P.; Tarasow, T. M.; Heeger, A. J.; Soh, H. T. *Proc. Natl. Acad. Sci. U.S.A.* **2009**, *106*, 2989.
(350) Mauk, M. G.; Ziober, B. L.; Chen, Z. Y.; Thompson, J. A.; Bau, H. H. *Oral-Based Diagnostics* **2007**, *1098*, 467.
(351) Pioch, D.; Jurgen, B.; Evers, S.; Maurer, K. H.; Hecker, M.; Schweder, T. *Appl. Microbiol. Biotechnol.* **2008**, *78*, 719.
(352) Grover, W. H.; Mathies, R. A. *Lab Chip* **2005**, *5*, 1033.
(353) Dubus, S.; Gravel, J. F.; Le Drogoff, B.; Nobert, P.; Veres, T.; Boudreau, D. *Anal. Chem.* **2006**, *78*, 4457.
(354) Ferreira, H. A.; Graham, D. L.; Feliciano, N.; Clarke, L. A.; Amaral, M. D.; Freitas, P. P. *IEEE Trans. Magn.* **2005**, *41*, 4140.
(355) Heer, R.; Eggeling, M.; Schotter, J.; Nohammer, C.; Pichler, R.; Mansfeld, M.; Bruckl, H. *J. Magn. Magn. Mater.* **2007**, *311*, 244.
(356) Chiou, C. H.; Huang, Y. Y.; Chiang, M. H.; Lee, H. H.; Lee, G. B. *Nanotechnology* **2006**, *17*, 1217.
(357) Chiou, C. H.; Lee, G. B. *J. Micromech. Microeng.* **2005**, *15*, 109.
(358) Mitnik, L.; Heller, C.; Prost, J.; Viovy, J. L. *Science* **1995**, *267*, 219.
(359) Kim, Y. S.; Morris, M. D. *Anal. Chem.* **1994**, *66*, 1168.
(360) Doyle, P. S.; Bibette, J.; Bancaud, A.; Viovy, J. L. *Science* **2002**, *295*, 2237.
(361) Dorfman, K. D.; Viovy, J. L. *Phys. Rev. E* **2004**, *69*, 011901.
(362) Minc, N.; Bokov, P.; Zeldovich, K. B.; Futterer, C.; Viovy, J. L.; Dorfman, K. D. *Electrophoresis* **2005**, *26*, 362.

(363) Minc, N.; Futterer, C.; Dorfman, K. D.; Bancaud, A.; Gosse, C.; Goubault, C.; Viovy, J. L. *Anal. Chem.* **2004**, *76*, 3770.
(364) Minc, N.; Slovakova, M.; Dorfman, K. D.; Futterer, C.; Bokov, P.; Bilkova, Z.; Smadga, C.; Taverna, M.; Viovy, J. L. *Houille Blanche-Revue Internationale De L Eau* **2006**, 51.
(365) Park, J. H.; Derfus, A. M.; Segal, E.; Vecchio, K. S.; Bhatia, S. N.; Sailor, M. J. *J. Am. Chem. Soc.* **2006**, *128*, 7938.
(366) Pipper, J.; Zhang, Y.; Neuzil, P.; Hsieh, T. M. *Angew. Chem., Int. Ed.* **2008**, *47*, 3900.
(367) Tsuchiya, H.; Okochi, M.; Nagao, N.; Shikida, M.; Honda, H. *Sens. Actuators, B: Chem.* **2008**, *130*, 583.
(368) Schotter, J.; Kamp, P. B.; Becker, A.; Puhler, A.; Reiss, G.; Bruckl, H. *Biosens. Bioelectron.* **2004**, *19*, 1149.
(369) Smistrup, K.; Bruus, H.; Hansen, M. F. *J. Magn. Magn. Mater.* **2007**, *311*, 409.
(370) Liu, Y. J.; Yao, D. J.; Chang, H. Y.; Liu, C. M.; Chen, C. *Biosens. Bioelectron.* **2008**, *24*, 558.
(371) Wang, S. X.; Bae, S. Y.; Li, G. X.; Sun, S. H.; White, R. L.; Kemp, J. T.; Webb, C. D. *J. Magn. Magn. Mater.* **2005**, *293*, 731.
(372) Brzeska, M.; Panhorst, M.; Kamp, P. B.; Schotter, J.; Reiss, G.; Puhler, A.; Becker, A.; Bruckl, H. *J. Biotechnol.* **2004**, *112*, 25.
(373) Weizmann, Y.; Patolsky, F.; Lioubashevski, O.; Willner, I. *J. Am. Chem. Soc.* **2004**, *126*, 1073.
(374) Mulvaney, S. P.; Mattoussi, H. M.; Whitman, L. J. *BioTechniques* **2004**, *36*, 602.
(375) Stahl, P. L.; Gantelius, J.; Natanaelsson, C.; Ahmadian, A.; Andersson-Svahn, H.; Lundeberg, J. *Genomics* **2007**, *90*, 741.
(376) Tierno, P.; Reddy, S. V.; Roper, M. G.; Jofansen, T. H.; Fischer, T. M. *J. Phys. Chem. B* **2008**, *112*, 3833.
(377) Besse, P.-A.; Boero, G. *Appl. Phys. Lett.* **2002**, *80*, 4199.
(378) Lagae, L.; Wirix-Speetjens, R.; Liu, C. X.; Laureyn, W.; Borghs, G.; Harvey, S.; Galvin, P.; Ferreira, H. A.; Graham, D. L.; Freitas, P. P.; Clarke, L. A.; Amaral, M. D. *IEE Proc. Circuits Devices Syst.* **2005**, *152*, 393.
(379) Ejsing, L.; Hansen, M. F.; Menon, A. K.; Ferreira, H. A.; Graham, D. L.; Freitas, P. P. *J. Magn. Magn. Mater.* **2005**, *293*, 677.
(380) Koets, M.; van der Wijk, T.; van Eemeren, J.; van Amerongen, A.; Prins, M. W. J. *Biosens. Bioelectron.* **2009**, *24*, 1893.
(381) Bronzeau, S.; Pamme, N. *Anal. Chim. Acta* **2008**, *609*, 105.
(382) Liu, R. H.; Yang, J. N.; Lenigk, R.; Bonanno, J.; Grodzinski, P. *Anal. Chem.* **2004**, *76*, 1824.
(383) Fan, Z. H.; Mangru, S.; Granzow, R.; Heaney, P.; Ho, W.; Dong, Q. P.; Kumar, R. *Anal. Chem.* **1999**, *71*, 4851.
(384) Lien, K. Y.; Lee, W. C.; Lei, H. Y.; Lee, G. B. 2006 1st Ieee International Conference on Nano/Micro Engineered and Molecular Systems, 2006; Vols. *1*−*3*, p 668.
(385) Lien, K. Y.; Lee, W. C.; Lei, H. Y.; Lee, G. B. *Biosens. Bioelectron.* **2007**, *22*, 1739.
(386) Liu, C. J.; Lien, K. Y.; Weng, C. Y.; Shin, J. W.; Chang, T. Y.; Lee, G. B. *Biomed. Microdevices* **2009**, *11*, 339.
(387) Lien, K. Y.; Liu, C. J.; Lee, G. B. Mems 2008: 21st Ieee International Conference on Micro Electro Mechanical Systems, Technical Digest, 2008; p 66.
(388) Cho, Y. K.; Lee, J. G.; Park, J. M.; Lee, B. S.; Lee, Y.; Ko, C. *Lab Chip* **2007**, *7*, 565.
(389) Pipper, J.; Inoue, M.; Ng, L. F. P.; Neuzil, P.; Zhang, Y.; Novak, L. *Nat. Med.* **2007**, *13*, 1259.
(390) Barbee, K. D.; Huang, X. H. *Anal. Chem.* **2008**, *80*, 2149.
(391) Mulvaney, S. P.; Cole, C. L.; Kniller, M. D.; Malito, M.; Tamanaha, C. R.; Rife, J. C.; Stanton, M. W.; Whitman, L. J. *Biosens. Bioelectron.* **2007**, *23*, 191.
(392) Kwakye, S.; Goral, V. N.; Baeumner, A. J. *Biosens. Bioelectron.* **2006**, *21*, 2217.
(393) Shen, W. F.; Schrag, B. D.; Carter, M. J.; Xie, J.; Xu, C. J.; Sun, S. H.; Xiao, G. *J. Appl. Phys.* **2008**, *103*, 07a306.
(394) Graham, D. L.; Ferreira, H. A.; Feliciano, N.; Freitas, P. P.; Clarke, L. A.; Amaral, M. D. *Sens. Actuators, B: Chem.* **2005**, *107*, 936.
(395) Hong, J. W.; Studer, V.; Hang, G.; Anderson, W. F.; Quake, S. R. *Nat. Biotechnol.* **2004**, *22*, 435.
(396) Wellman, A. D.; Sepaniak, M. *Anal. Chem.* **2006**, *78*, 4450.
(397) Wellman, A. D.; Sepaniak, M. *Anal. Chem.* **2007**, *79*, 6622.
(398) Liu, Y. J.; Guo, S. S.; Zhang, Z. L.; Huang, W. H.; Baigl, D. M.; Chen, Y.; Pang, D. W. *J. Appl. Phys.* **2007**, *102*, 084911.
(399) Peyman, S. A.; Iles, A.; Pamme, N. *Chem. Commun.* **2008**, 1220.
(400) Herrmann, M.; Veres, T.; Tabrizian, M. *Lab Chip* **2006**, *6*, 555.
(401) Herrmann, M.; Roy, E.; Veres, T.; Tabrizian, M. *Lab Chip* **2007**, *7*, 1546.
(402) Lee, H.; Yasukawa, T.; Shiku, H.; Matsue, T. *Biosens. Bioelectron.* **2008**, *24*, 1000.
(403) Sista, R. S.; Eckhardt, A. E.; Srinivasan, V.; Pollack, M. G.; Palanki, S.; Pamula, V. K. *Lab Chip* **2008**, *8*, 2188.
(404) Lehmann, U.; de Courten, D.; Vandevyver, C.; Parashar, V. K.; Gijs, M. A. M. *Microelectron. Eng.* **2007**, *84*, 1669.
(405) Choi, J. W.; Oh, K. W.; Thomas, J. H.; Heineman, W. R.; Halsall, H. B.; Nevin, J. H.; Helmicki, A. J.; Henderson, H. T.; Ahn, C. H. *Lab Chip* **2002**, *2*, 27.
(406) Do, J.; Ahn, C. H. *Lab Chip* **2008**, *8*, 542.
(407) Morozov, V. N.; Morozova, T. Y. *Anal. Chim. Acta* **2006**, *564*, 40.
(408) Kim, K. S.; Park, J. K. *Lab Chip* **2005**, *5*, 657.
(409) Millen, R. L.; Kawaguchi, T.; Granger, M. C.; Porter, M. D.; Tondra, M. *Anal. Chem.* **2005**, *77*, 6581.
(410) Degre, G.; Brunet, E.; Dodge, A.; Tabeling, P. *Lab Chip* **2005**, *5*, 691.
(411) Ku, B. Y.; Chan, M. L.; Ma, Z.; Horsley, D. A. *J. Magn. Magn. Mater.* **2008**, *320*, 2279.
(412) Chung, S. H.; Hoffmann, A.; Bader, S. D.; Liu, C.; Kay, B.; Makowski, L.; Chen, L. *Appl. Phys. Lett.* **2004**, *85*, 2971.
(413) Chung, S. H.; Hoffmann, A.; Guslienko, K.; Bader, S. D.; Liu, C.; Kay, B.; Makowski, L.; Chen, L. *J. Appl. Phys.* **2004**, *97*, 10R101.
(414) Morozov, V. N.; Groves, S.; Turell, M. J.; Baileyt, C. *J. Am. Chem. Soc.* **2007**, *129*, 12628.
(415) Moser, Y.; Lehnert, T.; Gijs, M. A. M. *Lab Chip* **2009**, *9*, 3261.
(416) Caulum, M. M.; Henry, C. S. *Lab Chip* **2008**, *8*, 865.
(417) Cohen-Tannoudji, L.; Bertrand, E.; Baudry, J.; Robic, C.; Goubault, C.; Pellissier, M.; Johner, A.; Thalmann, F.; Lee, N. K.; Marques, C. M.; Bibette, J. *Phys. Rev. Lett.* **2008**, *100*, 108301.
(418) Dupont, E.; Labonne, E.; Vandevyver, C.; Lehmann, U.; Charbon, E.; Gijs, M. A. M. *Anal. Chem.* **2009**, DOI: 10.1021/ac902241j.
(419) Hermann, M.; Veres, T.; Tabrizian, M. *Anal. Chem.* **2008**, *80*, 5160.
(420) De Palma, R.; Reekmans, G.; Liu, C. X.; Wirix-Speetjens, R.; Laureyn, W.; Nilsson, O.; Lagae, L. *Anal. Chem.* **2007**, *79*, 8669.
(421) De Palma, R.; Reekmans, G.; Laureyn, W.; Borghs, G.; Maes, G. *Anal. Chem.* **2007**, *79*, 7540.
(422) Hahn, Y. K.; Jin, Z.; Kang, J. H.; Oh, E.; Han, M. K.; Kim, H. S.; Jang, J. T.; Lee, J. H.; Cheon, J.; Kim, S. H.; Park, H. S.; Park, J. K. *Anal. Chem.* **2007**, *79*, 2214.
(423) Mulvaney, S. P.; Myers, K. M.; Sheehan, P. E.; Whitman, L. J. *Biosens. Bioelectron.* **2009**, *24*, 1109.
(424) Soelberg, S. D.; Stevens, R. C.; Limaye, A. P.; Furlong, C. E. *Anal. Chem.* **2009**, *81*, 2357.
(425) Aytur, T.; Foley, J.; Anwar, M.; Boser, B.; Harris, E.; Beatty, P. R. *J. Immunol. Methods* **2006**, *314*, 21.
(426) Yang, S. Y.; Lien, K. Y.; Huang, K. J.; Lei, H. Y.; Lee, G. B. *Biosens. Bioelectron.* **2008**, *24*, 855.
(427) Tang, D.; Yuan, R.; Chai, Y. *Clin. Chem.* **2007**, *53*, 1323.
(428) Dittmer, W. U.; de Kievit, P.; Prins, M. W. J.; Vissers, J. L. M.; Mersch, M. E. C.; Martens, M. *J. Immunol. Methods* **2008**, *338*, 40.
(429) Kiely, J.; Hawkins, P.; Wraith, P.; Luxton, R. *IET Sci. Meas. Techn.* **2007**, *1*, 270.
(430) Bruls, D. M.; Evers, T. H.; Kahlman, J. A. H.; van Lankvelt, P. J. W.; Ovsyanko, M.; Pelssers, E. G. M.; Schleipen, J. J. H. B.; de Theije, F. K.; Verschuren, C. A.; van der Wijk, T.; van Zon, J. B. A.; Dittmer, W. U.; Immink, A. H. J.; Nieuwenhuis, J. H.; Prins, M. W. J. *Lab Chip* **2009**, DOI: 10.1039/B913960E.
(431) Chen, H. X.; Busnel, J. M.; Peltre, G.; Zhang, X. X.; Girault, H. H. *Anal. Chem.* **2008**, *80*, 9583.
(432) Chen, X.; Cui, D. F.; Liu, C. C. *Electrophoresis* **2008**, *29*, 1844.
(433) Lacharme, F.; Vandevyver, C.; Gijs, M. A. M. *Microfluid. Nanofluid.* **2009**, *7*, 479.
(434) Peyman, S.; Iles, A.; Pamme, N. The 11th International Conference on Miniaturized Systems for Chemistry and Life Sciences, μTAS 2007 Conference, Paris, France, 2007; p 1270.
(435) Shikida, M.; Takayanagi, K.; Honda, H.; Ito, H.; Sato, K. *J. Micromech. Microeng.* **2006**, *16*, 1875.
(436) De Palma, R.; Liu, C. X.; Barbagini, F.; Reekmans, G.; Bonroy, K.; Laureyn, W.; Borghs, G.; Maes, G. *J. Phys. Chem. C* **2007**, *111*, 12227.
(437) Morozova, T. Y.; Morozov, V. N. *Anal. Biochem.* **2008**, *374*, 263.
(438) Baudry, J.; Bertrand, E.; Lequeux, N.; Bibette, J. *J. Phys.: Condens. Matter* **2004**, *16*, R469.
(439) Baudry, J.; Rouzeau, C.; Goubault, C.; Robic, C.; Cohen-Tannoudji, L.; Koenig, A.; Bertrand, E.; Bibette, J. *Proc. Natl. Acad. Sci. U.S.A.* **2006**, *103*, 16076.
(440) Lai, J. J.; Nelson, K. E.; Nash, M. A.; S., H. A.; Yager, P.; Stayton, P. S. *Lab Chip* **2009**, *9*, 1997.
(441) Cole-Hamilton, D. J. *Science* **2003**, *299*, 1702.
(442) Abu-Reziq, R.; Alper, H.; Wang, D. S.; Post, M. L. *J. Am. Chem. Soc.* **2006**, *128*, 5279.
(443) Hu, A. G.; Yee, G. T.; Lin, W. B. *J. Am. Chem. Soc.* **2005**, *127*, 12486.
(444) Luo, S. Z.; Zheng, X. X.; Xu, H.; Mi, X. L.; Zhang, L.; Cheng, J. P. *Adv. Synth. Catal.* **2007**, *349*, 2431.
(445) Stevens, P. D.; Li, G. F.; Fan, J. D.; Yen, M.; Gao, Y. *Chem. Commun.* **2005**, 4435.
(446) Zheng, Y.; Stevens, P. D.; Gao, Y. *J. Org. Chem.* **2006**, *71*, 537.

(447) Li, J.; Zhang, Y. M.; Han, D. F.; Gao, Q.; Li, C. *J. Mol. Catal. A: Chem.* **2009**, *298*, 31.
(448) Lee, J.; Lee, D.; Oh, E.; Kim, J.; Kim, Y. P.; Jin, S.; Kim, H. S.; Hwang, Y.; Kwak, J. H.; Park, J. G.; Shin, C. H.; Hyeon, T. *Angew. Chem., Int. Ed.* **2005**, *44*, 7427.
(449) Kang, J. H.; Park, J. K. *Small* **2007**, *3*, 1784.
(450) Kang, J. H.; Park, J. K. Ieee 20th IEEE International Conference on Micro Electro Mechanical Systems (MEMS 2007), Kobe, Japan, 2007; p 99.
(451) Ding, S. J.; Xing, Y. C.; Radosz, M.; Shen, Y. Q. *Macromolecules* **2006**, *39*, 6399.
(452) Shokouhimehr, M.; Piao, Y. Z.; Kim, J.; Jang, Y. J.; Hyeon, T. *Angew. Chem., Int. Ed.* **2007**, *46*, 7039.
(453) Wang, Z. F.; Shen, B.; Zou, A. H.; He, N. Y. *Chem. Eng. J.* **2005**, *113*, 27.
(454) Wang, Z. F.; Xiao, P. F.; Shen, B.; He, N. Y. *Colloids Surf., A* **2006**, *276*, 116.
(455) Yoon, T. J.; Lee, W.; Oh, Y. S.; Lee, J. K. *New J. Chem.* **2003**, *27*, 227.
(456) Teunissen, W.; Bol, A. A.; Geus, J. W. *Catal. Today* **1999**, *48*, 329.
(457) Yi, D. K.; Lee, S. S.; Ying, J. Y. *Chem. Mater.* **2006**, *18*, 2459.
(458) Jun, C. H.; Park, Y. J.; Yeon, Y. R.; Choi, J. R.; Lee, W. R.; Ko, S. J.; Cheon, J. *Chem. Commun.* **2006**, 1619.
(459) Dyal, A.; Loos, K.; Noto, M.; Chang, S. W.; Spagnoli, C.; Shafi, K.; Ulman, A.; Cowman, M.; Gross, R. A. *J. Am. Chem. Soc.* **2003**, *125*, 1684.
(460) Gardimalla, H. M. R.; Mandal, D.; Stevens, P. D.; Yen, M.; Gao, Y. *Chem. Commun.* **2005**, 4432.
(461) Zheng, Y.; Duanmu, C.; Gao, Y. *Org. Lett.* **2006**, *8*, 3215.
(462) Bromberg, L.; Hatton, T. A. *Ind. Eng. Chem. Res.* **2005**, *44*, 7991.
(463) Stevens, P. D.; Fan, J. D.; Gardimalla, H. M. R.; Yen, M.; Gao, Y. *Org. Lett.* **2005**, *7*, 2085.
(464) Gao, X.; Yu, K. M. K.; Tam, K. Y.; Tsang, S. C. *Chem. Commun.* **2003**, 2998.
(465) Llopis, X.; Pumera, M.; Alegret, S.; Merkoci, A. *Lab Chip* **2009**, *9*, 213.
(466) Krenkova, J.; Foret, F. *Electrophoresis* **2004**, *25*, 3550.
(467) Slovakova, M.; Minc, N.; Bilkova, Z.; Smadja, C.; Faigle, W.; Futterer, C.; Taverna, M.; Viovy, J. L. *Lab Chip* **2005**, *5*, 935.
(468) Le Nel, A.; Minc, N.; Smadja, C.; Slovakova, M.; Bilkova, Z.; Peyrin, J. M.; Viovy, J. L.; Taverna, M. *Lab Chip* **2008**, *8*, 294.
(469) Li, Y.; Xu, X. Q.; Yan, B.; Deng, C. H.; Yu, W. J.; Yang, P. Y.; Zhang, X. M. *J. Proteome Res.* **2007**, *6*, 2367.
(470) Li, Y.; Yan, B.; Deng, C. H.; Yu, W. J.; Xu, X. Q.; Yang, P. Y.; Zhang, X. M. *Proteomics* **2007**, *7*, 2330.
(471) Liu, J. Y.; Lin, S.; Qi, D. W.; Deng, C. H.; Yang, P. Y.; Zhang, X. M. *J. Chromatogr.* **2007**, *1176*, 169.
(472) Jankovicova, B.; Rosnerova, S.; Slovakova, M.; Zverinova, Z.; Hubalek, M.; Hernychova, L.; Rehulka, P.; Viovy, J. L.; Bilkova, Z. 22nd International Symposium on Microscale Bioseparations and Methods for Systems Biology, Berlin, Germany, 2008; p 64.

CR9001929